QA.A47A35
Mic
INPC

STIC-ILL

From: Holleran, Anne
Sent: Monday, January 20, 2003 11:57 AM
To: STIC-ILL
Subject: refs. for 09/868,968

Please send copies of the following papers:

1.	Hoyoku,	Anticancer Res. (1999) 19(5A): 3663-3664
2.	Chamson-Reig	Endocrinology (1999) 140(8): 3573-3580
3.	Lixin,	J. Medicinal Chemistry 91998) 41(18): 3303-3306
4.	Yorek,	American J. Physiology (1998) 274(1, part1): C58-C71
5.	Nazih-Sanderson	Biochimica et Biophysica Acta (1997) 1346(1): 45-60
6.	Wattenberg	Cancer Research (1996) 56(22): 5132-5135
7.	Caro	Infection and Immunity (1996) 64(8): 3438-3441
8.	Seymour	Laboratory Investigation (1996) 75(3): 427-437
9.	Brunn	Cancer Chemotherapy (1994) 35(1): 71-79
10.	Kopp	Cancer Research (1990) 50(20): 6490-6496
11.	Tanino	Japanese J. Experimental Medicine (1972) 42(6): 575-582
12.	Eagle	Biochmistry (1963) 2(5): 1125-1126
13.	Caro	Biochem. Mol. Med. (1997) 61: 214-228

Anne Holleran
AU: 1642
Tel: 308-8892
RM: 8e03

mailbox: 8e12

INFECTION AND IMMUNITY, Aug. 1996, p. 3438–3441
0019-9567/96/$04.00+0

Vol. 64, No. 8

Structural Similarities among Malaria Toxins, Insulin Second Messengers, and Bacterial Endotoxin

H. N. CARO,[1]* N. A. SHEIKH,[2] J. TAVERNE,[2] J. H. L. PLAYFAIR,[2] AND T. W. RADEMACHER[1]

Molecular Medicine Unit, Department of Molecular Pathology,[1] and Department of Immunology,[2] University College London Medical School, London W1P 6DB, United Kingdom

Received 6 November 1995/Returned for modification 6 December 1995/Accepted 7 May 1996

Malaria toxin causes hypoglycemia and induction of tumor necrosis factor. Extracts of parasitized erythrocytes which were coeluted and copurified with one of the two subtypes of mammalian insulin-mimetic inositolphosphoglycans similarly induced fibroblast proliferation in the absence of serum. In addition, induction of tumor necrosis factor in macrophages by malaria toxin and by lipopolysaccharide from *Escherichia coli* was enhanced by pretreatment of these toxins with α-galactosidase. Thus, parasitized erythrocytes contain both soluble inositolphosphoglycan-like insulin second messengers and endotoxin-like lipidic molecules.

Since the severity of clinical manifestations of malaria is correlated with the presence of tumor necrosis factor (TNF) in the circulation (8, 13, 15), components of parasitized erythrocytes which induce its production and cause hypoglycemia (25) are customarily referred to as toxins (11). The TNF-inducing activity is associated with a phospholipid (1, 3) and is inhibited by inositol monophosphate (2). The hypoglycemia associated with malaria correlates with hyperinsulinemia (6). Toxin preparations also synergize with insulin in stimulating lipogenesis in adipocytes in vitro (26).

Insulin second messengers. Insulin second messengers are derived from membrane-associated glycosylphosphatidylinositol (GPI) (7). Inositolphosphoglycans (IPGs) are released outside the cell by the action of a phospholipase which is activated following receptor ligation by insulin. A family of structures with A- and P-type subfamilies which are functionally and chemically distinct exists, and their release is tissue specific (14). The A-type mediators mimic the lipogenic activity of insulin on adipocytes, whereas the P-type mediators mimic the glycogenic activity of insulin on muscle. Both A- and P-type mediators are mitogenic when added to fibroblasts in serum-free medium.

To see if parasitized erythrocytes contain IPG-like activities, they were extracted as described previously for rat and bovine tissues (14, 17). Female CD1 mice (Charles River Ltd., Margate, Kent, United Kingdom) infected with *Plasmodium yoelii* YM (from A. Holder, National Institute of Medical Research, London, United Kingdom) were bled, and washed erythrocytes (RBCs) containing more than 80% schizonts of *P. yoelii* were incubated at 37°C overnight at 2×10^8 cells per ml in 50 ml of Earle's balanced salt solution (Life Technologies Ltd.); uninfected RBCs at 2×10^9/ml were used as a control. They were then dried in a rotary evaporator and extracted by being boiled in 50 mM formic acid containing 1 mM EDTA and 1 mM β-mercaptoethanol and then centrifuged at 29,500 × *g* for 90 min. The supernatant was treated with charcoal (10 mg/ml) on ice and recentrifuged. The clear supernatant was diluted to 5 mM formic acid, adjusted to pH 6.0 with 10% NH_4OH, and shaken overnight with AG1X8 (formate form) resin (Bio-Rad, Hemel Hempstead, United Kingdom). The resin was then poured into a chromatography column and washed with water and 1 mM HCl (2 bed volumes of each). It was eluted with 10 mM HCl (5 bed volumes), yielding P-type IPG, followed by 50 mM HCl (5 bed volumes), yielding A-type IPG. The two fractions were adjusted to pH 4.0 with 10% NH_4OH and then dried, and each was dissolved in 200 μl of BSS and adjusted to pH 7.0. Rat liver after insulin infusion was also extracted as a positive control, and the presence of A-type (50 mM HCl eluate) and P-type (10 mM HCl eluate) IPGs was confirmed by their biological activities (14).

The two fractions obtained from erythrocytes were assayed for their ability to support proliferation of epidermal growth factor receptor-transfected T17 fibroblasts (gift from I. Varela-Nieto) in the absence of serum (18). Cells (10^4 per well) were grown overnight in 96-well plates in Dulbecco's modified Eagle's medium (DMEM [Life Technologies Ltd., Paisley, Scotland]) containing 10% fetal calf serum and 10 μg of ciprofloxacin (Ciproxin; Bayer, Newbury, Berkshire, United Kingdom) per ml, washed free of serum, and maintained in serum-free DMEM for a further 24 h. They were then incubated, in triplicate, with serial dilutions of the erythrocyte-derived fractions in serum-free DMEM, DMEM with 10% fetal calf serum, and P- and A-type mediators from rat liver (diluted 1/40) as controls. After 18 h, cells were pulsed with [^{3}H]thymidine (1 μCi per well; Amersham, Buckinghamshire, United Kingdom) for 4 h, detached by trypsinization, and harvested, and DNA-incorporated radioactivity was determined.

Extracts from parasitized but not from uninfected RBCs supported cell proliferation, the activity of the 10 mM eluate (P-type IPG) greatly exceeding that of the 50 mM eluate (A-type IPG) (Fig. 1). This activity was not directly related to their content of organic phosphate as determined by standard molybdate assay. Thus, the 10 mM eluate from parasitized RBCs contained 7.6 nmol/μl, compared with 28 nmol/μl in the 50 mM eluate. The uninfected RBC fractions contained 5.3 and 13.4 nmol/μl, respectively. The comparable fractions from rat liver contained 13.2 and 27.6 nmol/μl. The 10 mM fraction also stimulated pyruvate dehydrogenase phosphatase activity (data not shown). Proliferative activity was only found in the 50 mM eluate at the lowest dilution. Neither fraction induced TNF. The smaller amount of A-type activity supports the original observation that most toxin preparations had no direct effect on lipogenesis in adipocytes (26). Since the aqueous extracts we employed would not have contained lipid-soluble GPI

* Corresponding author. Mailing address: Molecular Medicine Unit, Department of Molecular Pathology, University College London Medical School, London W1P 6DB, United Kingdom. Phone: 44-171-580-5171. Fax: 44-171-380-9497. Electronic mail address: H.Caro@ucl.ac.uk.

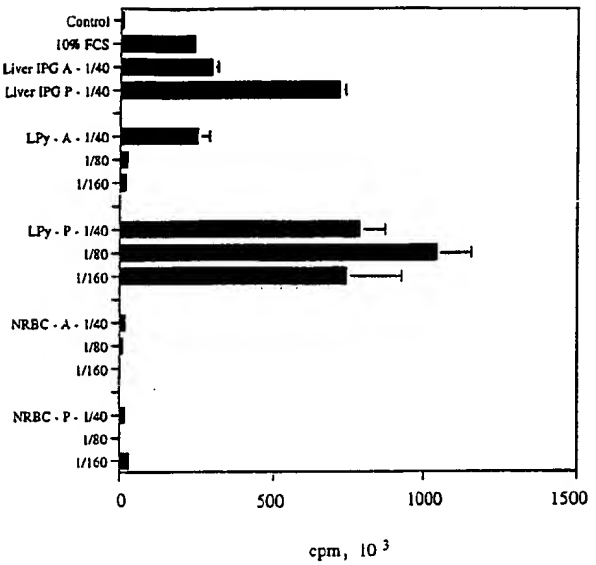

FIG. 1. IPG activity of malaria toxin assessed by proliferation of fibroblasts transfected with the human epidermal growth factor receptor. Cells were incubated in the absence of serum (control) or with serial dilutions made from the IPG-containing solutions of RBCs infected with *P. yoelii* (LPy) or normal RBCs (NRBC). As positive controls, 10% fetal calf serum (FCS) and A-type and P-type IPG, obtained from rat liver as described previously (14), were included (10 μl of stock solution represents the amount of mediator recovered from 800 mg (wet weight) of liver). Values are means ± standard deviations of triplicate determinations.

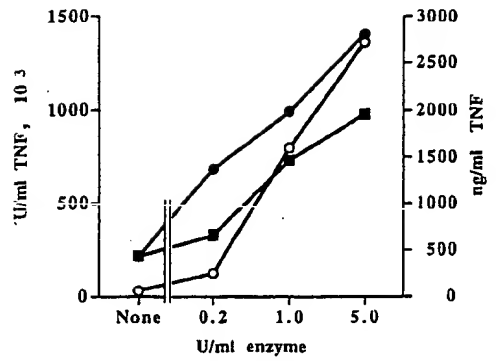

FIG. 2. Typical enhancement of the TNF-inducing ability of malaria toxin by treatment with α-galactosidase from two different sources. Serial dilutions of an extract of parasitized RBCs which (undiluted) induced 435 ng of TNF per ml as determined by ELISA and which induced 30,400 U/ml in the bioassay were incubated at pH 6.0 at 37°C overnight with a series of concentrations of α-galactosidase from Sigma or from Oxford GlycoSystems, boiled, neutralized, and then tested on macrophages for TNF induction by bioassay and ELISA. (Means of duplicate determinations are shown.) The amount of TNF that would have been induced by the original undiluted extract was then calculated. ○, units per milliliter by bioassay (enzyme from Sigma); ●, nanograms per milliliter by ELISA (enzyme from Sigma); ■, nanograms per milliliter by ELISA (enzyme from Oxford GlycoSystems).

structures, our results cannot be compared directly with those described by Schofield and Hackett (22).

Structural components of the malaria toxin. Structural components of malaria toxin which affect activity have been inferred from enzymatic and chemical treatments. TNF induction by malaria toxin is unaffected (3) by treatment with dilute HONO. This resistance to HONO distinguishes the active portion of lipidic TNF-inducing malaria toxin from GPI anchors of proteins which, like IPG, are degraded by HONO, because of the presence of a non-*N*-acetylated hexosamine residue. Glycoconjugates from parasites, such as lipophosphoglycans attached to the membrane via GPI anchors (16) and the glycan moiety of GPI-anchored proteins (27), contain α-galactose residues. Likewise, bacterial lipopolysaccharide (LPS) contains α-galactose residues (20). α-D-Galactosidase has also been shown to alter the antigenicity of an antigen in *Plasmodium falciparum* culture medium (12) which induces TNF (23). To see if the TNF-inducing activity of malaria toxin contained α-galactose residues, we treated both the malaria toxin and LPS with a preparation of α-galactosidase.

Mice bred here [(CBA × BALB/c)F_1 or (CBA × C57Bl)F_1] were infected with *P. yoelii* YM or *Plasmodium berghei* ANKA. Parasitized RBCs (10^8/ml) in BSS were incubated at 37°C overnight and then disrupted by freezing and thawing, digested overnight with 250 μg of pronase E (Sigma) per mg of protein (determined by Bio-Rad assay), boiled, treated with 25 μg of polymyxin B agarose (Sigma) per ml to eliminate endotoxin, filtered through a 0.2-μm-pore-size filter (Sartorius AG, Göttingen, Germany), and stored at 4°C (24). TNF induction from thioglycolate-induced peritoneal macrophages and enzyme-linked immunosorbent assays (ELISAs) for murine TNF were described previously (24). Polymyxin B (5 μg/ml) was included in all experiments with malaria toxin to exclude effects of contamination with LPS. A more sensitive one-plate procedure for TNF production and assay was also used (5). Cytotoxicity assays for TNF were done with L929 cells (23). Green coffee bean α-D-galactosidase was obtained from two sources (Sigma, Poole, Dorset, United Kingdom, and Oxford GlycoSystems, Ltd., Abingdon, Oxford, United Kingdom).

A significant increase in TNF induction in macrophages was reproducibly observed when more than a dozen different extracts of RBCs infected with *P. yoelii* and three infected with *P. berghei* (but not uninfected RBC controls that did not induce TNF) were pretreated with α-D-galactosidase. A typical titration showing dose-dependent enhancement of TNF induction by one sample of malaria toxin treated with increasing amounts of α-galactosidase is shown in Fig. 2. The amount of TNF enhancement by any concentration of α-galactosidase depended on toxin potency, with higher dilutions of toxin always showing greater enhancement. No TNF was induced from macrophages incubated with only 2 U of enzyme per ml, and no enhancement occurred with boiled enzyme, again excluding any contribution from contaminating LPS, which is heat stable. Macrophages treated with 2 U of enzyme per ml for 1 h at 37°C and then stimulated with toxin or 2 or 10 ng of LPS per ml did not secrete more TNF than untreated cells.

The α-galactosidase hydrolysis of *p*-nitrophenyl-α-D-galactopyranoside (αPNP-Gal) is optimal at pH 6.0 (4, 9) and undetectable at pH 8.0 (9), as we confirmed, but enhancement of TNF induction by malaria toxin was greatest at pH 8.0 (Fig. 3). The TNF-inducing activity of LPS was also enhanced with a pH profile similar to that of the toxin, indicating a homologous structure-function relationship. The degree of enhancement also varied with the concentration of LPS, and at higher concentrations, enhancement was also detectable at pH 6.0.

The most likely explanation for the lack of activity against αPNP-Gal at pH 8.0 is the presence of an α-galactosidase activity which does not hydrolyze this substrate. This was supported by the observation of batch-to-batch variability and the fact that the stability of the TNF-enhancing activity differed from that of the αPNP-Gal activity. Although all enzyme preparations were first dialyzed and adjusted to the same activity

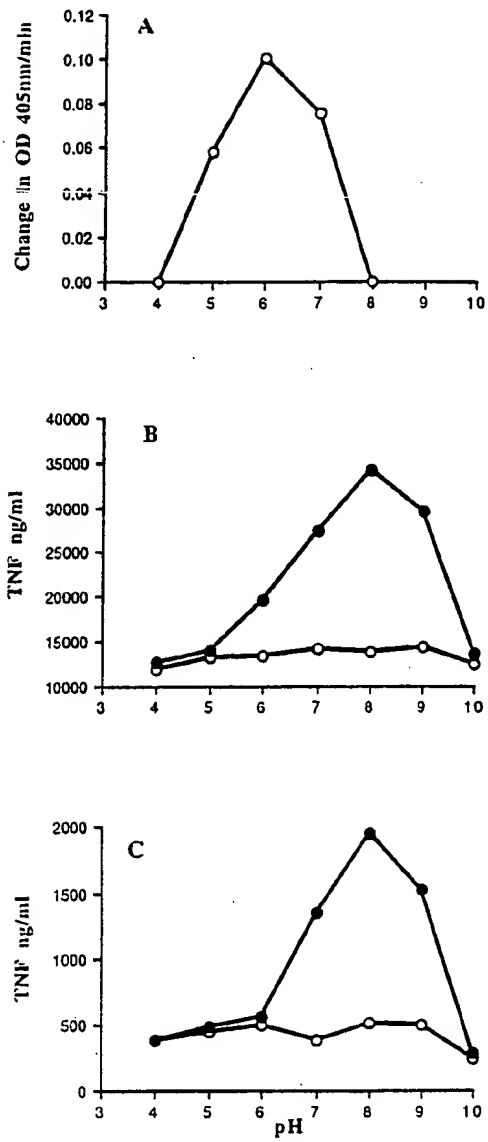

FIG. 3. Enhancement of TNF-inducing activity of malaria toxin and of LPS at different pHs compared with specific α-galactosidase activity. OD, optical density. Results from one of two experiments are shown. (A) Rate of reaction of 0.04 U of α-galactosidase per ml at 37°C with αPNP-Gal as substrate as determined over the first 3 min. (B and C) Malaria toxin from *P. yoelii* diluted 1/10 (B) and 50 ng of LPS per ml (C) were incubated overnight at 37°C with 2 U of α-galactosidase per ml and then boiled and tested on macrophages for TNF induction, as assayed by ELISA. Means of duplicate experiments are shown. O, samples incubated in buffer only, boiled, and then adjusted to neutral pH in RPMI 1640 medium as pH controls; ●, samples incubated with enzyme.

against αPNP-Gal, batches from different sources enhanced TNF activity to different degrees (as illustrated in Fig. 2). TNF-enhancing capacity deteriorated with storage at 4°C, although activity against the αPNP-Gal substrate did not. No differences were visible in a sodium dodecyl sulfate–10% polyacrylamide gel electrophoresis mini-gel system (Pharmacia, Uppsala, Sweden), with 4.5 μg of protein, between batches which did or did not enhance TNF activity. Apart from bovine serum albumin, all preparations contained three bands with sizes of 33, 29, and 27 kDa; 28- and 36.5-kDa isoforms were previously described (4). No β-galactosidase activity was detectable against βPNP-Gal at pH 6.0, nor did 0.8 U of β-galactosidase (Sigma, grade X from *E. coli*) per ml at any pH from 4 to 8 affect malaria toxin or LPS activity.

It is commonly found that not all exoglycosidase activities can be monitored with a PNP surrogate substrate. For example, while the α-(1,2)-, α-(1,3)-, and α-(1,6)-mannosidase activities of jack bean α-mannosidase can be assayed with PNP-mannoside, the α-(1,2)-mannosidase activity from *Aspergillus phoenicis* cannot, and only natural substrates can be used (10). This property is normally referred to as the aglycon specificity of an exoglycosidase. Further experiments are necessary to confirm that an α-galactosidase causes the enhancement.

The presence in parasitized erythrocytes of a soluble mediator which may have structural features homologous to the P-type IPG second messenger contrasts with the almost exclusive presence of A-type mediators from pathogenic mycobacteria (21). These mediators are pleiotropic and are released by a number of hormones and growth factors other than insulin (19). For example interleukin-2, adrenocorticotropin, insulin-like growth factor 1, epidermal growth factor, transforming growth factor β, and nerve growth factor all stimulate the hydrolysis of membrane-associated GPI and release IPG extracellularly. Clearly the existence of mediators in malaria which mimic those derived from mammalian tissue may lead to the elucidation of new parasitic pathogenic mechanisms.

This work was supported by grants from the Medical Research Council.

REFERENCES

1. **Bate, C. A. W., and D. Kwiatkowski.** 1994. A monoclonal antibody that recognizes phosphatidylinositol inhibits induction of tumor necrosis factor alpha by different strains of *Plasmodium falciparum*. Infect. Immun. 62:5261–5266.
2. **Bate, C. A. W., J. Taverne, and J. H. L. Playfair.** 1992. Detoxified exoantigens and phosphatidylinositol derivatives inhibit tumor necrosis factor induction by malarial exoantigens. Infect. Immun. 60:1894–1901.
3. **Bate, C. A. W., J. Taverne, E. Román, C. Moreno, and J. H. L. Playfair.** 1992. TNF induction by malaria exoantigens depends upon phospholipid. Immunology 75:129–135.
4. **Carchon, H., and C. K. D. de Bruyne.** 1975. Purification and properties of coffee-bean α-D-galactosidase. Carbohydr. Res. 41:175–189.
5. **de Groote, D., Y. Gevaert, M. Lopez, R. Gathy, F. Fauchet, I. Dehart, M. Jadoul, D. Radoux, and P. Franchimont.** 1993. Novel method for the measurement of cytokine production by a one-stage procedure. J. Immunol. Methods 163:259–267.
6. **Elased, K., and J. H. L. Playfair.** 1994. Hypoglycemia and hyperinsulinemia in rodent models of severe malaria infection. Infect. Immun. 62:5157–5160.
7. **Gaulton, G. N., and J. C. Pratt.** 1994. Glycosylated phosphatidylinositol molecules as second messenger. Semin. Immunol. 6:97–107.
8. **Grau, G. E., T. E. Taylor, M. E. Molyneux, J. J. Wirima, P. Vassalli, M. Hommel, and P.-H. Lambert.** 1989. Tumor necrosis factor and disease severity in children with falciparum malaria. N. Engl. J. Med. 320:1586–1591.
9. **Haibach, F., J. Hata, M. Mitra, M. Dhar, M. Harmata, P. Sun, and D. Smith.** 1991. Purification and characterization of a *Coffea canephora* α-D-galactosidase isozyme. Biochem. Biophys. Res. Commun. 181:1564–1571.
10. **Ichishima, E., M. Arai, Y. Shigematsu, H. Kumagai, and R. Sumida-Tanaka.** 1981. Purification of an acidic alpha-D-mannosidase from *Aspergillus saitoi* and specific cleavage of 1,2-alpha-D-mannosidic linkage in yeast mannan. Biochim. Biophys. Acta 658:45–53.
11. **Jakobsen, P. H., C. A. W. Bate, J. Taverne, and J. H. L. Playfair.** 1995. Malaria: toxins, cytokines and disease. Parasite Immunol. 17:223–231.
12. **Jakobsen, P. H., T. G. Theander, J. B. Jensen, K. Mølbak, and S. Jepsen.** 1987. Soluble *Plasmodium falciparum* antigens contain carbohydrate moieties important for immune reactivity. J. Clin. Microbiol. 25:2075–2079.
13. **Kern, P., C. J. Hemmer, J. van Damme, H.-J. Gruss, and M. Dietrich.** 1989. Elevated tumor necrosis factor α and interleukin-6 serum levels as markers for complicated *Plasmodium falciparum* malaria. Am. J. Med. 57:139–143.
14. **Kunjara, S., H. N. Caro, P. McLean, and T. W. Rademacher.** 1995. Tissue specific release of inositol phosphoglycans, p. 301–306. *In* J. Svasti et al. (ed.), Biopolymers and bioproducts: structure, function and applications. Dokya Publishing Co., Ltd., Bangkok, Thailand.
15. **Kwiatkowski, D., A. V. S. Hill, I. Sambou, P. Twumasi, J. Castracane, K. R. Manogue, A. Cerami, D. R. Brewster, and B. M. Greenwood.** 1990. TNF

concentration in fatal cerebral, non-fatal cerebral, and uncomplicated *Plasmodium falciparum* malaria. Lancet 336:1201–1204.
16. **McConville, M. J., and M. A. J. Ferguson.** 1993. The structure, biosynthesis and function of glycosylated phosphatidylinositols in the parasitic protozoa and higher eukaryotes. Biochem. J. 294:305–324.
17. **Nestler, J. E., G. Romero, L. C. Huang, C. G. Zhang, and J. Larner.** 1991. Insulin mediators are the signal transduction system responsible for insulin's actions on human placental steroidogenesis. Endocrinology 129:2951–2956.
18. **Pandiella, A., L. Beguinot, T. J. Velu, and J. Meldolesi.** 1988. Transmembrane signalling at epidermal growth factor receptors overexpressed in NIH 3T3 cells. Phosphoinositide hydrolysis, cytosolic Ca2+ increase and alkalinization correlate with epidermal-growth-factor-induced cell proliferation. Biochem. J. 294:223–228.
19. **Rademacher, T. W., H. Caro, S. Kunjara, D. Y. Wang, A. L. Greenbaum, and P. McLean.** 1994. Inositolphosphoglycan second messengers. Braz. J. Med. Biol. Res. 27:327–341.
20. **Raetz, C. R. H.** 1990. Biochemistry of endotoxins. Annu. Rev. Biochem. 59:129–170.
21. **Rook, G. A. W., H. N. Caro, E. Filley, S. Kunjara, and T. W. Rademacher.** *Mycobacterium vaccae* and *Mycobacterium tuberculosis* contain compounds that mimic the action of insulin second messengers derived from mammalian tissues. J. Biol. Chem., in press.
22. **Schofield, L., and F. Hackett.** 1993. Signal transduction in host cells by a glycosylphosphatidylinositol toxin of malaria parasites. J. Exp. Med. 177: 145–153.
23. **Taverne, J., C. A. W. Bate, D. Kwiatkowski, P. H. Jakobsen, and J. H. L. Playfair.** 1990. Two soluble antigens of *Plasmodium falciparum* induce tumor necrosis factor release from macrophages. Infect. Immun. 58:2923–2928.
24. **Taverne, J., N. Sheikh, J. B. de Souza, J. H. L. Playfair, L. Probert, and G. Kollias.** 1994. Anaemia and resistance to malaria in transgenic mice expressing human tumour necrosis factor. Immunology 82:397–403.
25. **Taylor, K., C. A. W. Bate, R. E. Carr, G. A. Butcher, J. Taverne, and J. H. L. Playfair.** 1992. Phospholipid-containing toxic malaria antigens induce hypoglycaemia. Clin. Exp. Immunol. 90:1–5.
26. **Taylor, K., R. E. Carr, J. H. L. Playfair, and E. D. Saggerson.** 1992. Malarial toxic antigens synergistically enhance insulin signalling. FEBS 311:231–234.
27. **Thomas, J. R., R. A. Dwek, and T. W. Rademacher.** 1990. Structure, biosynthesis, and function of glycosylphosphatidylinositols. Biochemistry 29:5413–5422.

Editor: S. H. E. Kaufmann

STIC-ILL R850.J3

From: Holleran, Anne
Sent: Monday, January 20, 2003 11:57 AM
To: STIC-ILL
Subject: refs. for 09/868,968

Please send copies of the following papers:

1.	Hoyoku,	Anticancer Res. (1999) 19(5A): 3663-3664
2.	Chamson-Reig	Endocrinology (1999) 140(8): 3573-3580
3.	Lixin,	J. Medicinal Chemistry 91998) 41(18): 3303-3306
4.	Yorek,	American J. Physiology (1998) 274(1, part1): C58-C71
5.	Nazih-Sanderson	Biochimica et Biophysica Acta (1997) 1346(1): 45-60
6.	Wattenberg	Cancer Research (1996) 56(22): 5132-5135
7.	Caro	Infection and Immunity (1996) 64(8): 3438-3441
8.	Seymour	Laboratory Investigation (1996) 75(3): 427-437
9.	Brunn	Cancer Chemotherapy (1994) 35(1): 71-79
10.	Kopp	Cancer Research (1990) 50(20): 6490-6496
11.	Tanino	Japanese J. Experimental Medicine (1972) 42(6): 575-582
12.	Eagle	Biochmistry (1963) 2(5): 1125-1126
13.	Caro	Biochem. Mol. Med. (1997) 61: 214-228

Anne Holleran
AU: 1642
Tel: 308-8892
RM: 8e03

mailbox: 8e12

[Japan. J. Exp. Med.
Vol. 42, 6, p. 575-582, 1972]

Studies on Tumor-Host Relationship

V. Effect of *myo*-Inositol on Tumor Cell Gr wth *in Vivo* and on the Resistant Activity of the Host

Takae TANINO, Koyu NARUMI and Toru TSUMITA

Department of Cell Chemistry, Institute of Medical Science, University of Tokyo
P.O. Takanawa, Tokyo 108, Japan

(Received for Publication, September 5, 1972)

Summary: In a syngenic mouse ascites tumor system: C3H/He mouse and mammary carcinoma cells (MM2), intraperitoneal injections of *myo*-inositol enhanced the growth of tumor cells. The tumor-bearing mice died in a shorter period than non-treated mice. The number of tumor cells increased 50% more and the mitotic tumor cells were found in 2.5 to 3 times more frequent than those of non-treated case. Survival rate of the mice after removal of tumor cells was lower than that of control mice. The titer of tumor cell growth inhibition activity of the serum and of the spleen cells decreased significantly.

It was demonstrated that *myo*-inositol affected cellular and humoral regulation process in tumor-bearing animals.

Introduction

myo-Inositol has been found in animal tissues as an important constituent of phospholipids and as a free form [1–5]. Phosphoinositides account for nearly all the combined inositol in the cell and are ubiquitous in the cell membrane system. As for free *myo*-inositol, it was at one time classified as an essential growth factor of the Vitamin B complex. However, there is as yet little evidence that free *myo*-inositol in the cell acts as coenzymes. Physiological significance of the free *myo*-inositol in animal tissues seems to be remained obscure, except the importance of the metabolic pool to be incorporated into the inositol lipids.

In the series of studies on the tumor-host relationship, we demonstrated that, when mouse ascites tumor cells were removed from the host in the late tumor-bearing period in a syngenic MM2-C3H/He mouse system, the treated mice survived for a long period afterwards without symptoms of tumor relapse [6]. In the serum of these survival mice, growth inhibition factor [7, 8] against MM2 cells and agglutination factor [9] were demonstrated and partly purified for characterization.

In this paper, it will be reported that free *myo*-inositol administered into tumor-bearing mice not only enhanced the tumor cell growth but also modified the tumor-host relationship. With respect to the latter phenomenon, *myo*-inositol seemed to abolish the formation of the growth inhibition factor.

Materials and Methods

Animals: C3H/He mice maintained in the Institute of Medical Science, University of Tokyo were used throughout. Syngenicity with respect to transplantation immunity

谷野隆江，鳴海孝佑，積田　亨（東京大学医科学研究所細胞化学研究部）

was cheked by skin graft.

Tumor cells: MM2 cells, transplantable ascites tumor cells derived from spontaneous mammary carcinoma of C3H/He mice were used [10].

Titration of resistant activity of mouse serum: The method was reported in detail previously [7]. The outline is as follows. A test serum was diluted stepwise with Krebs-Ringer-phosphate buffer at pH 7.4, and to 0.4 ml of the solution 2×10^4 MM2 cells were added. After incubation at 37°C for 30 minutes, the cell suspension was injected intraperitoneally into a healthy C3H/He mouse. The maximum dilution of the serum enough to prevent the tumor growth was used as a titer of the resistant activity of the serum.

myo-Inositol solution: myo-Inositol was dissolved in physiological saline and sterilized at 115°C for 30 minutes. The solution was injected intraperitoneally into mice. Repeated injections of 10 mg of *myo*-inositol in 0.5 ml of saline seven times *i.p.* every other day into mice did not affect the body weight increase of the mice.

Results

Effect of myo-inositol on tumor cell growth.

C3H/He mice inoculated with 2×10^5 MM2 cells usually died in 2–3 weeks after the inoculation. However, by injections of *myo*-inositol the tumor-bearing animals died in a shorter period than that of the control mice without the treatments. As shown in Fig. 1, two mg of *myo*-inositol dissolved in 0.5 ml of saline was injected into tumor-bearing mice seven times every other day beginning from the second day after the transplantation. Within following 2 weeks 50% of animals died due to the tumor growth, but in the control group without *myo*-inositol injections the rate was only 10% in the same period. It seemed evident that *myo*-inositol injections during the tumor-bearing period affected the tumor-host relationship, resulted in causing early tumor death. The number of tumor cells in the peritoneal cavity was measured by separating tumor cells and ascites at various tumor-bearing period. The result is shown in Fig. 2. From animals received *i.p.* 2 mg

Fig. 1. Effect of *myo*-inositol on survival rate of tumor-bearing mice.

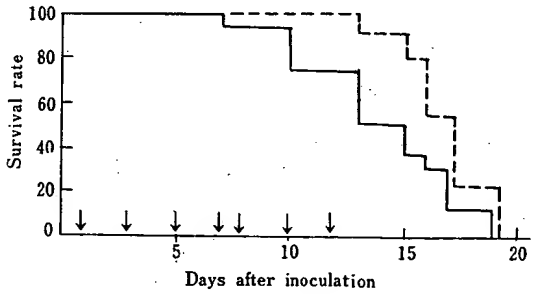

At 0 day, 2×10^5 MM2 cells were inoculated into C3H/He mice *i.p.* Survival rate represents percent of number of living mice to the total number of mice used. Arrows indicate *myo*-inositol injections, *i.p.*, 2 mg in 0.5 ml saline or 0.5 ml saline for the control. Solid line, *myo*-inositol-injected group; dotted line, saline-injected group.

Fig. 2. Increase of total number of tumor cells by *myo*-inositol treatment.

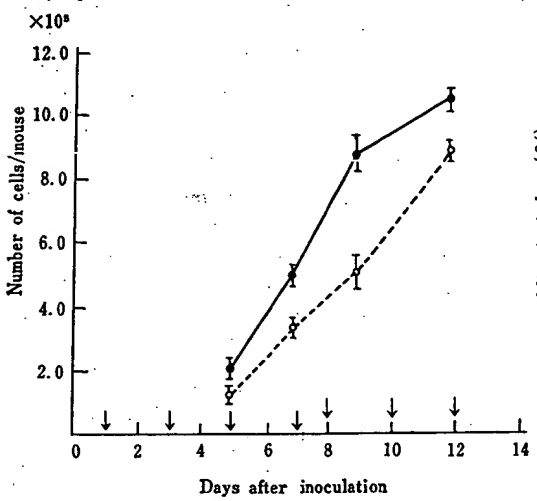

MM2 cells, 2×10^5 were inoculated into C3H/He mice *i.p.*, and at indicated day (arrow) 2 mg of *myo*-inositol in 0.5 ml saline was injected. Solid line *myo*-inositol-injected group; dotted line, saline-injected control group.

Fig. 3. Frequency of tumor cells in the mitosis in tumor-bearing mice treated with *myo*-inositol or D-mannitol.

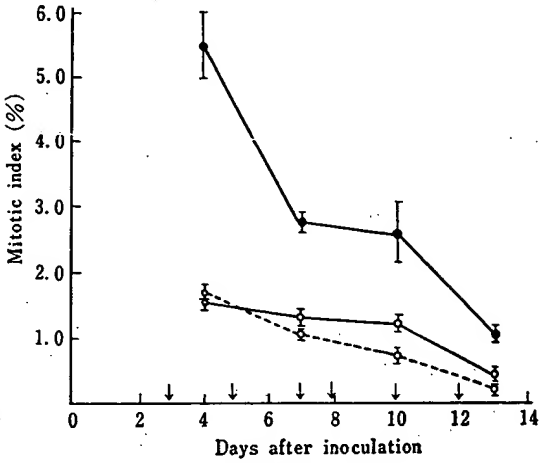

At 0 day 2×10^5 MM2 cells were inoculated *i.p.* into C3H/He mice and at indicated day (arrow) 2 mg of myo-inositol or D-mannitol dissolved in 0.5 ml saline was injected *i.p.*. Number of tumor cells of mitotic stage was counted from 1,000 cells on a smear stained with Wright's solution.

—●— *myo*-Inositol
—○— D-Mannitol
···○··· Saline.

of *myo*-inositol, the total tumor cell number was 20 to 50 percent more than that of non-treated mice. Within 9 days after the tumor transplantation, the difference of total cell number between treated and non-treated tumor-bearing mice was more predominant than that in the late period. The frequency of tumor cells of the mitotic stage was also found to be significantly higher in the tumor-bearing mice treated with *myo*-inositol than that of non-treated mice, as shown in Fig. 3.

Particularly, in the early tumor-bearing period, the mitotic index, percent of number of tumor cells in mitosis to the total cell number, was 5–6% with the treated mice, in contrast to 2% with non-treated animals. The high mitotic index of the treated group was kept throughout the whole tumor-bearing period. However, D-mannitol did not show such effect, but gave values similar to that of the saline control group. Therefore, it was considered that *myo*-inositol enhanced primarily the tumor cell division. The enhancement would result in the increase of tumor cell number in the tumor-bearing mice. The high death rate in the early tumor-bearing period was probably due in part at least to the growth promoting effect of *myo*-inositol.

The inositol injections into the tumor-bearing mice did not cause any morphological changes of tumor cells except more frequent occurrence of cells in the mitotic stage. However, extensive hemorrhages in the peritoneal cavity and adhesions of the tumor tissue in a solid form onto the mesenterium and omentum were observed in the mice which died in the early tumor-bearing period. With the non-treated group, the occurrence of the

adhesion of solid tumor tissues was found in 10% of the tumor-bearing animals, but with the inositol-treated group it was observed in 50% of mice. These results would suggest that *myo*-inositol was not only able to bring about the enhancement of tumor cell growth but also change the tumor-host relationship, resulted in the hemorrhage, infiltration of tumor cells into host tissues.

Decrease of survival rate by myo-inositol injection.

As reported previously, the tumor-bearing mice survived without relapse of tumor growth for a long period afterwards by a treatment of removing the tumor cells and ascites fluid at the late tumor-bearing period. During the studies on the mechanism, it was elucidated that sera of the survived mouse contained growth inhibition factor(s) and tumor cell agglutination factor(s). These factors were partly purified and characterized [8, 9]. The former designated as RFs was able to inhibit tumor cell growth *in vivo*. These facts indicated that the host mice produced RFs in the late tumor-bearing period and prevented the tumor relapse after the removal of tumor cells. From this viewpoint, effects of *myo*-inositol on the tumor-bearing mice were examined. At first, experiments were designed to determine whether *myo*-inositol affected the survival rate. C3H/He mice of various ages were inoculated with 2×10^5 MM2 cells and at the late tumor-bearing period (on the 13th day after the inoculation) tumor cells and ascites fluid were removed with a syringe as reported previously [6]. *myo*-Inositol was injected *i.p.* 7 times every other day after the inoculation. Table 1 shows the results. In the control group, which was inoculated with MM2 cells, injected 7 times with 0.5 ml of saline instead of *myo*-inositol solution, 60 to 79% of the total mice survived without any symptom of tumor re-growth. The rate was in accordance with those reported in the previous papers. However, the survival rates (20–30%) of the test group injected with *myo*-inositol, 2 mg or 10 mg, were considerably lower than those of the control group. Particularly, when mice of 8 weeks'

Table 1

Effect of *myo*-inositol on survival rate.

Age of mice (weeks)	Inositol dose (mg)	Tumor growth *	Survival rate (%)
8.0	2.0	8/9	11
8.0	0	3/8	62
8.0	2.0	8/10	20
8.0	0	3/10	70
16.0	10.0	7/10	30
16.0	0	4/10	60
19.0	2.0	10/15	33
19.0	10.0	9/15	27
19.0	0	3/14	79

MM2 cells 2×10^5 were transplanted into C3H/He mice of indicated ages and on the 13th day after the inoculation tumor cells and ascites fluid were withdrawn with a syringe. During the tumor-bearing periods, *myo*-inositol dissolved in 0.5 ml saline was injected *i.p.* 7 times on every other day. For the control group, 0.5 ml of saline was injected in the same way. After the removal of tumor cells, mice were under observation at least for 30 days to check tumor re-growth. The survival rate was figured out in percent of mice without tumor growth to the total mice used.

* A ratio of number of dead mice due to tumor growth to the total number of test mice.

age were employed, the survival rates were 11% in contrast to the control survival rate, 62%. With respect to the survival rate, both groups received *myo*-inositol 2 mg and 10 mg gave the same result and no difference was found. A trend was pointed out that the survival rates depended on mouse ages and mice of younger age gave lower rates than those of 17 weeks' age. In the test group, more than 50% of mice died within 2–3 days after the tumor cell removal. Hemorrhage in the peritoneal cavity and infiltration of tumor cells as solid tumor were also found.

Serum resistant activity of the survival mouse received myo-inositol.

The low survival rate of the test group suggested that the tumor-host relationship was modified by the *myo*-inositol injections. Therefore, RFs activity of mouse serum was assayed and the results are shown in TABLE 2. *myo*-Inositol was injected at a dose of 10 mg or 2 mg to the tumor-bearing mice. On the 7th day after the tumor removal, the mouse serum was prepared. The growth inhibition factor RFs was found in the control mice and the titer in the serum was 150, that is, 0.4 ml of 1: 150 diluted serum abolished completely the viability of 2×10^4 MM2 cells. On the other hand, the activity in the sera of inositol-injected group was only one third or none as compared with those of the control groups. These results indicated that inositol inhibited the formation of RFs of the host and consequently the activity of the sera was kept at a lower level than that of non-treated mice. It appeared that the low growth inhibition activity in the host mice was responsible in part at least, for the frequent relapse of tumor growth.

Cellular resistant activity of the survival mice received myo-inositol.

In addition to the humoral growth inhibition activity, cellular inhibition activity was demonstrated with spleen cells of the survival mice. Tumor cells lost the viability *in vivo* when the host mice had been injected with a definite number of spleen cells of the survival mouse [6].

To examine whether cellular activity was also affected by *myo*-inositol treatment, following experiment was carried out. Spleen cells were prepared from two sources: for a control, the spleen was excised from the survival mouse and free cells were prepared accord-

TABLE 2

Inhibition of *myo*-inositol on the titer of RFs of survival mouse serum.

Treatment		Tumor growth				
		Serum dilution				
Inositol (mg)	No. of injection, *i.p.*	×10	×20	×50	×150	RFs activity of serum
2	7		4/4		4/4	−
0	7		0/4		0/4	+
2	7	0/5		0/5	3/5	±
10	7	0/5		0/5	5/5	±
0	7			0/5	0/5	+
2	7	0/5		0/5	5/5	±
0	7			0/5	0/5	+

C3H/He mice were inoculated *i.p.* with 2×10^5 MM2 tumor cells and were injected *i.p.* with saline solution of *myo*-inositol 0.5 ml or saline alone on every other day. On the 13th day, tumor cells and ascites fluid were removed. Seven days after the removal, sera were prepared from all mice and pooled for the assay of RFs activity. The method of titration of RFs activity is descibed in MATERIALS AND METHODS.

TABLE 3

Effect of *myo*-inositol on growth-inhibition activity of spleen cells prepared from survival mice.

Donor		Recipient	Results
Treatment*	No. of spleen cells injected into recipient mice	Tumor growth**	Growth inhibition activity of spleen cells
myo-inositol 2 mg×7	1×10^8	4/4	−
	0.8×10^8	8/10	−
Saline 0.5 ml×7	1×10^8	0/4	+
	0.8×10^8	0/8	+

Spleen tissues were excised from survival C3H/He mice treated with *myo*-inositol as described in TABLE 2. The spleen cells were injected *i.p.* into recipient C3H/He mice, which were challenged with 2×10^5 MM2 cells 24 hours later. For the following 30 days, the recipient mice were observed with respect to tumor growth. In detail see the text.

TABLE 4

Effective dose and number of injections of *myo*-inositol to decrease survival rate.

Age of mice (weeks)	*myo*-Inositol injection			Tumor growth	Survival rate (%)*
	Dose (mg)	No. of injection	Period days after inoculation		
8.5	10	1	0	7/15	53 (92)
9.5	2	5	0–7	15/16	6 (79)
9.5	2	4	9–12	9/11	18 (79)
				12/15	20 (92)

Indicated amount of *myo*-inositol was dissolved in 0.5 ml of saline and was injected into the tumorbearing C3H/He mice, *i.p.*

* Number in parenthesis indicates the rate of control group received 0.5 ml of saline, *i.p.*, during the same period.

ing to the method reported previously. For the test group, spleen cells were obtained from survived C3H/He mice, those were injected 7 times with 0.5 ml of *myo*-inositol solution (2 mg).

These two kinds of spleen cells were injected *i.p.* into healthy mice at a dose of $0.8–1.0\times10^8$ cells per mouse. After 24 hours, challenge inoculation was made by transplanting 5×10^5 MM2 cells intraperitoneally. The results are shown in TABLE 3. Mice of control groups did not show tumor growth as expected from the previous paper and all animals survived. However, animals of test groups pre-treated with spleen cells of inositol-treated mice died due to the tumor growth. It was evident, therefore, that spleen cells of the inositol-treated mice had no activity to make the host resistant to the tumor growth. As far as these results were concerned, the *myo*-inositol treatment prevented not only formation of the humoral factor RFs but also of cellular factor which were able to make the host reject tumor cells.

Effective dose and period of inositol injections for the decrease of survival rate.

In the above experiments, inositol was injected on every other day during the tumor-bearing period. TABLE 4 summarized the effect of *myo*-inositol administered on three

different stages of the tumor-bearing period: a single injection at the same time with tumor cell inoculation, repeated injections either within 7 days after the inoculation or in the late period [7–13 days]. The decrease of the survival rate was most distinctly found in the case of the repeated administration in the first one week after the inoculation. By the treatment in the late period, the decrease was also evident but was a slightly lower than the above case. However, a single dose of *myo*-inositol, 10 mg did not gave a comparable grade of decrease of the survival rate to that of the repeated injections. It seemed indicating that continuous administration was required to modify the tumor-host relationship.

Taking into consideration that survival rates of control groups varied by experiment in a range from 50% to 100%, the value (53%) due to a single dose was to be read as a result of no effect of the treatment.

Discussion

The results presented here in the above section, indicate that *myo*-inositol influences the tumor-host relationship. The effects will be considered from both sides, tumor cell and host. The first point is the enhancement of tumor cell growth and cell division by the inositol administration. In fact, the number of tumor cells and the mitotic index were significantly higher in the treated group than in the control. The growth promoting activity of *myo*-inositol (10^{-5}–10^{-6} M) was reported with cultured cells [11, 12]. The relation between *myo*-inositol and the spindle formation in the mitosis was also described by Chargaff *et al.* [13]. Therefore, it seems reasonable to consider that a very small part of injected *myo*-inositol (about 10 mg/mouse) accelerated the cell growth. However, the direct effect on the tumor cells could not explain the different response of the host against the tumor growth. The repeated injections of *myo*-inositol inhibited the formation of humoral growth inhibition factor RFs and abolished the same activity of spleen cells of the host. As reported previously, RFs was of macroglobulin nature and was fractionated in α- and β-globulin portions by electrophoresis [8]. RFs was not strictly specific to MM2 cells but was able to make non-viable several kinds of mouse tumor cells. It was adsorbed on the surface of the tumor cells. At present, RFs is regarded as tumor cell-binding protein produced by the host response to the tumor cell surface. Inhibition of RFs formation would take place under following conditions. A possibility is that inositol affects RFs-producing organs of the host and consequently no RFs activity appears in the survival mouse serum. An evidence, which will be reported separately, indicates that lymphoid organs of C3H/He mice are responsible for the formation of RFs [14]. It is not known yet whether *myo*-inositol inhibits the function of the lymphatic system.

It is also conceivable that inositol affects the tumor cell surface so as to minimize "heterogeneous" features. RFs is absorbed with MM2 cells but not with normal liver cells of C3H/He mice. It suggests that tumor cells have specific binding sites on the surface but normal cells do not. As pointed out by Warner [15, 16], *scyllo*-inositol, an isomer of *myo*-inositol has a similar structure to structural water in biological system. He suggested that these cyclitols could be inserted into the structural water by replacement. Webb [17] reported that *myo*-inositol replaced the water requirement under dehydrating condition. Physical properties of *myo*-inositol seem to have a role on the modification of the heterogeneous surface structure of MM2 cells, in other words, masking antigenic sites.

Recently, the authors reported a similar effect of *myo*-inositol on induction of experimental allergic encephalomyelitis (EAE). When EAE antigen was incubated with *myo*-inositol prior to sensitization of guinea pigs, the EAE-inducing activity decreased. In this case,

the effect of inositol was not effective when inositol and the antigen were administered independently into animals through different route [18].

The fact that myo-inositol showed some effect on the tumor-bearing host seems to be important to elucidate the biological significance of free inositol present in animal tissues.

Acknowledgement

The authors wish to express their gratitude to Professor emeritus Yukichi Kimura, University of Tokyo for the criticism and encouragements.

References

[1] **Platt, B. S.** and **Glock, G. E.:** *Biochem. J.*, **37,** 709 (1943).
[2] **Hartree, E. F.:** *Biochem. J.*, **66,** 131 (1957).
[3] **Dawson, R. M. C.** and **Freinkel, N.:** *Biochem. J.*, **78,** 606 (1961).
[4] **Narumi, K., Arita, M., Kitagawa, A., Kumazawa, A.** and **Tsumita, T.:** *Japan. J. Exp. Med.*, **39,** 399 (1969).
[5] **Narumi, K.** and **Tsumita, T.:** *Japan. J. Exp. Med.*, **39,** 409 (1969).
[6] **Kimura, Y.** and **Tanino, T.:** *Japan. J. Exp. Med.*, **36,** 371 (1966).
[7] **Tanino, T.:** *Japan. J. Exp. Med.*, **38,** 383 (1968).
[8] **Tanino, T.:** *Japan. J. Exp. Med.*, **38,** 393 (1968).
[9] **Tanino, T.** and **Tsumita, T.:** *Japan. J. Exp. Med.*, **42,** 401 (1972).
[10] **Yamamoto, T.:** Report of US-Japan Cooperation Program, Planning Meeting of Chemotherapy Screening (1964).
[11] **Eagle, H., Oyama, V. I., Levy, M.** and **Freeman, A.:** *J. Biol. Chem.*, **226,** 191 (1957).
[12] **Eagle, H., Oyama, V. I., Levy, M.** and **Freeman, A.:** *Science*, **123,** 845 (1956).
[13] **Murray, M. R., DeLam, H. H.** and **Chargaff, E.:** *Exp. Cell Res.*, **2,** 165 (1951).
[14] **Tanino, T.:** To be published in *Japan. J. Exp. Med.*, **43,** (1973).
[15] **Warner, D. T.:** *In* "Annual Report in Medical Science Chemistry, 1969" (C. K. Cain, ed.), Academic Press, N. Y., p. 256 (1970).
[16] **Warner, D. T.:** *Ann. N. Y. Acad. Sci.*, **125,** Art. 2, 605 (1965).
[17] **Webb, S. J.** and **Bhorjee:** *Canad. J. Biochem.*, **46,** 691 (1968).
[18] **Tsumita, T., Nagai, Y.** and **Saito, M.:** *Japan. J. Exp. Med.*, **42,** 587 (1972).

STIC-ILL RC261.A1 A68

From: Holleran, Anne
Sent: Monday, January 20, 2003 11:57 AM
To: STIC-ILL
Subject: refs. for 09/868,968

Please send copies of the following papers:

1.	Hoyoku,	Anticancer Res. (1999) 19(5A): 3663-3664
2.	Chamson-Reig	Endocrinology (1999) 140(8): 3573-3580
3.	Lixin,	J. Medicinal Chemistry 91998) 41(18): 3303-3306
4.	Yorek,	American J. Physiology (1998) 274(1, part1): C58-C71
5.	Nazih-Sanderson	Biochimica et Biophysica Acta (1997) 1346(1): 45-60
6.	Wattenberg	Cancer Research (1996) 56(22): 5132-5135
7.	Caro	Infection and Immunity (1996) 64(8): 3438-3441
8.	Seymour	Laboratory Investigation (1996) 75(3): 427-437
9.	Brunn	Cancer Chemotherapy (1994) 35(1): 71-79
10.	Kopp	Cancer Research (1990) 50(20): 6490-6496
11.	Tanino	Japanese J. Experimental Medicine (1972) 42(6): 575-582
12.	Eagle	Biochmistry (1963) 2(5): 1125-1126
13.	Caro	Biochem. Mol. Med. (1997) 61: 214-228

Anne Holleran
AU: 1642
Tel: 308-8892
RM: 8e03

mailbox: 8e12

ANTICANCER RESEARCH *19*: 3663-3664 (1999)

Suppression of Lung and Liver Carcinogenesis in Mice by Oral Administration of *Myo*-inositol

HOYOKU NISHINO[1], MICHIAKI MURAKOSHI[1,2], MITSUHARU MASUDA[1], HARUKUNI TOKUDA[1], YOSHIKO SATOMI[1], MARI ONOZUKA[1], SHINO YAMAGUCHI[1], PING BU[1], ATSUSHI TSURUTA[3], KAZUTO NOSAKA[4], MASAKI BABA[5] and NOBUO TAKASUKA[6]

[1]Department of Biochemistry, [3]Second Department of Surgery, and [4]Department of Chemistry, Kyoto Prefectural University of Medicine, Kawaramachi-Hirokoji, Kamigyo-ku, Kyoto 602-8566;
[2]Research Planning and Administration Department, Research and Development Headquarters, Lion Corporation, Hirai, Edogawa-ku, Tokyo 132-0035; and [5]Department of Natural Medicine and Phytochemistry, Meiji Pharmaceutical University, Nozawa, Setagaya-ku, Tokyo 154-0003; [6]Chemotherapy Division, National Cancer Center Research Institute, Tsukiji, Chuo-ku, Tokyo 104-0045, Japan

Abstract. *It has been reported that myo-inositol can inhibit carcinogenesis in various organs, such as the mammary gland, colon and lung. In the present study, at first, inhibitory effects of myo-inositol on lung carcinogenesis were confirmed. Then, the influence of myo-inositol on liver carcinogenesis in mice was investigated. In C3H/He male mice, the rate of spontaneous liver carcinogenesis is known to be high. Using this experimental model, the effects of oral administration of myo-inositol (added into the drinking water at the concentration of 1%) were assessed. Significant suppression of liver carcinogenesis was observed in mice treated with myo-inositol for 40 weeks. In the control group without myo-inositol administration, 88% of the animals developed liver tumors, whereas in the myo-inositol-supplemented group, the incidence of liver tumors was 38% ($p<0.05$). The average number of liver tumors per mouse was also decreased significantly by myo-inositol treatment; from 7.8 in the control group to 0.8 in the myo-inositol-supplemented group ($p<0.01$). Thus, myo-inositol may be useful for cancer chemoprevention in the liver, as well as the lung.*

The optimal way for dealing with the cancer problem may be prevention. Chemoprevention provides one means of obtaining this objective. In the present study, *myo*-inositol was assessed for its value for this purpose.

Studies of cancer prevention by *myo*-inositol have their origin in the work of Shamsuddin *et al.* First, they showed that inositol hexaphosphate (phytate) inhibits carcinogen-induced neoplasia in the colon and mammary gland. Then, they also found that *myo*-inositol inhibits tumor formation to a similar magnitude under the same conditions as phytate (1). They pointed out the possibility that dephosphorylated products are the actual inhibitors when phytate is given orally, since their studies showed phytate to be quickly absorbed from the stomach and upper small intestine and distributed as inositol monophosphate and *myo*-inositol.

Subsequently, myo-inositol was also shown to inhibit neoplasia in the lung and forestomach by Estensen and Wattenberg (2).

In the present study, the inhibitory effects of *myo*-inositol on pulmonary tumor formation were first confirmed. Then, the potential of *myo*-inositol was assessed to suppress liver tumorigenesis.

Correspondence to: Dr Hoyoku Nishino.

Key Words: Myo-inositol, chemoprevention, liver carcinogenesis.

Materials and Methods

Chemicals. Myo-inositol was obtained from Wako Pure Chemical Industries, Ltd., Osaka. 4-Nitroquinoline 1-oxide (4NQO) and glycerol were purchased from Nacalai Tesque Co., Kyoto.

Lung carcinogenesis experiment. The animals used were 6-week-old male ddY mice purchased from Shizuoka Laboratory Animal Center, Shizuoka. 4NQO was dissolved in a mixture of olive oil and cholesterol (20:1), and 0.3 mg/mouse was given by single s.c. injection on the first experimental day. A 10% solution of glycerol in water was given as tumor promoter from the beginning of experimental week 5 for 25 weeks. *Myo*-inositol (final concentration: 1%) was mixed in the drinking water during the promoting period. Mice were killed at experimental week 30 by cervical dislocation. At autopsy, the lungs were fixed *via* intratracheal instillation of 10% formaldehyde. After separation of each pulmonary lobe, the numbers of induced tumors were counted under a microscope.

Liver carcinogenesis experiment. Male C3H/He mice, which have a high incidence of spontaneous liver tumor development, were used. Eight-week-old mice were purchased from Shizuoka Laboratory Animal Center, Shizuoka. *Myo*-inositol (final concentration: 1%) was mixed in drinking water and given for 40 weeks. Mice were killed at experimental

0250-7005/99 $2.00+.40

Table I. *Effect of myo-inositol on two-stage lung carcinogenesis in ddY mice.*

Condition	(n)	Tumor-bearing mice (%)	Tumors per mouse
Control	(12)	92	4.9[a]
myo-Inositol (1%)	(12)	75	2.0[a]

[a]$p<0.05$.

Table II. *Effect of myo-inositol on spontaneous liver carcinogenesis in C3H/He male mice.*

Condition	(n)	Tumor-bearing mice (%)	Tumors per mouse
Control	(17)	88[a]	7.8[b]
myo-Inositol (1%)	(13)	38[a]	0.8[b]

[a]$p<0.05$, [b]$p<0.01$

week 40 by cervical dislocation, following which they were autopsied, and the numbers of liver tumors were counted.

Results

Suppression of lung carcinogenesis. As shown in Table I, oral administration of *myo*-inositol resulted in a decrease of the mean number of lung tumors per mouse, to about 41% of the value for the control group ($p<0.05$). *Myo*-inositol also showed a tendency toward decreasing the percentage of tumor-bearing mice, although the difference was not statistically significant. Histologically, most tumor nodules were so-called type II adenomas.

Suppression of liver carcinogenesis. As shown in Table II, oral administration of *myo*-inositol resulted in a decrease of the mean number of liver tumors per mouse, to about 10% of the number in the control group; *i.e.*, 7.8 in the control group without *myo*-inositol administration, and 0.8 in *myo*-inositol-supplemented group ($p<0.01$). *Myo*-inositol also decreased significantly the percentage of tumor-bearing mice; *i.e.*, in the control group, 88% mice developed liver tumors, whereas in the *myo*-inositol-supplemented group, the incidence of liver tumors was 38% ($p<0.05$).

Discussion

Phytate has a broad distribution in plant foods. It occurs in relatively large concentrations in crops, such as rice, and in beans and seeds. Phytate is converted in some part into *myo*-inositol in the stomach and intestine after oral intake. In addition, free form *myo*-inositol and lipid-bound *myo*-inositol also occur naturally. Thus, *myo*-inositol itself, besides phytate, seems to be warrant assessment of its benefit for human health more precisely.

Myo-inositol has been used clinically to minimize diabetic neuritis and cataract formation. It can be consumed at high dose levels without evidence of toxicity; the administration schedule employed entailed dose levels of several grams per day over long periods of time, and in none of these studies was toxicity encountered.

Myo-inositol has also been used in premature infants with respiratory distress syndrome since it modulates production of pulmorary surfactant.

The available information indicates that *myo*-inositol is a safe material. Since the feature of safety is a most important aspect in cancer prevention, *myo*-inositol seems to be suitable to use as a cancer chemopreventive agent. For example, *myo*-inositol may find application as an active principle in "functional foods" for cancer chemoprevention. (Functional foods means modulated foodstuffs which possess health promoting functions. Their development for cancer prevention is the most urgent.)

In the present study, the potency to suppress liver tumorigenesis was proven to be extremely high. Thus, *myo*-inositol may be valuable for cancer prevention in the liver as well as the colon, mammary gland and lung.

The mechanism of the anti-carcinogenic action of *myo*-inositol is not known yet. Its elucidation is essential before *myo*-inositol can be put into practical use.

Acknowledgements

We thank L. W. Wattenberg for advice and helpful comments. This work was supported in part by grants from the Ministry of Education, Science, Sports and Culture, the Ministry of Health and Welfare (The 2nd-term Comprehensive 10-year strategy for Cancer Control), the Program for Promotion of Basic Research Activities for Innovative Biosciences, the Program of Fundamental Studies in Health Sciences of the Organization for Pharmaceutical Safety and Research, SRF, and the Plant Science Research Foundation, Japan.

References

1 Vucenic I, Yang G-Y and Shamsuddin AM: Inositol hexaphosphate and inositol inhibit DMBA-induced rat mammary cancer. Carcinogenesis *16:* 1055-1058, 1995.

2 Estensen RD and Wattenberg LW: Studies of chemopreventive effects of myo-inositol on benz[α]pyrene-induced neoplasia of the lung and forestomach of female A/J mice. Carcinogenesis *14:* 1975-1977, 1993.

Received December 28, 1998
Accepted February 24, 1999

RC261·A1 C2
mic

STIC-ILL

From: Holleran, Anne
Sent: Monday, January 20, 2003 11:57 AM
To: STIC-ILL
Subject: refs. for 09/868,968

Please send copies of the following papers:

1.	Hoyoku,	Anticancer Res. (1999) 19(5A): 3663-3664
2.	Chamson-Reig	Endocrinology (1999) 140(8): 3573-3580
3.	Lixin,	J. Medicinal Chemistry 91998) 41(18): 3303-3306
4.	Yorek,	American J. Physiology (1998) 274(1, part1): C58-C71
5.	Nazih-Sanderson	Biochimica et Biophysica Acta (1997) 1346(1): 45-60
6.	Wattenberg	Cancer Research (1996) 56(22): 5132-5135
7.	Caro.	Infection and Immunity (1996) 64(8): 3438-3441
8.	Seymour	Laboratory Investigation (1996) 75(3): 427-437
9.	Brunn	Cancer Chemotherapy (1994) 35(1): 71-79
10.	Kopp	Cancer Research (1990) 50(20): 6490-6496
11.	Tanino	Japanese J. Experimental Medicine (1972) 42(6): 575-582
12.	Eagle	Biochmistry (1963) 2(5): 1125-1126
13.	Caro	Biochem. Mol. Med. (1997) 61: 214-228

Anne Holleran
AU: 1642
Tel: 308-8892
RM: 8e03

mailbox: 8e12

[CANCER RESEARCH 50, 6490–6496, October 15, 1990]

Suramin Alters Phosphoinositide Synthesis and Inhibits Growth Factor Receptor Binding in HT-29 Cells[1]

Reinhard Kopp[2] and Andreas Pfeiffer

Departments of Surgery and Internal Medicine II, Klinikum Grosshadern, University of Munich, West Germany

ABSTRACT

Initiation of cell growth frequently involves activation of growth factor receptor-coupled tyrosine kinases and stimulation of the phosphoinositide second messenger system. The antitrypanosomal and antifiliarial drug suramin has been shown to exert antiproliferative activities by inhibition of growth factor receptor binding. We therefore investigated the effect of suramin on epidermal growth factor receptor-binding characteristics and, additionally, searched for effects on basal or cholinergically stimulated phospholipid metabolism in HT-29 cells.

Suramin caused a dose-dependent and noncompetitive inhibition of ^{125}I-epidermal growth factor binding (concentration producing 50% inhibition, 44.2 μg/ml) but did not alter muscarinic receptor binding. Suramin did not affect the basal ^{32}P incorporation into phosphoinositides at concentrations of <200 μg/ml suramin. In contrast, the carbachol-stimulated enhancement of ^{32}P incorporation into phosphatidic acid, phosphatidylinositol, and polyphosphoinositides was reduced by 48–95% in the presence of 100 μg/ml suramin. Thus, phosphoinositide and diacylglycerol kinases involved in basal and receptor-stimulated phosphoinositide metabolism may be localized in different subcellular compartments, which can be dissociated by the use of suramin. Direct measurements of phosphatidylinositol kinase and diacylglycerol kinase activities showed a potent inhibition when treated with suramin. Suramin did not affect the stimulation of phospholipase C by carbachol, determined by release of [^{3}H]inositol phosphates in [^{3}H]myoinositol-prelabeled cells.

Our data indicate that suramin potently inhibits phosphoinositide resynthesis under stimulated conditions. Additionally, we confirm the inhibitory effects of suramin on epidermal growth factor receptor binding in a human intestinal cell line. The inhibitory effects of suramin on phospholipid metabolism may play a role in the antiproliferative actions of this drug.

INTRODUCTION

Regulation of proliferation seems to be mediated by two different signaling pathways (1). Binding of growth factors, such as EGF,[3] transforming growth factor α, insulin-like growth factor 1, or insulin, to specific receptors leads to activation of tyrosine-specific protein kinases, an intrinsic property of this receptor family (2). Other growth factors, such as PDGF, bombesin, or thrombin, additionally mediate their mitogenic signals by activating the phosphoinositide system. This results in a specific receptor-coupled hydrolysis of the membrane phospholipid PIP_2 into the metabolically active second messengers inositol trisphosphate and DAG (3, 4). Inositol trisphosphate and its metabolites cause an increase of intracellular calcium levels and a stimulation of calcium/calmodulin kinases. Diacylglycerol activates protein kinase C, a family of Ca^{2+}-sensitive and phospholipid-dependent isoenzymes, known to phosphorylate regulatory proteins and to elevate cytosolic pH levels (5, 6). Activation of protein kinase C by phorbol esters and elevation of intracellular calcium levels by calcium ionophores have been shown to be mitogenically active cofactors during the initiation of DNA synthesis (7–10).

HT-29 colon carcinoma cells have recently been shown to produce EGF/transforming growth factor α and insulin-like growth factor 1-like activities (11), indicating a possible autocrine proliferative effect of these growth factors. Whether other signal transduction pathways are involved during the transmission of mitogenic signals to the nucleus is presently unknown. Previous experiments in our laboratory demonstrated that the phosphoinositide system of HT-29 cells shows a rapid carbachol-induced stimulation of phosphatidylinositol metabolism via muscarinic M_3 receptors, as measured by an enhanced release of inositol phosphates (12).

The antitrypanosomal and antifiliarial drug suramin was reported to selectively dissociate growth factors (EGF, heparin-binding growth factor 2, PDGF, and TGF β) from their receptors and to produce antiproliferative effects in lymphocytes and fibroblasts (13–18). These effects were proposed to occur by inhibition of growth factor receptor binding, direct binding f suramin to the PDGF, modified interaction of growth factor receptor and autosecreted oncogene products, or inhibition f specific DNA polymerases. Reports available at present did not investigate a possible interference of suramin with the phosphoinositide system.

Therefore, we investigated the effect of suramin on EGF receptor binding and searched for a possible involvement of phosphoinositide metabolism in unstimulated and carbachol-treated cells.

We report that suramin inhibited ^{125}I-EGF binding to HT-29 colon carcinoma cells, causing a complete disappearance of the high affinity-binding site and a reduction of binding capacity of the low affinity site. Additionally, suramin potently inhibited phosphoinositide synthesis and generation of phosphatidic acid after cholinergic stimulation, most likely due to reduction of phosphoinositide and diacylglycerol kinase activities. Suramin did not affect the activation of phospholipase C when incubated with carbachol.

MATERIALS AND METHODS

Materials. All reagents were of analytical grade and purchased from Merck (Darmstadt, West Germany) unless indicated otherwise. *N*-(2-(hydroxymethyl)piperazine-*N'*-2-ethanesulfonic acid was from Serva (Heidelberg, West Germany). Dulbecco's modified Eagle's medium, HBSS, and fetal calf serum were from Gibco (Karlsruhe, West Germany). DE-52 was purchased from Whatman (Milestone, United Kingdom). Phosphatidylinositol and sn-1,2-diacylglycerol were from Sigma (Taufkirchen, West Germany). [^{3}H]NMS, [^{3}H]myoinositol, and [^{32}P]P_i were from Amersham Buchler (Dreieich, West Germany) and suramin (Germanin) from Bayer (Leverkusen, West Germany).

Received 12/13/89; accepted 7/2/90.

The costs of publication of this article were defrayed in part by the payment of page charges. This article must therefore be hereby marked *advertisement* in accordance with 18 U.S.C. Section 1734 solely to indicate this fact.

[1] This work was supported by the Wilhelm Sander-Stiftung (grant 86.018.1). Part of this study was presented at the Annual Meeting of the American Gastroenterological Society, Washington, DC, May 1989 (Gastroenterology, 1989, abstract).

[2] To whom requests for reprints should be addressed, at Chirurgische Klinik, Klinikum Grosshadern, Folab B VE01–320, Universität München, Marchioninistr. 15, 8000 München 70, West Germany.

[3] The abbreviations used are: EGF, epidermal growth factor; PA, phosphatidic acid; PI, phosphatidylinositol; PIP, phosphatidylinositol-4-phosphate; PIP_2, phosphatidylinositol-4,5-bisphosphate; HBSS, Hank's balanced salt solution; NMS, *N*-methylscopolamine; PDGF: platelet-derived growth factor; DAG, diacylglycerol; ED_{50}, 50% effective dose.

Cell Culture. Cells were obtained from the American Type Culture Collection (Rockville, MD), subcultured with 0.05% trypsin/1 mM EDTA in Dulbecco's modified Eagle's medium,, c ntaining 6% fetal calf serum, 1 mM pyruvic acid, 2 mM glutamine, 100 units/ml penicillin, 50 units/ml streptomycin, and 200 IU/ml nystatin in 75-cm^2 disposable tissue culture flasks in a humidified atmosphere of 5% CO_2/95% air. For the experiments, cells were seeded at a density of 2×10^5 cells in 24-well flat bottom tissue culture plates (Falcon, Heidelberg, West Germany) and grown until subconfluency ($0.7–1.0 \times 10^6$ cells/well).

Determination of Inositol Phosphate Accumulation. For measurements of inositol phosphate release, cells were preincubated with [^{3}H] myoinositol (2 μCi/ml) for 48 h, until complete isotopic equilibrium was achieved. Accumulation of inositol phosphates was measured in the presence of LiCl (10 mM), known to inhibit the degradation of inositol monophosphates (19). Cells were stimulated for 30 min and inositol phosphate release was determined as described previously (20) using the Dowex ion exchange technique (21). Inositol phosphate release was linear during incubations up to 30 min.

Phospholipid Turnover. For investigations of phospholipid turnover, cells were cultured in phosphate-free HBSS [containing 1 mM pyruvic acid, 2 mM glutamine, 20 mM *N*-(2-(hydroxymethyl)piperazine-*N'*-2-ethanesulfonic acid, and 3.7 g/liter $NaHCO_3$] for 60 min prior to the experiment and then incubated under nonequilibrium conditions in HBSS (PO_4-free) with [^{32}P]P_i (10 μCi/ml) and simultaneously with indicated substances at 36.5°C for 30–60 min in a shaking water bath. Incubations were terminated by aspirating the incubation medium, followed by two rapid washes with ice-cold HBSS and addition of ice-cold methanol. Cells were scraped off into polypropylene tubes and phospholipids were extracted as described before (20). Separation of lipids was performed by thin-layer chromatography according to the system described by Jolles *et al.* (22) after pretreatment of silica gel plates (Merck DC 60) with 50% ethanol, 1% potassium oxalate, and 2 mM EDTA (23). Phospholipids were stained with iodine vapor, exposed to autoradiography film (Amersham Hyperfilm) for 48–76 h, and identified by comigration with lipid standards (Sigma). Identity of separated phospholipids was controlled by means of two-dimensional thin-layer chromatography, using the above described solvent in the first dimension and $CHCl_3/CH_3OH/NH_4OH$ (45/35/10, v/v/v) in the second dimension.

PI and DAG Kinase Activity. PI kinase activity was determined according to the method described by Tuazon and Traugh (24). Briefly, cells were sonicated (3 × 30 s) in buffer A containing 20 mM Tris-HCl, 1 mM EDTA, 1 mM ethyleneglycol bis(β-aminoethyl ether)-*N,N,N',N'*-tetraacetic acid, 10 mM 2-mercaptoethanol, 10 μM cyclic AMP, and 0.15% Triton X-100 (pH 7.5). PI and DAG kinases were partially purified by DEAE chromatography (DE 52, 200-μl packed volume) in microtubes, and kinases were eluted with buffer A containing 300 mM NaCl (500 μl). PI and DAG, used as substrates, were stored in chloroform solutions, dried under an N_2 stream, redissolved in ethanol (final 0.1%) and buffer B (40 mM Tris-HCl, 0.375% Triton X-100, 75 mM 2-mercaptoethanol, and 0.25 mM sodium vanadate), and sonicated. The assay was performed at 30°C in a volume of 50 μl and started by the addition of $MgCl_2$ and [γ-^{32}P]ATP [final assay concentrations: 20 mM Tris-HCl, 10 mM $CaCl_2$, 0.1 mM sodium vanadate, 30 mM 2-mercaptoethanol, 0.15% Triton X-100, 0.20 mM [γ-^{32}P]ATP (specific activity, 100–200 cpm/pmol)]. The assay was stopped after 15 min with EDTA (final concentration, 20 mM) and nonradioactive ATP (final concentration, 7 mM). After the addition of 1 N HCl (200 μl), phospholipids were extracted with 400 μl of $CHCl_3$/MeOH (2/1, v/v) and the lower phase was transferred to new tubes. The lipid phase was reextracted with 400 μl $CHCl_3$. Pooled lipid phases were evaporated to dryness by N_2 and separation of phospholipids and determination of incorporated radioactivity was performed as described above.

Binding Studies. The cells were incubated in HBSS (0.5 ml) in the presence of ^{125}I-labeled EGF (specific activity, 80–150 μCi/μg) for 60 min at room temperature. Cells were then rinsed twice with cold HBSS and dissolved in 0.5 M NaOH, and specifically bound radioactivity was measured in a Beckman gamma counter. Similar results were obtained in experiments at 4°C, performed to prevent internalization of receptors. For determination of cholinergic receptors, cells were incubated with 0.25 nM [^{3}H]NMS (specific activity, 72 Ci/mmol) for 60 min in HBSS at room temperature. Total bound radioactivity was measured by liquid scintillation spectrophotometry. Specific receptor binding varied between 10 and 30% (5–10,000 cpm/well added) for EGF receptor binding and 3–5% (6,000 cpm/well added) for [^{3}H]NMS binding.

Murine EGF (Collaborative Research) was iodinated as described previously (25) and specific activity was estimated by the self-displacement technique (26).

Statistical Methods. Data are reported as means ± SE from three or more independent experiments. SEM was <10% if not indicated otherwise. For statistical calculations Student's *t* test for paired samples was used. The data were analyzed using the computerized nonlinear least-squares regression programs LIGAND and ALLFIT (26, 27).

RESULTS

Effect of Suramin on EGF Binding. The effect of suramin on EGF binding was assessed by means of radioreceptor assays with ^{125}I-labeled EGF. ^{125}I-EGF binding in untreated HT-29 cells was best fitted using a model of two binding sites, with a K_d high of 7.8 pM and a K_d low of 250 pM, corresponding to 1,400 and 35,000 binding sites/single cell. Scatchard analysis after pretreatment with 50 μg/ml suramin for 60 min revealed a complete disappearance of the high affinity-binding sites and

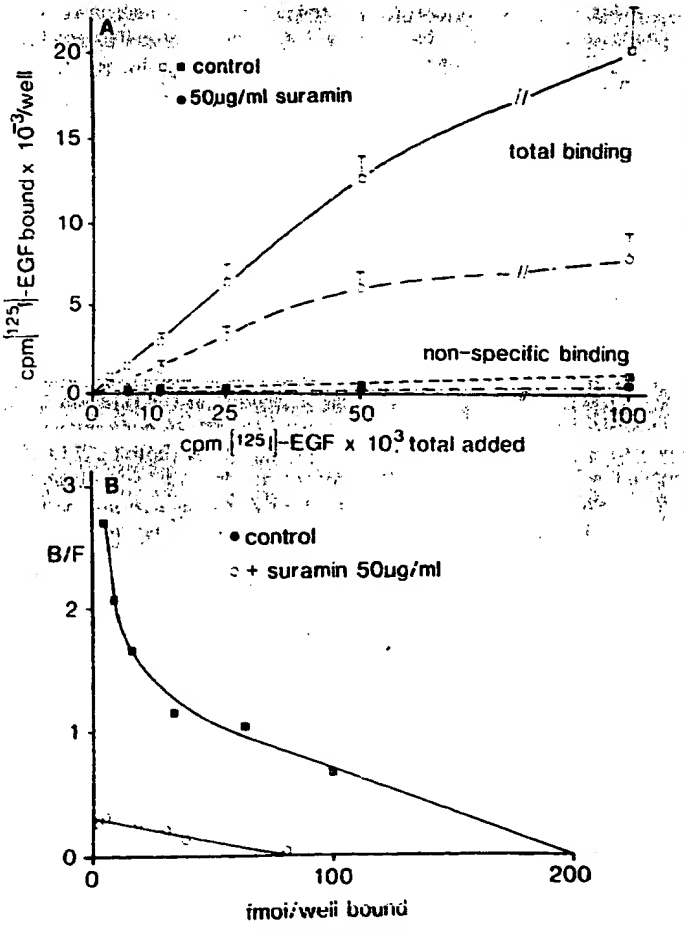

Fig. 1. Effect of suramin on ^{125}I-EGF binding. Cells were labeled with ^{125}I-EGF for 60 min at room temperature with or without suramin. ^{125}I-EGF was added 10 min prior to the addition of suramin. Data show cpm/well of totally bound ligand of one experiment performed in triplicate (*A*). Nonspecific binding was determined by adding unlabeled EGF (100 ng/ml) to the incubation medium. Two further experiments revealed identical results. *B*, data plotted according to Scatchard. Results were fitted with the LIGAND program (27).

a 54% reduction in receptor capacity from 106 fmol to 49 fmol/10^6 cells ($P < 0.01$), indicating a n ncompetitive mode of action (Fig. 1).

Investigation of EGF receptor binding in the presence of increasing concentrations of suramin showed a dose-dependent decrease of specifically bound ^{125}I-EGF with a concentration producing 50% inhibition of 44.2 ± 22.0 μg/ml suramin (Fig. 2). The effect of suramin on EGF receptor binding was >80% after an incubation time of <30 min and persisted during long-term treatment with suramin (100 μg/ml) for at least 24 h (not shown).

Effect of Suramin on Basal Phospholipid Metabolism. The receptor-activated breakdown of phospholipids is closely linked to the subsequent resynthesis of those phospholipids involved in the hydrolysis by phospholipase C. To investigate the effect of suramin on phospholipid metabolism in HT-29 cells, ^{32}P incorporation in untreated and cholinergically stimulated cells was determined.

Pretreatment of the cells with suramin for 60 min (Fig. 3) showed no changes in the basal ^{32}P labeling of phosphoinositides and phosphatidic acid at concentrations up to 200 μg/ml. At concentrations >200 μg/ml suramin caused a reproducible 1.5-fold increase in labeling of [^{32}P]phosphatidylinositol (ED_{50}, 307 ± 89 μg/ml), suggesting either an increased activity of specific kinases or an increase in the total amount of the lipid.

Effect of Suramin on Carbachol-activated Phospholipid Metabolism. To investigate the effect of suramin on stimulated phospholipid turnover, the cells were incubated with the cholinergic agonist carbachol (0.2 mM), either alone or in the presence of suramin. Carbachol significantly increased the incorporation (60-min incubation) of ^{32}P into phosphatidic acid (1.5-fold) and phosphatidylinositol (4.3-fold) (Fig. 4; Table 1). ^{32}P contents of PIP and PIP_2 were increased to a lesser extent (30–50%) after 60 min of cholinergic stimulation, since the metabolism f these phospholipids is very rapid. The turnover of other major lipids, such as phosphatidylcholine and phosphatidylethanolamine, was not markedly affected (Table 1).

In the presence of suramin (100 μg/ml, 60-min pretreatment) ^{32}P incorporation of phospholipids was significantly decreased into phosphatidylinositol (48% inhibition, $P < 0.01$), phosphatidic acid (90%, $P < 0.01$), phosphatidylinositol-4-phosphate

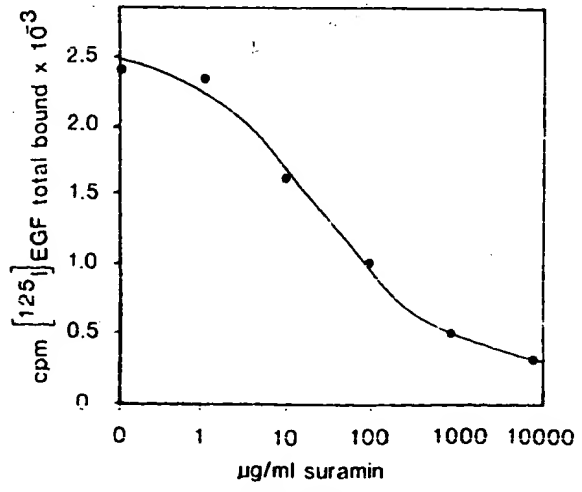

Fig. 2. Dose-response curve of ^{125}I-EGF binding to HT-29 cells in the presence of suramin. Data show means ± SEM of three independent experiments performed in triplicate. ^{125}I-EGF was added 10 min prior to the addition of various concentrations of suramin. The curve was analyzed with the ALLFIT program.

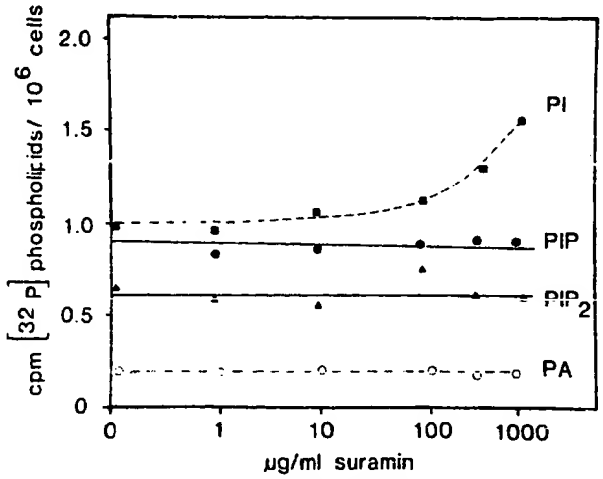

Fig. 3. Basal ^{32}P incorporation into phospholipids in the presence of suramin. Cells were incubated with phosphate-free HBSS (60 min) and various concentrations of suramin 2 min prior to the addition of 10 μCi/ml [^{32}P]P_i. After 60 min of incubation lipid extraction was performed as described in "Materials and Methods." Phospholipids were separated by thin-layer chromatography and exposed to autoradiography film, and radioactivity was determined by Cerenkov counting. Data show means ± SEM of three experiments, each performed in triplicate.

(95%, $P < 0.05$), and phosphatidylinositol-4,5-bisphosphate (95% inhibition, $P < 0.05$), during a 30-min incubation period, as shown in Fig. 5. These experiments indicated an effect of suramin on stimulated phosphoinositide synthesis. The inhibitory effects of suramin on carbachol-stimulated synthesis of PA, PI, PIP, and PIP_2 were constantly observed during time course experiments for up to 60 min. Suramin did not have major effects on ^{32}P labeling of phosphatidylcholine under basal conditions or in the presence of carbachol (data not shown).

Determination of PI Kinase and DAG Kinase Activities. The experiments performed with whole cells showed a potent reduction of ^{32}P incorporation into phosphoinositides and a decrease in phosphatidic acid synthesis. To get a more precise estimate of the target of suramin action we determined PI and DAG kinase activities. As shown in Fig. 6 suramin treatment potently inhibited both PI kinase and DAG kinase activities with half-maximal inhibitory effects achieved at concentrations of 14.2 ± 2.7 μg/ml (PI kinase) and 20.4 ± 5.7 μg/ml (DAG kinase). Furthermore, the addition of a crude preparation of PIP as substrate for PIP kinase indicated a similar inhibition of PIP kinase activity in the presence of suramin (95% inhibition using 200 μg/ml suramin) (not shown).

Effect of Suramin on Inositol Phosphate Accumulation. To assess effects on phospholipase C activity, cells were prelabeled with [^{3}H]myoinositol for 24 h and then stimulated with increasing concentrations of carbachol alone or in the presence of 500 μg/ml suramin. As shown in Fig. 7, incubations with suramin for 60 min and 24 h (not shown) did not affect cholinergically stimulated release of inositol phosphates [control: ED_{50}, 15 μM; suramin (500 μg/ml): ED_{50}, 17 μM], indicating that suramin did not alter receptor-activated hydrolysis of polyphosphoinositides by phospholipase C.

Estimation of Total Phospholipid Mass after Suramin Treatment. Suramin may cause changes in the total amount of phosphoinositides and thereby reduce stimulated metabolism due to a decrease in substrate. Therefore, we measured the incorporation of [^{3}H] myoinositol int ph sphoinositides after 48 h of labeling, when isotopic equilibrium was achieved. Separation of PI, PIP, and PIP_2 by thin-layer chromatography did

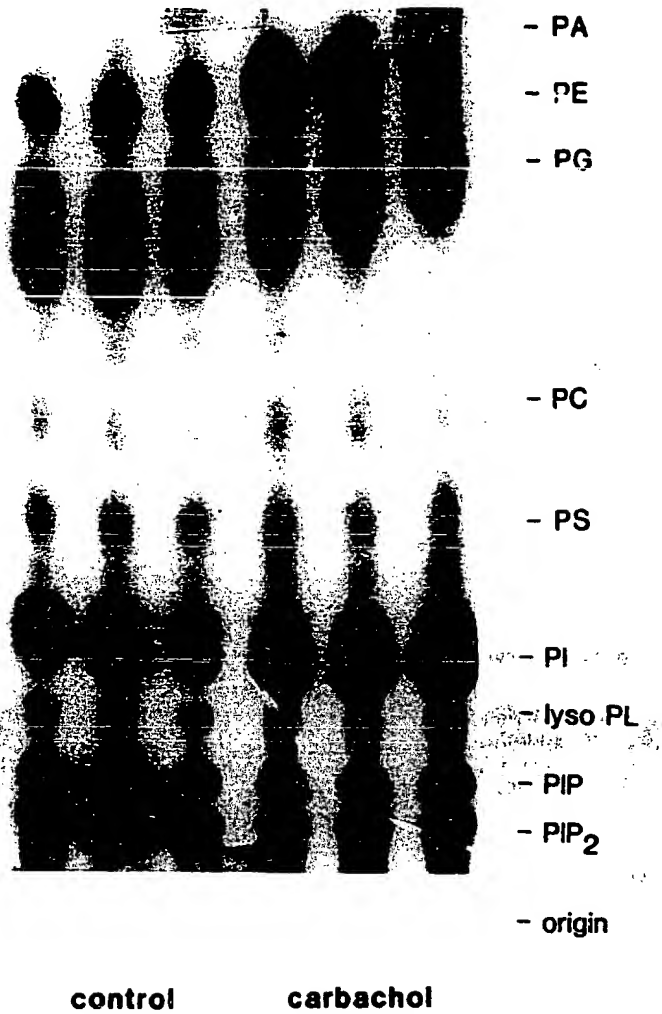

Fig. 4. [^{32}P]P_i incorporation into phospholipids. Autoradiography shows ^{32}P labeling of phospholipids into untreated HT-29 cells (control) and after incubation with carbachol (0.2 mM, 60 min). Phospholipids were extracted and separated as described in "Materials and Methods." Autoradiography films were exposed for 48 h at room temperature. RF values were as follows: PIP_2, 0.10; PIP, 0.15; PI, 0.31; phosphatidylcholine (PC), 0.51; phosphatidylglycerol (PG), 0.71; phosphatidylethanolamine (PE), 0.82; PA, 0.90.

n t reveal any significant change of the [^{3}H]inositol content of each investigated phospholipid (not shown), after incubations with suramin at concentrations up to 1 mg/ml, indicating that changes of stimulated phospholipid turnover seem to be more likely due to alterations of phospholipid kinase activities.

Binding t Muscarinic Receptors in the Presence of Suramin. Another possibility to explain the reduction f carbachol-stimulated phospholipid metabolism by suramin would be an interaction of the drug with muscarinic receptors n HT-29 cells. Results in Fig. 8 show that muscarinic receptor binding, as measured by incubations with [^{3}H]NMS, was not affected by suramin at concentrations up to 1.0 mg/ml, after an incubation time of 60 min or 24 h (not shown) and therefore did not account for the alterations of cholinergically stimulated phospholipid turnover.

DISCUSSION

The antiprotozoal drug suramin potently inhibited stimulated phosphoinositide metabolism in HT-29 cells most likely because of a direct interference with kinase activities involved in phospholipid synthesis. Suramin caused a dose-dependent inhibition of carbachol-stimulated phosphoinositide synthesis and generation of phosphatidic acid, without affecting phospholipase C activity or basal phosphoinositide metabolism at concentrations <200 μg/ml suramin. In addition, investigation of EGF receptor characteristic in the presence of suramin confirmed the previously reported inhibitory effect of suramin on growth factor receptor binding.

Since several reports have shown that initiation of cell growth involves activation of the phosphoinositide system (1, 28), our data indicate that antiproliferative effects of suramin could also be produced by changes in the phospholipid-dependent second messenger release and therefore may need a critical reevaluation. The known properties of suramin on growth factor receptor binding, its inhibitory activities on retroviral reverse transcriptase (17, 18), and the effects on phosphoinositide metabolism reported in this study may indicate a potential anticancer activity of this compound.

In HT-29 cells suramin showed a noncompetitive inhibition of ^{125}I-EGF binding, as indicated by Scatchard analysis. This is in agreement with the noncompetitive effects of suramin on DNA polymerases found in lymphoid cells (15) and inhibition of GTPase activities in neuroblastoma cells (29) but is in contrast to reports of Betsholtz *et al.* (30) and Williams *et al.* (31), who found a competitive inhibition of PDGF recept r binding and growth factor-induced mitogenic activity by suramin. The reported inhibitory effect on EGF binding seems to include tyrosine kinase-coupled receptors but, remarkably, did not affect muscarinic receptors, which belong to the family of the G-protein-coupled receptors, such as the β-adrenergic receptors and the rhodopsins.

Table 1 *Effect of carbachol (0.2 mM) on ^{32}P incorporation into phospholipids in HT-29 cells*

Results of ^{32}P labeling into phospholipids (60 min) of untreated and carbachol-stimulated HT-29 cells. ^{32}P incorporation was performed under nonequilibrium conditions. Lipids were extracted and separated as described in "Materials and Methods." Data represent two independent experiments, each performed in triplicate.

	Control (100%) (cpm ^{32}P incorporation)		Carbachol [cpm ^{32}P incorporation (%)]	
Phospholipid	Experiment 1	Experiment 2	Experiment 1	Experiment 2
Phosphatidic acid	682	823	1053	1201 (150)[a]
Phosphatidylinositol	955	955	4060	4296 (438)[a]
Phosphatidylinositol-4-phosphate	745	418	1013	734 (155)[b]
Phosphatidylinositol-4,5-bisphosphate	1346	466	1565	745 (138)
Phosphatidylethanolamine	416	328	443	365 (111)
Phosphatidylcholine	623	655	679	699 (108)

[a] $P < 0.01$.
[b] $P < 0.05$.

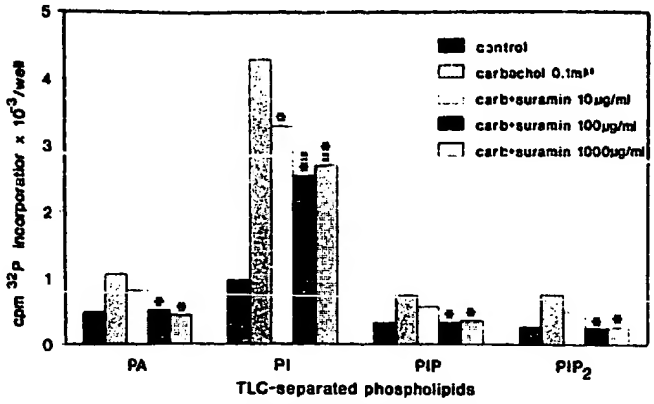

Fig. 5. Effect of suramin on carbachol-stimulated [^{32}P]phospholipid labeling. ^{32}P incorporation under nonequilibrium conditions was performed in unstimulated cells (control) and during incubation (30 min) of HT-29 cells with carbachol (carb) (0.1 mM), in the presence of indicated concentrations of suramin (0.1–1000 µg/ml). Data show results of three independent experiments, each performed in triplicate. *, $P < 0.05$; **, $P < 0.01$, as compared to carbachol-stimulated ^{32}P content of indicated phospholipids. TLC, thin-layer chromatography.

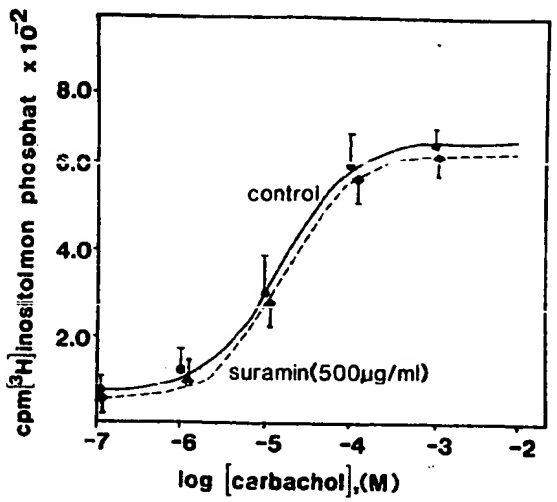

Fig. 7. Effect of suramin on inositol phosphate accumulation. Cells were stimulated with indicated concentrations of carbachol for 30 min, either alone or after pretreatment with suramin for 60 min (500 µg/ml). Results represent means ± SEM (*bars*) of three independent experiments performed in triplicate. A 24-h pretreatment with suramin gave similar results (data not shown).

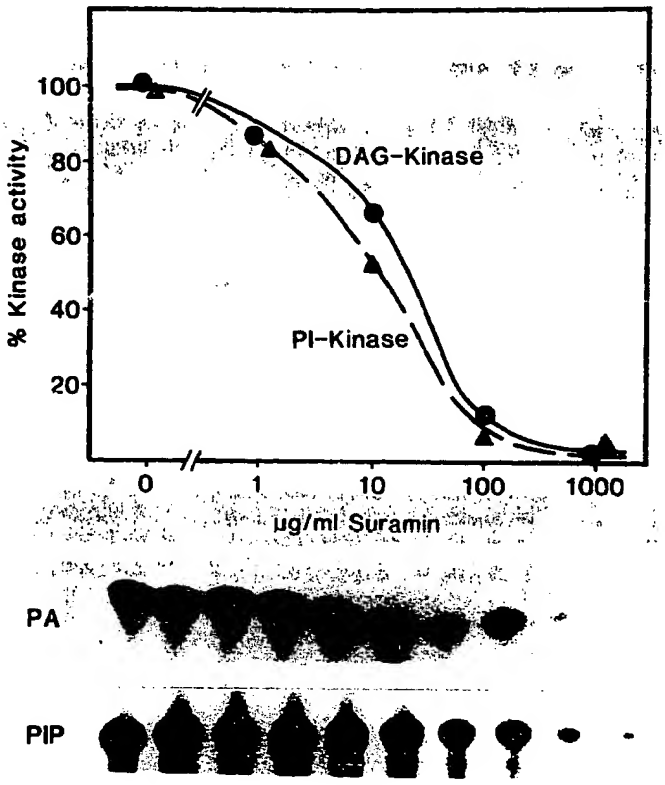

Fig. 6. Determination of PI and DAG kinase activity. PI and DAG kinase from whole cell homogenates were eluted from DEAE cellulose as described in "Materials and Methods." Phosphatidylinositol (200 µg/ml) and diacylglycerol (100 µg/ml) were used as substrates and ^{32}P incorporation in PIP and PA was measured. Phospholipids were extracted, separated by thin-layer chromatography, and exposed to autoradiography film. [^{32}P]phospholipids comigrating with commercial standards of PIP and PA were scraped into vials and radioactivity was determined by Cerenkov counting. Data show results (means ± SEM) of PI and DAG kinase activity in the presence of suramin from three independent experiments, each performed in duplicate. Autoradiographs show representative experiments demonstrating ^{32}P content in PIP and PA, representing PI and DAG kinase activity, respectively. Specific kinase activity of PIP and DAG kinase corresponds to 163 and 107 cpm/min/tube, respectively.

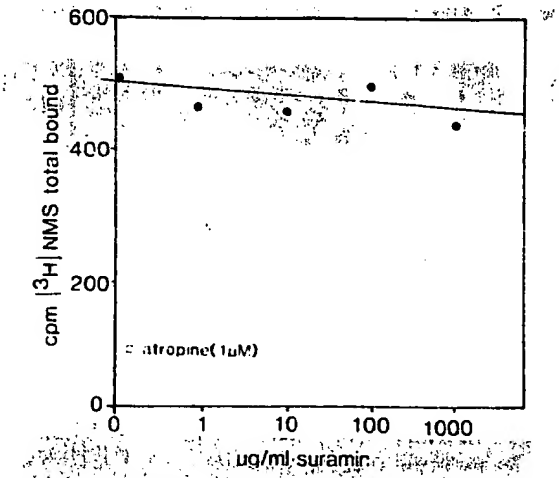

Fig. 8. Effect of suramin on muscarinic receptor binding. Data show muscarinic receptor binding on HT-29 cells by determination with [^{3}H]*N*-methylscopolamine (0.25 nM) in the presence of the indicated concentrations of suramin. Cells were pretreated with suramin 60 min prior to the addition of tritiated NMS. Results represent means of one typical experiment out of three, each performed in triplicate.

The reduction of ^{32}P incorporation by suramin into phosphatidylinositol, polyphosphoinositides, and phosphatidic acid was observed only in the presence of carbachol, indicating a reduced phospholipid synthesis under stimulated c nditions. Inositol phosphate release representing phospholipase C activity was not altered by suramin during a 30-min stimulation with carbachol. The fact that phospholipase C did not appear to be inhibited by suramin despite inhibition of resynthesis of phosphoinositides suggests that cellular pools of phosphoinositides were sufficient to serve as a substrate for phospholipase C-induced hydrolysis. However, under conditions of long-term stimulation, such as growth factor-induced cell proliferation, a permanently activated phosphoinositide metabolism should be dependent on active phospholipid kinase-mediated phosphoinositide resynthesis. Therefore, growth inhibitory effects of suramin may involve inhibition of phosphoinositide synthesis. In addition, previ us reports have indicated a proliferative potential f phosphatidic acid, depending n the content f unsaturated fatty acid residues (32). Since ur results show a potent inhibition of phosphatidic acid synthesis by an inhibition of diacylglycerol kinase, this effect may contribute t the antiproliferative effects of suramin.

Remarkably, suramin showed divergent effects on basal and stimulated phosphoinositide metabolism. These findings would support the hyp thesis that cells use different phospholipid pools or kinases for basal and receptor-activated phospholipid metabolism. This suggesti n would also explain our results, which indicate that incubation with suramin (0.1–1 mg/ml) for up to 24 h did not change phosphoinositides quantitatively and did not interfere with basal phosphoinositide turnover.

Suramin did not alter basal ^{32}P incorporation into phospholipids at lower concentrations, although carbachol-stimulated ^{32}P labeling was potently inhibited (Figs. 3 and 5). However, direct measurements of PI kinase and DAG kinase in cell homogenates showed a potent reduction of PI kinase and DAG kinase (Fig. 6). These results may lead to speculations that kinases involved in basal phospholipid metabolism might be localized in compartments not easily accessible for suramin by exogenous addition to the culture medium.

The ^{32}P labeling of unstimulated HT-29 cells in the presence f suramin resulted in an increase of [^{32}P]phosphatidylinositol at concentrations >200 μg/ml. However, the increase of basal phosphatidylinositol metabolism did not alter carbachol-activated phospholipase C activity. This may be expected due to a possible increase in substrate. The inhibition of carbachol-stimulated PI turnover, which was present already at 10 times lower concentrations of suramin (Fig. 6), was also observed at these high concentrations of 1 mg/ml suramin. This again may indicate a dissociation of basal and stimulated phosphoinositide synthesis. Furthermore, suramin inhibited carbachol-stimulated resynthesis of PI, while basal PI turnover was increased at higher concentrations of suramin. This might suggest additi nal effects of suramin on pathways related to phosphatidylinositol synthesis, which may involve PI synthase activity or the metabolism of CDP-diacylglycerol.

Several reports of the pathways involved in the resynthesis of phosphatidylinositol and phosphatidylglycerol in type II pneumocytes described a common CDP-diacylglycerol pool for the *de novo* synthesis of phosphatidylinositol in microsomal preparations (33, 34). In our experiments with HT-29 cells suramin potently reduced the ^{32}P labeling of a phospholipid comigrating with phosphatidylglycerol (concentration producing 50% inhibition, <50 μg/ml).[4] We speculate from these data that suramin may additionally inhibit the synthesis of phosphatidylglycerol, probably due to a decrease of CDP-diacylglycerol glycerol phosphate phosphatidyltransferase activity. This would explain the reported increase of basal phosphatidylinositol resynthesis, due to a predominant use of CDP-diacylglycerol pools for phosphatidylinositol formation. Furthermore, this may suggest a connective pathway between these two phospholipids during basal and stimulated phosphoinositide turnover and possibly indicates an auxiliary pathway for the resynthesis of phosphatidylinositol in intestinal cells. However, further experiments will be necessary to clearly demonstrate the effect of suramin on additional pathways involved in phosphatidylinositol synthesis.

Misset and Opperdoes (35) reported inhibition of various phosphoglycerol kinases in *Trypanosoma brucei* by suramin, suggesting that the inhibitory activity of the negatively charged compound suramin on phosphokinases may be related to its affinity to kinases with high isoelectric point values. Butler *et al.* (29) reported a noncompetitive interaction of suramin with a pertussis toxin-sensitive GTP-binding protein in neuronal cell membranes involved in opioid receptor function. Our findings d n t indicate that the reduction f stimulated phosphoinositide turnover by suramin is due to reduced GTPase activity in HT-29 cells, since carbachol-activated in sit l phosphate release was not affected. Changes in the labeling of cellular ATP pools after suramin treatment are unlikely to account f r the changes in [^{32}P]P_i incorporation, since suramin caused divergent effects on various phospholipids.

In A 431 cells, a cell line overexpressing EGF receptors, EGF was found to increase the phosphorylation of phosphoinositides, although results concerning the correlation between the activation of the phosphoinositide system and Ca^{2+} or Na^+/H^+ fluxes are controversial at present (36, 37). Since HT-29 cells were reported to produce EGF-like growth factors (11) suramin could reduce ^{32}P contents of phosphoinositides as a result f decreased autocrine stimulation of phosphoinositide metabolism. In this case suramin should show measurable effects n basal phosphoinositide metabolism. In contrast, our results indicate that suramin-induced changes of phosphoinositide metabolism were not due to a reduction of EGF receptor-mediated autocrine stimulation of phosphoinositide metabolism. Incubation of HT-29 cells with EGF at concentrations varying from 0.1 to 1000 ng/ml did not stimulate the phosphoinositide system as measured by inositol phosphate release or determination of ^{32}P incorporation into membrane phospholipids.[5]

Recent reports have shown inhibitory effects of suramin on protein kinase C activity (38). Since PI kinase is positively regulated by protein kinase C (39) and DAG kinase has been shown to be a protein kinase C substrate (40), suramin may interfere with mechanisms of phosphoinositide resynthesis mediated by protein kinase C.

In summary, we report remarkable effects of suramin on stimulated phosphoinositide metabolism, due to inhibition f PI kinase and DAG kinase activities. This indicates that effects of suramin on second messenger-related phospholipid metabolism need to be considered when suramin is used during investigation of growth factor-related metabolic pathways. Since development and proliferation of tumor cells may be related to increased metabolic activities of growth factor-dependent pathways, persistent retroviral replication, or altered phosphoinositide metabolism, the effects of suramin on phosphoinositide synthesis reported in this study may support the probable value of suramin as a potential anticancer drug.

ACKNOWLEDGMENTS

The authors wish to thank Professor G. Paumgartner for his continuous support.

REFERENCES

1. Berridge, M. J., Brown, K. D., Irvine, R. F., and Heslop, J. P. Phosphoinositides and cell proliferation. J. Cell. Sci., *3* (Suppl.): 187–198, 1985.
2. Ushiro, H., and Cohen, S. Identification of phosphotyrosine as a product of epidermal growth factor-activated proteinkinase in A-431 cell membranes. J. Biol. Chem., *255:* 8363–8365.
3. Berridge, M. J., and Irvine, R. F. Inositol trisphosphate, a novel second messenger in cellular signal transduction. Nature (London), *312:* 315–321, 1984.
4. Berridge, M. J. Inositoltrisphosphate and diacylglycerol: two interacting second messengers. Annu. Rev. Biochem., *56:* 159–193, 1987.
5. Nishizuka, Y. The role of protein kinase C in cell surface signal transduction and tumor promotion. Nature (London), *308:* 693–698, 1984.
6. Nishizuka, Y. Studies and perspectives of proteinkinase C. Science (Washington DC), *233:* 305–312, 1986.

[4] Unpublished results.

[5] Unpublished data.

7. Kaibuchi, K., Taki, Y., and Nishizuka, Y. Protein kinase C and calcium ion in mitogenic response of macrophage-depleted human peripheral lymphocytes. J. Biol. Chem., *260:* 1366–1369, 1985.
8. Graeme, R. G., Gordon, J., Michell, H. R., and Brown, G. Synergism between diacylglycerols and calcium ionophore in the induction of human B cell proliferation mimics the inositol lipid polyphosphate breakdown signals induced by cross linking surface immunglobulin. Biophys. Biochem. Res. Commun., *131:* 484–481, 1985.
9. Moolenaar, W. H., Tertoolen, L. G. J., and de Laat, S. W. Phorbol esters and diacylglycerol mimic growth factors in raising cytoplasmic pH. Nature (London), *312:* 371–374, 1984.
10. Rozengurt, E., Rodriguez-Pena, A., Coombs, M., and Sinnet-Smith, J. Diacylglycerol stimulates DNA-synthesis and cell division in mouse 3T3-cells: role of Ca^{2+}-sensitive phospholipid dependent protein kinase. Proc. Natl. Acad. Sci. USA, *81:* 5748–5752. 1984.
11. Culouscou, J. M., Remacle-Bonnet, M., Garrouste, F., Marvaldi, J., and Pommier, G. Simultaneous production of IGF-I and EGF competing growth factors by HT-29 human colon cancer line. Int. J. Cancer, *40:* 646–652, 1987.
12. Kopp, R., Lambrecht, G., Mutschler, E., Moser, U., Tacke, R., and Pfeiffer, A. HT-29 colon-carcinoma cells contain muscarinic M_3 receptors coupled to phosphoinositide metabolism. Eur. J. Pharmacol., *172:* 397–405, 1989.
13. Coffey, J. R., Leof, E. B., Shipley, G. D., and Moses, H. L. Suramin inhibition of growth factor receptor binding and mitogenity in AKR-2B cells. J Cell. Physiol., *132:* 143–148, 1987.
14. Hosang, M. Suramin binds to platelet derived growth factor and inhibits its biological activity. J. Cell. Biochem., *29:* 265–273, 1985.
15. Huang, S. S., and Huang, J. S. Rapid turnover of the platelet-derived growth factor receptor in sis-transformes cells and reversal by suramin. J. Biol. Chem., *263:* 12608–12618.
16. Spigelman, Z., Dowers, A., Kennedy, S., DiSorbo, D., O'Brien, M., Barr, R., and McCaffrey, R. Antiproliferative effects of suramin on lymphoid cells. Cancer Res., *47:* 4694–4698, 1987.
17. De Clercq, E. Suramin, a potent inhibitor of the reverse transcriptase of RNA tumor viruses. Cancer Lett., *8:* 9–22, 1979.
18. Rupprecht, R. M., Rossini, L. D., Haseltine, W. A., and Broder, S. Suppression of retroviral propagation and disease by suramin in murine systems. Proc. Natl. Acad. Sci. USA, *82:* 7733–7737, 1985.
19. Berridge, M. J., Downes, P., and Hanley, M. R. Lithium amplifies agonist dependent phosphatidylinositol response in brain and salivary glands. Biochem. J., *220:* 345–360, 1984.
20. Pfeiffer, A., Rochlitz, H., Herz A., and Paumgartner, G. Stimulation of acid secretion and phosphoinositol production by rat parietal cell muscarinic M_2 receptors. Am. J. Physiol., *254:* G622–629, 1988.
21. Downes, C. P., and Michell, R. H. The phosphoinositide phosphodiesterase of erythrocyte membranes. Biochem. J., *198:* 133–140, 1981.
22. Jolles, J., Zwiers, H., Dekker, A., Wirtz, K. W. A., and Gispen, W. H. Corticotropin-(1–24)-tetracosapeptide affects protein phosphorylation and polyphosphoinositide metabolism in rat brain. Biochem. J., *194:* 283–291, 1981.
23. Wilson, D. B., Neufeld, E. J., and Majerus, P. W. Phosphoinositide interconversion in thrombin-stimulated human platelets. J. Biol. Chem., *260:* 1046–1051, 1985.
24. Tuazon, P. T., and Traugh, J. A. Phosphatidylinositol kinases from rabbit reticulocytes. Methods Enzymol., *141:* 210–222, 1987.
25. Carpenter, G., and Cohen, S. ^{125}I-labeled human epidermal growth factor. J Cell. Biol., *71:* 159–171, 1979.
26. De Lean, A., Munson, P. J., and Rodbard, D. Simultanous analysis families of sigmoidal curves: application to bioassay. radioligand assay, and physiological dose-response curves. Am. J. Physiol., *235:* E97–102, 1978.
27. Munson, P. J., and Rodbard, D. LIGAND: a versatile computerized approach for characterization of ligand-binding systems. Anal. Biochem., *107:* 220–239, 1980.
28. Taylor, M. V., Metcalf, J. C., Hesketh, T. R., Smith, G. A., and Moore, J. P. Mitogens increase phosphorylation of phosphoinositides in thymocytes. Nature (London), *312:* 462–465, 1984.
29. Butier, S. J., Kelly, E. C., McKenzie, F. R., Guild, S. B. Wakelam, M. J. O., and Milligan, G. Differential effects of suramin on the coupling of receptors to individual species of pertussis-toxin-sensitive guanine-nucleotide-binding proteins. Biochem. J., *251:* 201–205, 1988.
30. Betsholtz, C., Johnsson, A., Heldin, C. H., and Westermark, B. Efficient reversion of simian sarcoma virus—transformation and inhibition of growth factor-induced mitogenesis by suramin. Proc. Natl. Acad. Sci. USA, *83:* 6440–6444, 1986.
31. Williams, L. T., Tremble, P., Lavin, M. F., and Sunday, M. E. Platelet-derived growth factor receptors form a high affinity state in membrane preparations. J. Biol. Chem., *259:* 5287–5294, 1984.
32. Moolenaar, W. H., Kruijer, W., Tilly, B. C., Verlaan, I., Bierman, A. J., and Laat, S. W. Growth factor-like action of phosphatidic acid. Nature (London), *323:* 171–173, 1987.
33. Post, M., and van Golde, L. M. G. Metabolic and developmental aspects of the pulmonary surfactant system. Biochem. Biophys. Acta, *947:* 249–286, 1988.
34. Rüstow, B., Nakagawa, Y., Rabe, H., Waku, K., and Kunze, D. Species pattern of phosphatidylinositol from lung surfactant and a comparison of the species pattern of phosphatidylinositol and phosphatidylglycerol synthesized *de novo* in lung microsomal fractions. Biochem. J., *254:* 67–71, 1988.
35. Misset, O., and Opperdoes, F. R. The phosphoglycerate kinases from *Trypanosoma bruzei*. A comparison of the glycosomal and cytosolic isoenzymes and their sensitivity towards suramin. Eur. J. Biochem., *162:* 493–500, 1987.
36. Macara, I. G. Activation of $^{45}Ca^{2+}$ influx and Na^+/H^+ exchange by epidermal growth factor and vanadate in A 431 cells is independent of phosphatidylinositol turnover and is inhibited by phorbolester and diacylglycerol. J. Biol. Chem., *261:* 9321–9327, 1986.
37. Pike, L. J., and Eakes, A. T. Epidermal growth factor stimulates the production of phosphatidylinositol monophosphate and the breakdown of polyphosphoinositides in A431 cells. J. Biol. Chem., *262:* 1644–1651, 1987.
38. Hensey, C. E., Boscoboinik, D., and Azzi, A. FEBS Lett., *258:* 156–158, 1989.
39. de Chaffoy de Courcelles, D., Roevens, P., and van Belle, H. FEBS Lett., *173:* 389–393, 1984.
40. Kanoh, H., Yamada, K., Sakane, F., and Imaizumi, T. Phosphorylation of diacylglycerol kinase *in vitro* by protein kinase C. Biochem. J., *258:* 455–462, 1989.

RC261.A1C2
Thiri

STIC-ILL

From: Holleran, Anne
Sent: Monday, January 20, 2003 11:57 AM
To: STIC-ILL
Subject: refs. for 09/868,968

Please send copies of the following papers:

1.	Hoyoku,	Anticancer Res. (1999) 19(5A): 3663-3664
2.	Chamson-Reig	Endocrinology (1999) 140(8): 3573-3580
3.	Lixin,	J. Medicinal Chemistry 91998) 41(18): 3303-3306
4.	Yorek,	American J. Physiology (1998) 274(1, part1): C58-C71
5.	Nazih-Sanderson	Biochimica et Biophysica Acta (1997) 1346(1): 45-60
6.	Wattenberg	Cancer Research (1996) 56(22): 5132-5135
7.	Caro	Infection and Immunity (1996) 64(8): 3438-3441
8.	Seymour	Laboratory Investigation (1996) 75(3): 427-437
9.	Brunn	Cancer Chemotherapy (1994) 35(1): 71-79
10.	Kopp	Cancer Research (1990) 50(20): 6490-6496
11.	Tanino	Japanese J. Experimental Medicine (1972) 42(6): 575-582
12.	Eagle	Biochmistry (1963) 2(5): 1125-1126
13.	Caro	Biochem. Mol. Med. (1997) 61: 214-228

Anne Holleran
AU: 1642
Tel: 308-8892
RM: 8e03

mailbox: 8e12

[CANCER RESEARCH 56, 5132–5135, November 15, 1996]

Advances in Brief

Chemopreventive Effects of *myo*-Inositol and Dexamethasone on Benzo[a]pyrene and 4-(Methylnitrosoamino)-1-(3-pyridyl)-1-butanone-induced Pulmonary Carcinogenesis in Female A/J Mice[1]

Lee W. Wattenberg[2] and Richard D. Estensen

Department of Laboratory Medicine and Pathology, University of Minnesota, Minneapolis, Minnesota 55455

Abstract

The objective of the present investigation was to prevent cancer of the lung by use of chemopreventive agents. Administrations of diets containing added *myo*-inositol or dexamethasone singly or in combination (the latter being the most potent) are being studied for this purpose. In previous work, the two compounds were shown to inhibit benzo(*a*)pyrene [B(*a*)P]-induced pulmonary adenoma formation in female A/J mice when fed during the postinitiation period [*i.e.*, starting 1 week after the last of three administrations of B(*a*)P by oral intubation]. In the present investigation, a longer administration schedule was used, which encompasses both the initiation and the postinitiation stages of carcinogenesis. The feeding of the test compounds was started 2 weeks prior to the first dose of carcinogen and continued for the duration of the experiment. Under these conditions, reductions in tumor formation were: *myo*-inositol, 64%; dexamethasone, 56%; and both together, 86% ($P < 0.001$ for all three). Addition of both compounds resulted in the largest inhibition that has been achieved with this experimental model as used in these investigations. Studies have begun of inhibition of 4-(methylnitrosamino)-1-(3-pyridyl)-1-butanone-induced pulmonary adenoma formation by *myo*-inositol and dexamethasone. The two compounds inhibit pulmonary carcinogenesis when fed singly or in combination. When fed throughout the entire protocol, reductions in tumor formation were: *myo*-inositol, 46%; dexamethasone, 41%; and both together, 71% ($P < 0.001$ for all three). The results of these investigations demonstrate that *myo*-inositol and dexamethasone inhibit pulmonary adenoma formation resulting from exposures to two major pulmonary carcinogens, B(*a*)P and 4-(methylnitrosamino)-1-(3-pyridyl)-1-butanone.

Introduction

The present investigation is part of a continuing effort to develop effective chemoprevention of carcinogenesis of the lungs. In previous studies, addition of *myo*-inositol and dexamethasone to the diet singly or in combination (the latter being the most potent) was found to reduce B(*a*)P[3]-induced pulmonary adenoma formation when the diet was fed during the postinitiation period (1). There is a great need for compounds that can inhibit pulmonary neoplasia when given during the postinitiation period of the carcinogenic process. Few chemopreventive agents have been shown to have this property (2, 3). The first demonstration of the chemopreventive effects of *myo*-inositol was in carcinogenesis of the large bowel. In this work, *myo*-inositol and inositol hexaphosphate (phytate) were both found to prevent carcinogen-induced neoplasia of this organ site when administered in the postinitiation period. Most of the experiments were done using inositol hexaphosphate (4–6). This compound is a common constituent of a large number of foods of plant origin (7), in which *myo*-inositol can also be present. In addition, *myo*-inositol can be formed within the intestinal tract as a result of hydrolysis of inositol hexaphosphate by the enzyme phytase, which occurs in the intestinal mucosa (8). Much of the ingested inositol hexaphosphate is hydrolyzed to inositol (8). The use of inositol hexaphosphate as a chemopreventive agent presents a problem in that it is a chelating agent (9). *myo*-Inositol does not have this property. It has exceedingly little toxicity, which makes it an attractive compound for study. It has been administered to humans and animals in high doses without producing adverse reactions (1, 10, 11). *myo*-Inositol has been shown to increase pulmonary surfactant synthesis when administered to immature animals (12). Other than this, very little information exists as to any effects it has on the lung. The mechanism(s) by which it inhibits carcinogenesis is not known.

The second compound under investigation is dexamethasone, a synthetic glucocorticoid. This compound has been shown to inhibit carcinogenesis of the skin, forestomach, and lungs of the mouse when given in the postinitiation period (1, 13, 14). In initiation/promotion experiments of epidermal carcinogenesis of the mouse, dexamethasone as well as other glucocorticoids have been found to be highly effective inhibitors when administered in the promotion phase of the study (13, 14). Dexamethasone has also been found to inhibit B(*a*)P-induced pulmonary adenoma formation and squamous cell carcinogenesis of the forestomach in female A/J mice when given in the postinitiation period (1). Dexamethasone has a large number of biological effects, including the capacity to mature type 2 alveolar cells, the major cell type occurring in pulmonary tumors in the experimental model used in the present study (15–19). Which effect or combination of effects is responsible for the cancer prevention properties of dexamethasone has not been established.

In earlier studies, both *myo*-inositol and dexamethasone were shown to inhibit pulmonary adenoma formation in female A/J mice when administered in the postinitiation period (1). The selection of this period of the carcinogenic process for study was based on data demonstrating this attribute in other tissues as described above. In the present investigation, the effects of the two compounds administered during an earlier period of the carcinogenic process (*i.e.*, starting 2 weeks prior to the first administration of carcinogen and continuing until 7 days after the last dose) have been studied. In addition, experiments have been carried out in which the compounds were fed throughout the entire course of the experiment. The prior experiments with *myo*-inositol and dexamethasone as inhibitors of pulmonary tumor formation were limited to those in which B(*a*)P was used as the carcinogen. In the experimental work presented here, the capacity of the two compounds to prevent pulmonary adenoma formation resulting from the administration of a second important pulmonary carcinogen, NNK, has been determined (20, 21).

Received 7/26/96; accepted 10/2/96.

The costs of publication of this article were defrayed in part by the payment of page charges. This article must therefore be hereby marked *advertisement* in accordance with 18 U.S.C. Section 1734 solely to indicate this fact.

[1] This work was supported by Grant RD-380 from the American Cancer Society and a grant from the Minnesota Soybean Research and Promotion Council.

[2] To whom requests for reprints should be addressed, at Department of Laboratory Medicine and Pathology, 6-133 Jackson Hall, University of Minnesota, Minneapolis, MN 55455.

[3] The abbreviations used are: B(*a*)P, benzo(*a*)pyrene; NNK, 4-(methylnitrosamino)-1-(3-pyridyl)-1-butanone.

Table 1 *Effects of myo-inositol and dexamethasone on B(a)P-induced pulmonary adenoma formation in female A/J mice*

Experiment	Group designation	Dietary additions: Preinitiation + initiation periods[a]	Dietary additions: Postinitiation period[b]	Pulmonary adenomas: No. of tumors per mouse	Pulmonary adenomas: % inhibition[c]	Pulmonary adenomas: Weight gain[d] (g)
1	C-C[e]	None	None	13.5 ± 5.0[f]		8
	myo-C	*myo*-inositol	None	10.9 ± 4.3	19	8
	C-*myo*	None	*myo*-Inositol	9.3 ± 3.8[g]	31	9
	myo-myo	*myo*-Inositol	*myo*-Inositol	6.5 ± 3.3[h,i]	52	11
2	C-C	None	None	17.5 ± 6.1		5
	C-Dex	None	Dexamethasone	9.3 ± 0.4[j]	47	4
3	C-C	None	None	16.5 ± 8.1		7
	myo-C	*myo*-inositol	None	11.2 ± 3.9[k]	32	5
	Dex-C	Dexamethasone	None	13.2 ± 3.9	20	7
	myo-myo	*myo*-Inositol	*myo*-Inositol	5.9 ± 2.8[l,m]	64	6
	Dex-Dex	Dexamethasone	Dexamethasone	7.3 ± 2.7[l,m]	56	6
	(*myo* + Dex)-(*Myo* + Dex)	*myo*-Inositol + dexamethasone	*myo*-Inositol + dexamethasone	2.3 ± 2.3[l]	86	5

[a] At 7 weeks of age, female A/J mice were randomized by weight into groups of 15 mice. At that time, they were placed on diets to be fed for 4 weeks. This time period has been designated "Preinitiation + initiation periods" and includes the 2 weeks prior to the first dose of B(*a*)P, the week during which the B(*a*)P was administered, and 1 week subsequent to the last dose of the carcinogen B(*a*)P (Fig. 1*A*). Concentrations of the test compounds throughout the experiments were: *myo*-inositol, 1%; dexamethasone, 0.5 mg/kg of diet.

[b] Dietary additions starting 1 week after the last administration of B(*a*)P and continuing for the duration of the protocol (Fig. 1*B*).

[c] Mean number of tumors in the control group minus the number in the test group divided by the number in the control group × 100.

[d] From the time of randomization until the termination of the protocol.

[e] C-C, no additions; *myo*, *myo*-inositol; Dex, dexamethasone.

[f] Mean ± SD.

[g] C-*myo vs.* C-C (experiment 1), $P < 0.05$.

[h] *myo-myo vs.* C-C (experiment 1), $P < 0.001$.

[i] *myo-myo vs.* C-*myo* (experiment 1), $P < 0.05$.

[j] C-Dex *vs.* C-C (experiment 2), $P < 0.05$.

[k] *myo*-C *vs.* C-C (experiment 3), $P = 0.054$.

[l] *myo-myo vs.* C-C (experiment 3), Dex-Dex *vs.* C-C (experiment 3), and (*myo* + Dex)-(*myo* + Dex) *vs.* C-C (experiment 3), $P < 0.001$.

[m] *myo-myo vs.* (*myo* + Dex)-(*myo* + Dex) and Dex-Dex *vs.* (*myo* + Dex)-(*myo* + Dex), $P < 0.001$.

Materials and Methods

Chemicals. The chemicals used were *myo*-inositol (>99% purity) and dexamethasone (>99% purity; Sigma Chemical Co., St. Louis, MO); B(*a*)P (>98% purity; Aldrich Chemical Co., Milwaukee, WI); and NNK (>99% purity; National Cancer Institute Carcinogen Repository, Midwest Research Institute, Kansas City, MO).

Animal Experiments. Female A/J mice obtained from the Jackson Laboratories (Bar Harbor, ME) were used in all experiments. The animals were fed a semipurified diet consisting of 27% vitamin-free casein, 59% starch, 10% corn oil, 4% salt mix (USP XIV), and a complete mixture of vitamins (Teklad, Madison, WI). At 7 weeks of age, the mice were randomized by weight into groups of 15. They were reweighed at weekly intervals. At 9 weeks of age, the animals were given the initial administration of the carcinogen to be used in the experiment. In experiments in which the carcinogen used was B(*a*)P, the dose of carcinogen used was 2 mg in 0.2 ml of cottonseed oil given by oral intubation. The administrations of B(*a*)P were repeated at 4 and 7 days after the initial dose. In animals receiving NNK, the dose was 1.6 mg in 0.1 ml of saline given i.p. Two administrations were given, the second 1 week after the first. Protocols with both carcinogens were terminated 21 weeks after the last dose of carcinogen, at which time the mice were autopsied. Pulmonary adenomas were counted on the surface of the lung using the procedure of Shimkin, as previously described (22, 23). Three administration schedules for the chemopreventive agents were used (Fig. 1). In the first of these, the mice were given the test compounds starting 2 weeks prior to the initial administration of the carcinogen, and the administration of the test compounds was continued until 1 week after the last dose of the carcinogen was given (Fig. 1*A*). This schedule has been designated "preinitiation and initiation periods." In the second administration schedule, the test compounds were fed starting 1 week after the last administration of carcinogen and were continued for the duration of the protocol (Fig. 1*B*). This schedule has been designated the "postinitiation period." The third schedule entailed administering the test agents starting 2 weeks prior to the first dose of carcinogen and continuing until the end of the experiment, (Fig. 1*C*).

Statistical Analysis. Differences between groups in an experiment were examined by means of ANOVA or, in the case of inhomogeneous variances, by the nonparametric Kruskal-Wallis test. Statistical results by nonparametric and parametric tests were the same. If the overall test was significant, pairwise comparisons were carried out by means of two-sample *t* tests with pooled or separate variance estimates, depending on whether the variances were similar ($P > 0.2$) or different. No adjustment for multiple testing was made for these *t* tests because each comparison was important on its own. The statistical package SAS was used.

Results

In Table 1, the results of administration of *myo*-inositol and dexamethasone on B(*a*)P-induced pulmonary adenoma formation are presented. In experiment 1, the effects of feeding *myo*-inositol during the three time schedules shown in Fig. 1 are presented. The first schedule (Fig. 1*A*) entails feeding *myo*-inositol during the preinitiation and initiation periods [*i.e.*, starting 2 weeks prior to the first administration of B(*a*)P and continuing until 1 week after the last administration of the carcinogen]. When *myo*-inositol was fed during this time frame, a small inhibition of pulmonary adenoma formation was found, which was not statistically significant. A larger inhibitory effect occurred when the *myo*-inositol was fed in the postinitiation period (Fig. 1*B*). When *myo*-inositol was given throughout the entire protocol, an additive effect was obtained (Fig. 1*C*). Experiment 2 demonstrates that dexamethasone fed in the postinitiation period results in a reduction of pulmonary tumors. The data in experiment 3 again show that *myo*-inositol has a small inhibitory effect when given in the preinitiation and initiation periods. Dexamethasone produces a small but

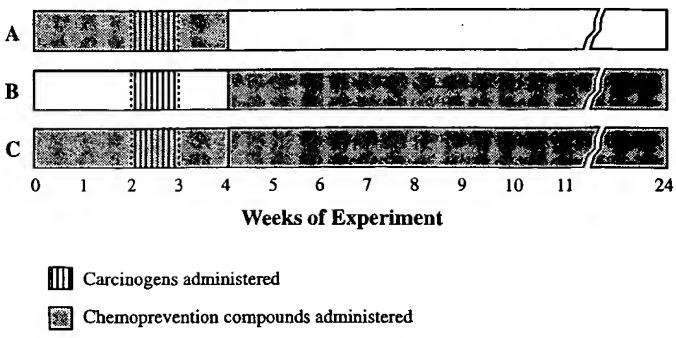

Fig. 1. Schematic presentation of the experimental protocol.

Table 2 *Effects of myo-inositol and dexamethasone on NNK-induced pulmonary adenoma formation in female A/J mice*

Group designation	Dietary additions[a]	Pulmonary adenomas		
		No. of tumors per mouse	% inhibition[b]	Weight gain[c] (g)
C-C[d]	None	19.2 ± 5.3[e]		6
myo-myo	*myo*-Inositol	10.3 ± 4.3[f,g]	46	5
Dex-Dex	Dexamethasone	11.3 ± 4.1[f,h]	41	6
(*myo* + Dex)-(*myo* + Dex)	*myo*-Inositol + dexamethasone	5.5 ± 2.8[f]	71	5

[a] At 7 weeks of age, female A/J mice were randomized by weight into groups of 15 mice. At that time, they were placed on their experimental diets containing the additions shown. These diets were continued for the duration of the protocol. Concentrations of the test compound were: *myo*-inositol, 1%; dexamethasone, 0.5 mg/kg of diet.
[b] Calculations as for Table 1.
[c] From time of randomization until the termination of the protocol.
[d] C-C, no additions, *myo*, *myo*-inositol; Dex, dexamethasone.
[e] Mean ± SD.
[f] *myo-myo*, Dex-Dex, and (*myo* + Dex)-(*myo* + Dex) *vs.* C-C, $P < 0.001$.
[g] *myo-myo vs.* (*myo* + Dex)-(*myo* + Dex), $P < 0.005$.
[h] Dex-Dex *vs.* (*myo* + Dex)-(*myo* + Dex), $P < 0.001$.

statistically insignificant inhibitory effect when fed during this time interval. In experiment 3, *myo*-inositol and dexamethasone were administered separately or in combination throughout the entire experiment (Fig. 1*C*). Each of the compounds, when fed separately, produces a high level of inhibition. When they are fed together, an additive effect occurs. The 86% inhibition shown with the combined feeding of both inhibitors throughout the experiment is the largest that has been observed in any study that we have performed with this experimental model as we use it.

In Table 2, the effects of administration of *myo*-inositol, dexamethasone, or both together throughout the entire experiment on NNK-induced pulmonary adenoma formation are shown. As is the case with the use of B(*a*)P as the carcinogen, both compounds, when given separately, inhibit pulmonary adenoma formation. Feeding the two compounds together results in a greater reduction in pulmonary tumor formation than feeding each separately.

Discussion

Although cancer of the lungs is the principal cause of cancer deaths in the United States and many other industrialized countries, effective chemoprevention of this neoplasm has not been achieved. In animal models, a number of compounds (blocking agents) can prevent the occurrence of this cancer when administered prior to or simultaneously with exposure to chemical carcinogens, but few are effective when given in the postinitiation period (3, 24). Both of the compounds studied in the present investigation inhibit pulmonary tumor formation when administered in the postinitiation period. When given in the preinitiation and initiation periods, *myo*-inositol produced a small but statistically insignificant inhibition; dexamethasone had even less effect. The two compounds had not been studied previously under these conditions. Although these data are not definitive, they are of importance in that there is always the possibility that a compound that can inhibit in one stage of the carcinogenic sequence may enhance carcinogenesis when given in another stage. In the studies carried out with *myo*-inositol and dexamethasone, this certainly is not the case.

The capacity of the glucocorticoid dexamethasone to inhibit pulmonary adenoma formation is of interest in that this compound has been found to inhibit cancers of squamous cell origin as well as those of glandular origin. Cancers of the lung can arise from different cell types. The predominant ones are glandular and squamous. Studies of the capacity of dexamethasone to inhibit squamous cell carcinogenesis of the lung have not been reported. If this compound does prevent cancers of both cellular origins, it would be particularly attractive. A major problem with the use of dexamethasone as a chemopreventive agent, as well as other glucocorticoids that have systemic effects, is toxicity. However, a number of topically active glucocorticoids with minimal systemic effects have been developed and could prove applicable for use as chemopreventive agents in the respiratory tract if administered by aerosol.

Prior studies of inhibition of pulmonary adenoma formation by *myo*-inositol and dexamethasone have been limited to B(*a*)P as the carcinogen. In the present work, the two compounds have been shown to inhibit pulmonary carcinogenesis resulting from administrations of NNK in this tumor model. B(*a*)P and NNK are representative of two major classes of lung carcinogens to which humans are exposed, indicating that *myo*-inositol and dexamethasone may be useful as chemopreventive agents in this organ site.

References

1. Estensen, R. D., and Wattenberg, L. W. Studies of chemopreventive effects of *myo*-inositol on benzo[*a*]-pyrene-induced neoplasia of the lung and forestomach of female A/J mice. Carcinogenesis (Lond.), *14:* 1975–1977, 1993.
2. Benner, S. E., Lippman, S. M., and Hong, W. K. Current status of retinoid chemoprevention of lung cancer. Oncology, *9:* 205–210, 1995.
3. Wattenberg, L. W. Prevention, therapy, basic science and the resolution of the cancer problem. Cancer Res., *53:* 5890–5896, 1993.
4. Shamsuddin, A. M., Ullah, A., and Chakravarthy, A. K. Inositol and inositol hexaphosphate suppress cell proliferation and tumor formation in CD-1 mice. Carcinogenesis (Lond.), *10:* 1461–1463, 1989.
5. Shamsuddin, A. M., and Sakamoto, K. Antineoplastic action of inositol compounds. *In:* L. Wattenberg, M. Lipkin, C. W. Boone, and G. J. Kelloff (eds.), Cancer Chemoprevention, pp. 285–308. Boca Raton, FL: CRC Press, 1992.
6. Shamsuddin, A. M., and Ullah, A. Inositol hexaphosphate inhibits large intestinal cancer in F344 rats 5 months after induction by azoxymethane. Carcinogenesis (Lond.), *10:* 625–626, 1989.
7. Reddy, W. R., Sathe, S. K., and Salunkhe, D. K. Phytates in legumes and cereals. Adv. Food Res., *28:* 1–92, 1982.
8. Cooper, J. R., and Gowing, H. S. Mammalian small intestinal phytase (EC 3.1.3.8). Br. J. Nutr., *50:* 673–678, 1983.
9. Morris, E. R. Phytate and mineral bioavailability. *In:* E. Graf (ed.), Phytic Acid, pp. 55–77. Minneapolis, Pilatus Press, 1986.
10. Gregersen, G. *Myo*-inositol supplementation. *In:* P. J. Dyck, P. K. Thomas, A. K. Asbury, A. I. Winegrad, and D. Porte (eds.), Diabetic Neuropathy, pp. 188–189. Philadelphia, W. B. Saunders Co., 1987.
11. Gregersen, G., Bertelsen, B., Harbo, H., Larsen, E., Andersen, J. R., Helles, A., Schmiegelow, M., and Christensen, J. E. J. Oral supplementation of *myo*-inositol: effects on peripheral nerve function in human diabetics and on the concentration in plasma, erythrocytes, urine and muscle tissue in human diabetics and normals. Acta Neurol. Scand., *67:* 164–172, 1983.
12. Hallman, M., Bry, K., Hoppu, K., Lappi, M., and Pohjavuori, M. Inositol supplementation in premature infants with respiratory distress syndrome. New Engl. J. Med., *326:* 1233–1239, 1992.
13. Belman, S., and Troll, W. The inhibition of croton oil-promoted mouse skin tumorigenesis by steroid hormones. Cancer Res., *32:* 450–454, 1972.
14. Verma, A. K., Garcia, C. T., Ashendel, C. L., and Boutwell, R. K. Inhibition of 7-bromomethylbenz[a]nthracene-promoted mouse skin tumor formation by retinoic acid and dexamethasone. Cancer Res., *43:* 3045–3049, 1983.
15. Kresch, M. J., and Gross, I. The biochemistry of fetal lung development. Clin. Perinatol., *14:* 481–507, 1987.
16. Gross, I. Regulation of fetal lung maturation. Am. J. Physiol., *259:* L337–L344, 1990.
17. Jonat, C., Rahmsdorf, H. J., Park, K-K., Cato, A. C. B., Gebel, S., Ponta, H., and Herrlich, P. Antitumor promotion and antiinflammation: down-modulation of AP-1 (Fos/Jun) activity by glucocorticoid hormone. Cell, *62:* 1189–1204, 1990.
18. Mouhieddine, O. B., Cazals, V., Kuto, E., LeBouc, Y., and Clement, A. Glucocor-

ticoid-induced growth arrest of lung alveolar epithelial cells is associated with increased production of insulin-like growth factor binding protein-2. Endocrinology, *137:* 287–295, 1996.

19. Wu, C-C., Croxtall, J. D., Perretti, M., Bryant, C. E., Thiemermann, C., Flower, R. J., and Vane, J. R. Lipocortin 1 mediates the inhibition by dexamethasone of the induction by endotoxin of nitric oxide synthase in the rat. Proc. Natl. Acad. Sci. USA, *92:* 3473–3477, 1995.
20. Hecht, S. S., and Hoffman, D. Tobacco-specific nitrosamines, an important group of carcinogens in tobacco and tobacco smoke. Carcinogenesis (Lond.), *9:* 785–884, 1988.
21. Hecht, S. S., Isaacs, S., and Trushin, N. Lung tumor induction in A/J mice by the tobacco smoke carcinogens 4(methylnitrosamino)-1-(3-pyridyl)-1-butanone and benzo[a]pyrene: a potentially useful model for evaluation of chemopreventive agents. Carcinogenesis (Lond.), *15:* 2721–2725, 1994.
22. Shimkin, M. B. Induced pulmonary tumors in mice. II. Reactions of lungs in strain A mice to carcinogenic hydrocarbons. Arch. Pathol., *29:* 235–255, 1940.
23. Shimkin, M. B. Pulmonary tumors in experimental animals. Adv. Cancer Res., *3:* 223–267, 1955.
24. Wattenberg, L. W. Chemoprevention of cancer by naturally occurring and synthetic compounds. *In:* L. Wattenberg, M. Lipkin, C. W. Boone, and G. J. Kelloff (eds.), Cancer Chemoprevention, pp. 19–39. Boca Raton, FL: CRC Press, 1992.

STIC-ILL

ND9 RB1.L2 4/28539

From: Holleran, Anne
Sent: Monday, January 20, 2003 11:57 AM
To: STIC-ILL
Subject: refs. for 09/868,968

Please send copies of the following papers:

9345198

1.	Hoyoku,	Anticancer Res. (1999) 19(5A): 3663-3664
2.	Chamson-Reig	Endocrinology (1999) 140(8): 3573-3580
3.	Lixin,	J. Medicinal Chemistry 91998) 41(18): 3303-3306
4.	Yorek,	American J. Physiology (1998) 274(1, part1): C58-C71
5.	Nazih-Sanderson	Biochimica et Biophysica Acta (1997) 1346(1): 45-60
6.	Wattenberg	Cancer Research (1996) 56(22): 5132-5135
7.	Caro	Infection and Immunity (1996) 64(8): 3438-3441
8.	Seymour	Laboratory Investigation (1996) 75(3): 427-437
9.	Brunn	Cancer Chemotherapy (1994) 35(1): 71-79
10.	Kopp	Cancer Research (1990) 50(20): 6490-6496
11.	Tanino	Japanese J. Experimental Medicine (1972) 42(6): 575-582
12.	Eagle	Biochmistry (1963) 2(5): 1125-1126
13.	Caro	Biochem. Mol. Med. (1997) 61: 214-228

Anne Holleran
AU: 1642
Tel: 308-8892
RM: 8e03

mailbox: 8e12

0023-6837/96/7503-427$03.00/0
LABORATORY INVESTIGATION

Vol. 75, No. 3, p. 427, 1996
Printed in U.S.A.

Vascular Endothelial Growth Factor Stimulates Protein Kinase C-Dependent Phospholipase D Activity in Endothelial Cells

Leonard W. Seymour, Mahmood A. Shoaibi, Ashley Martin, Asif Ahmed, Paul Elvin, David J. Kerr, and Michael J. O. Wakelam

CRC Institute for Cancer Studies (MS, MJOW, DJK, LWS); Department of Obstetrics and Gynecology (AA), University of Birmingham School of Medicine, Birmingham, United Kingdom; and Zeneca Pharmaceuticals (PE), Alderley Park, Macclesfield, Cheshire, United Kingdom

SUMMARY: Many tumors produce vascular endothelial growth factor (VEGF), a paracrine factor acting selectively on endothelial cells. VEGF has many effects on cultured endothelial cells and mediates angiogenesis and enhanced vascular permeability in vivo. The endothelial signal transduction pathways of VEGF represent novel targets for cancer therapy because they are readily accessible to systemically administered drugs. We have examined VEGF-stimulated signals generated in HUVEC to identify potential targets for therapeutic intervention. The transphosphatidylation reaction has been used to monitor phospholipase D (PLD) activity; total inositol phosphates have been measured after prelabeling of cells with [^{3}H]myoinositol; and intracellular free calcium has been measured using Fura-2 fluorescence. After HUVEC-stimulation with VEGF, there is an early influx of calcium (maximal by 100 seconds) followed by activation of PLD (half maximal by 100 seconds, EC_{50} 70 pM). The PLD activity was inhibited by reducing extracellular calcium (150 nM, 50% inhibition), exposure to 12-*O*-tetradecanoylphorbol 13 acetate (200 nM, 24 hours, 100% inhibition), Roche 31.8220 (10 μM, 15 minutes, 72% inhibition), or genestein (100 μM, 30 minutes, 56% inhibition), which suggests a dependence on both protein kinase C and tyrosine phosphorylation. Activation of phospholipase C-catalyzed hydrolysis of phosphatidylinositol-4,5-bisphosphate was inferred from the production of inositol phosphates, although this response was slower (half maximal by 3 minutes). The phospholipase C activity was also dependent on influx of calcium and was partially inhibited by low (150 nM) extracellular calcium. PLD may be involved in mediating a number of endothelial responses to tumor-secreted VEGF, notably cytoskeleton-dependent effects such as the cell migration involved in angiogenesis. This signal transduction pathway could represent an accessible and vulnerable target for cancer therapeutic intervention and has the novelty of being located within normal cells rather than tumor cells. (*Lab Invest 1996, 75:427–437*).

VEGF is a paracrine-acting peptide growth factor implicated in tumor growth and development (Plate et al, 1992; Senger et al, 1993; Ferrara, 1995). It is produced by many tumors at advanced stages of malignancy (Brown et al, 1993, 1995), and its production is further regulated by hypoxia, showing particularly high expression in areas of tumor adjacent to zones of necrosis (Shweiki et al, 1992). VEGF protein is secreted from tumor cells and localizes in extracellular stores, mediating paracrine activities on tumor-associated endothelial cells. VEGF (also known as vascular permeability factor) is thought to play an important role in regulating tumor vascular permeability (Senger et al, 1983), angiogenesis (Klagsbrun and Soker, 1993), and even the angiogenesis involved in metastasis (Takahashi et al, 1995).

The biological effects of VEGF on endothelial cells are mediated through the specific membrane receptors known as KDR and *flt*-1, both Class III tyrosine kinase-linked receptors (Terman et al, 1992; Devries et al, 1992). Physiologic responses include chemotaxis, mitogenesis, and release of proteolytic enzymes and their inhibitors, as well as a stimulation of capillary tube formation, which is synergistic with basic fibroblast growth factor (bFGF; Pepper et al, 1991, 1992). The precise signaling pathways that mediate these responses have not yet been elucidated, although they represent an interesting target for potentially selective therapeutic intervention because they may involve biochemical processes not constitutively activated in normal cells.

Received May 7, 1996.
Address reprint requests to: Dr. Seymour, CRC Institute for Cancer Studies, University of Birmingham School of Medicine, Edgbaston, Birmingham, United Kingdom B15 2TT. Fax: 44 121 414 3263.
This work was supported by the Cancer Research Campaign (LWS, MAS, DJK) and the Wellcome Trust (AM, AA, MJOW).

Activation of the low-affinity, high-capacity VEGF receptor (known as KDR) is thought to mediate actin reorganization, membrane ruffling, chemotaxis, and mitogenicity, whereas the functions of the high-affinity, low-capacity VEGF receptor (known as *flt*-1) are less clearly understood (Waltenberger et al, 1994). Both endothelial VEGF receptors are known to undergo autophosphorylation after agonist binding, with phosphorylation of *Src* family members occurring after stimulation of *flt*-1 (Waltenberger et al, 1994). Although there are contradictory reports of phosphatidylinositol 3'-kinase activation and tyrosine phosphorylation of phospholipase C (PLC)-γ (Waltenberger et al, 1994; Guo et al, 1995), a role for phospholipid messengers in post-receptor VEGF signaling is clearly suggested by the PLC-mediated hydrolysis of phosphatidylinositol-4,5-bisphosphate (Brock et al, 1991).

Phospholipase D (PLD) is also emerging as a significant signaling enzyme and is known to be regulated variously by tyrosine phosphorylation, protein kinase C (PKC) (Cook and Wakelam, 1992), and small molecular weight G proteins such as Arf, Rho (Kuribara et al, 1995), and Ral (Jiang et al, 1995). A role for PLD has been tentatively suggested in cytoskeletal reorganization (Ha and Exton, 1993) and possibly even in metastasis (Pai et al, 1994), which makes it an intriguing candidate for activation by VEGF. Such a signal could represent a useful target for selective therapeutic intervention. The purpose of this study was to elucidate the phospholipid signal pathways stimulated by VEGF in endothelial cells and to specifically identify whether VEGF is capable of stimulating PLD-mediated hydrolysis of phosphatidylcholine.

Results

VEGF Stimulation of Endothelial Cell Growth

VEGF stimulated a maximum rise of HUVEC proliferation over 72 hours to 250% of control, with an EC_{50} of 20 pM. Basic fibroblast growth factor (bFGF) stimulated a rise to ≥380% of control, with an EC_{50} ≥500 pM (Fig. 1).

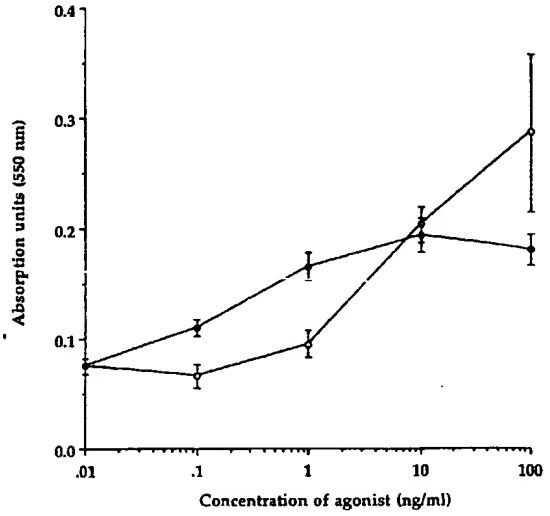

Figure 1.
Mitogenicity of VEGF and bFGF on HUVEC in vitro. Cells were stimulated with agonists at the concentrations shown. After 67 hours, MTT was added to each well (500 μg/ml), and cell viability was assessed (67 to 72 hours) by reduction of MTT to an insoluble formazan salt as determined by dissolution in dimethylsulfoxide and spectrophotometric absorption at 550 nm. ○, bFGF; ●, VEGF bars, SE.

Measurement of Phospholipase D Activity

To determine whether VEGF was able to stimulate PLD activity, changes in [^{3}H] phosphatidylbutanol (PtdButOH) were measured in [^{3}H]palmitate-labeled HUVEC in the presence of 30 mM butan-1-ol. [^{3}H] PtdButOH formation is catalyzed by the transferase activity of PLD and serves as a definitive marker of PLD activity. After exposure of HUVEC to a mitogenic concentration of VEGF (10 ng/ml, approximately 600 pM), [^{3}H] PtdButOH increased rapidly (Fig. 2A) with time to half maximal stimulation of 100 seconds, although the level continued to increase up to at least 5 minutes. In the absence of stimulus, there was no significant change in levels of [^{3}H] PtdButOH. The ability of VEGF to increase [^{3}H] PtdButOH levels was dose-dependent, with EC_{50} about 70 pM (Fig. 2B). The dose-response curve was bell-shaped (data not shown) with a peak response at approximately 5 nM VEGF. Co-administration of VEGF (1 to 10 ng/ml) and bFGF (1 to 10 ng/ml) showed no synergistic effects on PLD activation (data not shown). A known stimulator of PLD activity in HUVEC, 12-*O*-tetradecanoylphorbol 13 acetate (TPA; 100 nM), was used as a positive control.

Involvement of PKC in Regulation of VEGF-Stimulated PLD Activity

The possible involvement of PKC in mediating VEGF-stimulated [^{3}H] PtdButOH formation was investigated using various strategies. Initially, cells were depleted of cellular PKC activity by prolonged exposure to TPA (200 nM, 24 hours). Under these conditions, the formation of [^{3}H] PtdButOH in response to subsequent VEGF challenge (1, 10, or 100 ng/ml) was completely abolished (Fig. 3A). TPA itself, again used as a control, was also unable to stimulate a response in these cells.

Most common isoforms of PKC (α, β_I, β_{II}, and γ but not δ, ε, η, and ζ) are dependent on calcium influx for

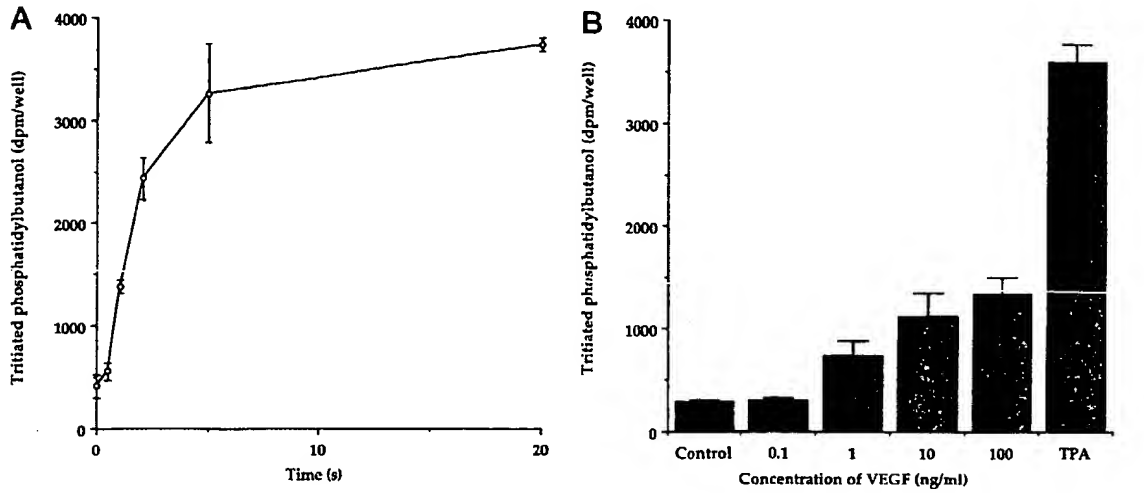

Figure 2.
Effect of VEGF on [^{3}H]PtdButOH formation in HUVEC. Cells were prelabeled with [^{3}H]palmitic acid, preincubated with butan-1-ol, then stimulated with VEGF (Time 0). A, Time course of PLD response after the addition (Time 0) of 10 ng/ml of VEGF. B, Influence of VEGF dose on PLD response measured 20 minutes after addition of VEGF. TPA (200 nM) was used as a positive control. Points are the mean of triplicate determination from a single experiment, typical of three others; bars represent the SE.

activation (Lopez et al, 1995), and this can be prevented by performing experiments in low (150 nM) calcium buffer, approximately equal to the intracellular concentration of free calcium. VEGF (10 or 100 ng/ml) stimulation of endothelial cells under these low-calcium conditions showed an approximate 50% decrease in [^{3}H] PtdButOH formation compared with normal calcium controls (Fig. 3B), which suggests the involvement of a calcium signal upstream of the PLD activity.

Finally, the Roche compound 31.8220, widely used as a selective inhibitor of PKC, was applied to cells (10 μM, 15 minutes) and mediated 72% inhibition of [^{3}H] PtdButOH formation in response to subsequent addition of VEGF (100 ng/ml; Fig. 3C).

Taken together, these data indicate that the PLD activity stimulated by VEGF within HUVEC is partially dependent on PKC activity, which indicates the probability of a serine/threonine phosphorylation stage in the regulation of its activation.

Involvement of Tyrosine Phosphorylation in Regulation of VEGF-Stimulated PLD Activity

Preincubation of cells with genestein (100 μM, 30 minutes), an inhibitor of tyrosine kinases, led to an approximate 56% fall in the levels of [^{3}H] PtdButOH formation mediated by subsequent challenge with VEGF (100 ng/ml; Fig. 3C). Despite the nonspecific nature of genestein inhibition, this result does suggest the involvement of tyrosin phosphorylation upstream of the PLD activity.

Measurement of Intracellular Calcium

The ability of low extracellular calcium levels to inhibit phospholipase D activity suggested that calcium influx formed an intrinsic part of the signaling process. We measured VEGF-stimulated changes in intracellular free calcium by monitoring the fluorescence intensity of intracellular Fura-2. To facilitate routine quantification, suspension cultures of HUVEC were used.

When assayed in full medium, thrombin (2 U/ml; used as a positive control) evoked a rapid increase in [Ca^{2+}]i (Fig. 4A), which quickly returned to levels near basal. VEGF (10 or 100 ng/ml) evoked a relatively slow rise in [Ca^{2+}]i levels, which were maximal after approximately 100 seconds and declined to an elevated plateau (approximately 80% of maximum) over the next 200 seconds (Fig. 4B). These results are compatible with a greater proportion of the elevated [Ca^{2+}]i being released from intracellular stores for thrombin than for VEGF, and this possibility was subsequently examined using extracellular EGTA.

Preincubation of HUVEC in EGTA (10 mM, 5 minutes) had relatively little effect on the initial elevation of [Ca^{2+}]i mediated by thrombin, although the signal that was generated declined to basal levels within 150 seconds of agonist challenge (Fig. 5A). This suggests that the influx of extracellular Ca^{2+} had been abolished, although th r l ase of Ca^{2+} from intracellular stores (presumably mediated by inositol 1,4,5-trisphosphate) was essentially unaffected. In contrast,

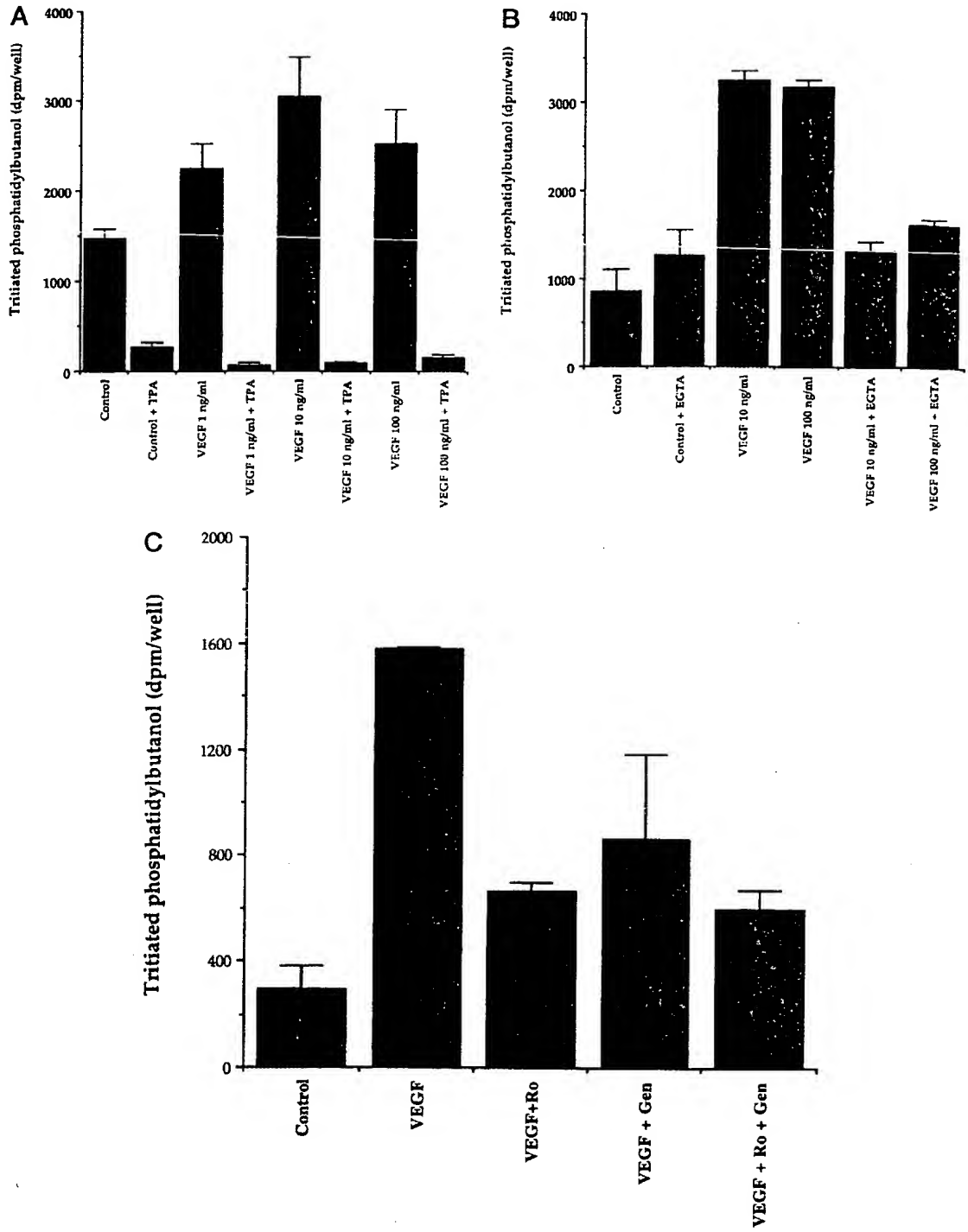

Figure 3.

Inhibition of VEGF-stimulated PLD activity by PKC antagonists and genestein. Cells were prelabeled with [^{3}H]palmitic acid, preincubated with butan-1-ol, then stimulated for 20 minutes with (A) 0:1, 10 and 100 ng/ml of VEGF with or without TPA pretreatment (200 nM, 24 hours) or (B) 0, 10, and 100 ng/ml of VEGF in the presence or absence of EGTA (1 mM, added 1 minute before VEGF) or (C) 100 ng/ml of VEGF with or without Roche 31.8220 (10 mM, added 15 minutes before VEGF), genestein (100 mM, added 30 minutes before VEGF), or with both Roche 31.8220 and genestein. Columns represent the mean of triplicate determination from a single experiment, typical of three others; the bars represent the SE

the elevation of $[Ca^{2+}]i$ in response to VEGF was completely abolished by preincubation in extracellular EGTA (Fig. 5B). This result was un xpected and suggests either that VEGF normally mediates no release of Ca^{2+} from intracellular stores or that mobilization of intracellular Ca^{2+} is itself dependent on an influx of Ca^{2+} from outside the cell, perhaps after activation of an ion channel.

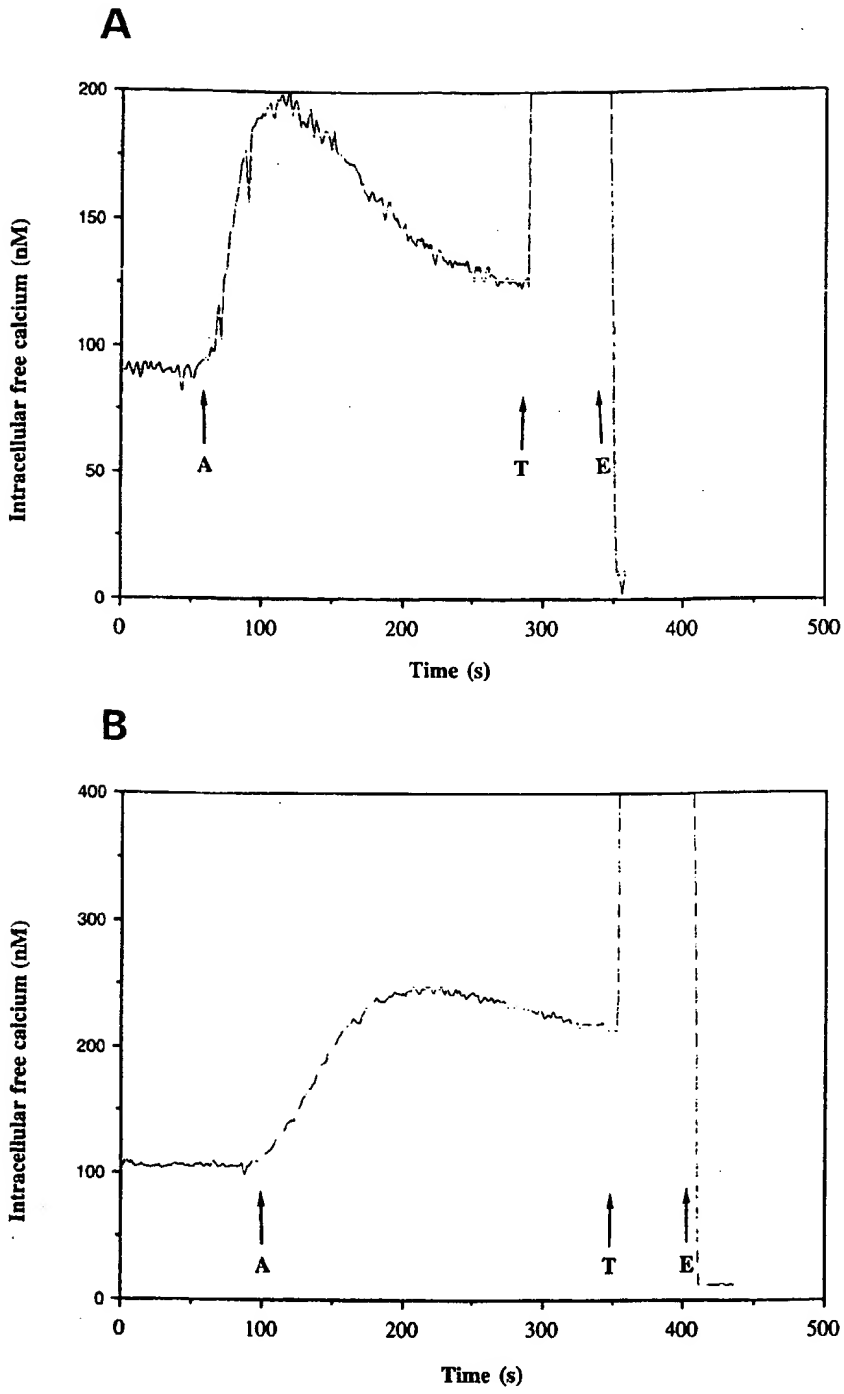

Figure 4.
Effect of VEGF on mobilization of intracellular calcium. Cells were loaded with Fura-2 AM dye for 45 minutes and then stimulated with (A) 2 U/ml of thrombin or (B) 100 ng/ml of VEGF. Intracellular free calcium levels were measured as described in the text. Agonists (*A*), Triton X-100 (*T*), and EGTA (*E*) were added when shown. The results presented are typical of three separate experiments.

Measurement of Inositol Phosphate Production

To elucidate the possible involvement of PLC activity in mediating cellular responses to VEGF, accumulation of [^{3}H]inositol phosphat s in HUVEC prelabeled with [^{3}H]myoinositol was measured in the presence of 10 mM LiCl. HUVEC exposed to a mitogenic concentration of VEGF (100 ng/ml) showed a gradual increase in th level of [^{3}H] inositol phosphates, which was measurabl aft r 2 minutes and continued increasing up to past 10 minutes (Fig. 6). In the absence of

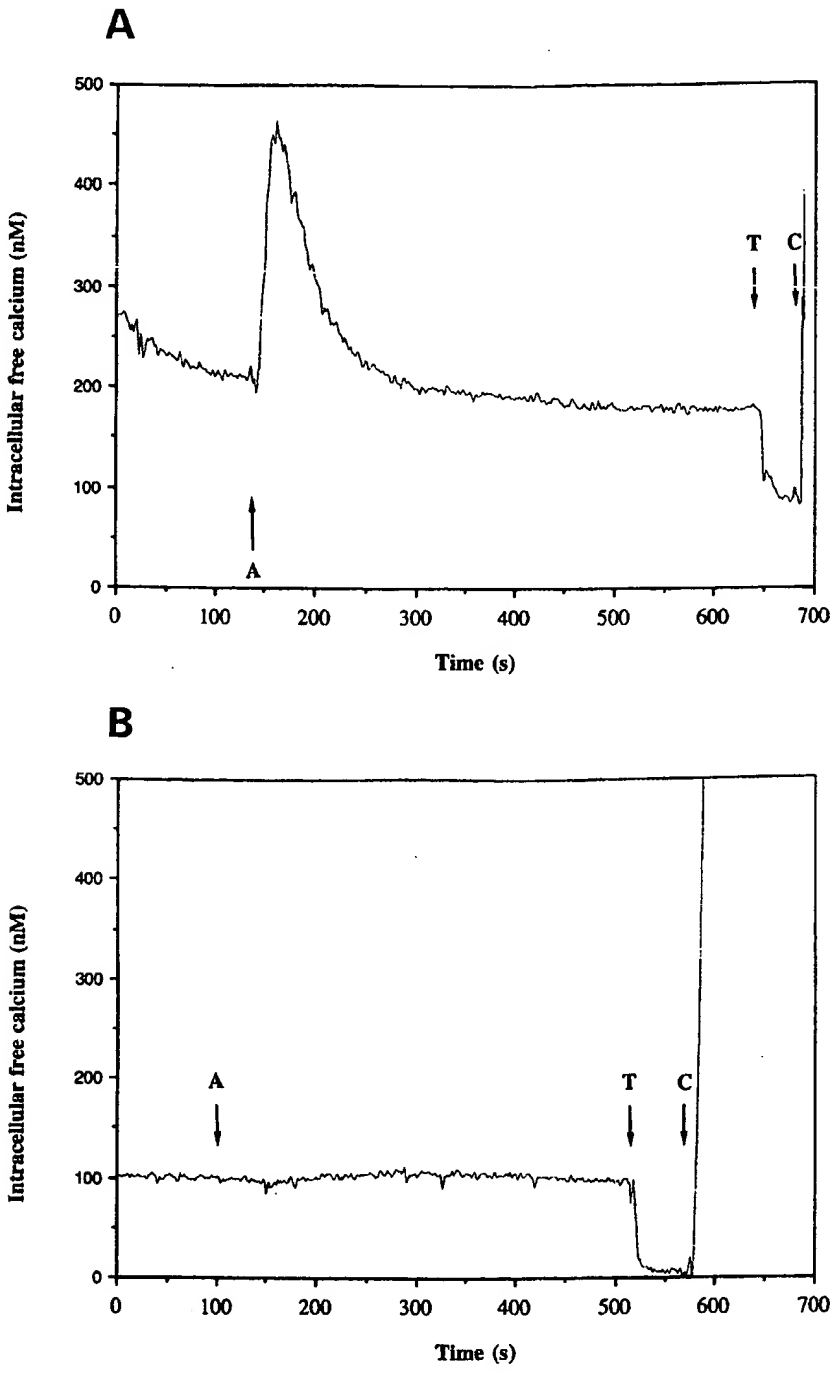

Figure 5.
Effect of VEGF on intracellular calcium in the presence of EGTA. Cells were loaded with Fura-2-AM dye for 45 minutes and then incubated with 10 mM EGTA for 5 minutes. Cells were then stimulated with (A) 2 U/ml of thrombin or (B) 100 ng/ml of VEGF. Intracellular free calcium levels were measured as described in the text. Agonists (*A*), Triton X-100 (*T*), and $CaCl_2$ (*C*) were added when shown. The results presented are typical of three separate experiments.

stimulus, there was no significant increase in levels of [^{3}H]inositol phosphates over the 20-minute period. Examination of the [Ca^{2+}]i traces over an extended time course (data not shown) gave no indication of a biphasic calcium response, which suggests that the high levels of inositol phosphates produced 10 to 20 minutes after VEGF stimulation do not lead to further elevated intracellular calcium. It is possible, however, that a second phase of [Ca^{2+}]i increase may be masked by the first.

When [^{3}H]inositol-labelled cells w re incubated in EGTA (1 mM) throughout the xposure to VEGF (100

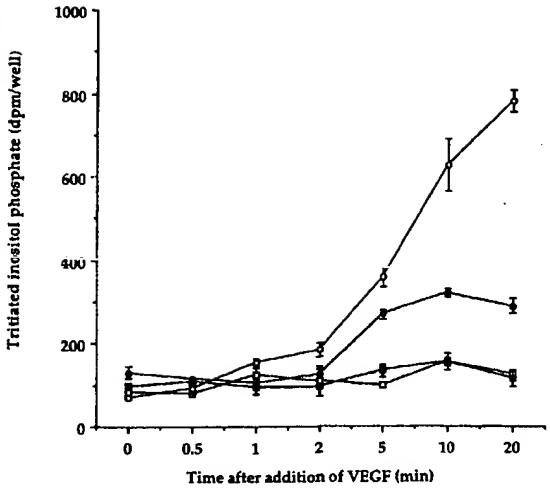

Figure 6.

Time course of VEGF stimulation of inositol phosphate formation in HUVEC. Cells were loaded with [^{3}H]myoinositol and incubated with (○) or without (□) 100 ng/ml of VEGF for varying lengths of time. Inositol phosphate generation was measured as described in the text. In some experiments, HUVEC were washed with EGTA (1 mM) and then stimulated with VEGF (100 ng/ml) in low-calcium buffer (●). An EGTA/low-calcium buffer control, without the addition of VEGF, was also performed (■). Points represent the mean of triplicate determination from a single experiment, typical of three others; the bars represent SE.

ng/ml), total production of [^{3}H]inositol phosphates was decreased compared with that detected in normal calcium-containing medium (Fig. 6) and reached a plateau 5 to 10 minutes after addition of VEGF.

Discussion

VEGF is of central importance to the maintenance and growth of many solid tumors (Kim et al, 1993), influencing vascularization of primary and metastatic growths (Ferrara, 1995; Takahashi et al, 1995) and the enhanced permeability of tumor-associated vasculature, which results in increased extravasation of proteins for clotting and stromal expansion (Senger et al, 1993). The paracrine action of VEGF on endothelial cells represents a promising target for therapeutic intervention because functional endothelial cells are easily accessible from the bloodstream. Agents capable of selective inhibition of the effects of VEGF on endothelial cells could, therefore, be of significant therapeutic interest.

There are various approaches to inhibiting VEGF stimulation of endothelial cells, including the use of anti-VEGF antibodies (Kim et al, 1993), receptor antagonists, or dominant negative VEGF receptor mutants introduced into endothelial cells (Millauer et al, 1994). We focused on the identification of post-receptor signaling pathways that may be susceptible to inhibition by low molecular weight agents suitable for systemic application. In this context, phospholipid signaling represents a promising opportunity for therapeutic intervention. Although some anticancer agents are known to inhibit phospholipid signaling pathways (eg, ether lipid analogu ET-18-OCH_3, suramin (Powis, 1994)), selective inhibition of these pathways has not been strategically pursued in cancer therapy. The demonstration that VEGF stimulates phospholipase D activity in endothelial cells, therefore, presents a novel therapeutic target not previously described.

PLD is rapidly activated by the addition of VEGF to HUVEC (time to half maximal stimulation is 100 seconds) and seems dependent on PKC as well as tyrosine phosphorylation. A similar time scale and pattern of regulation was reported for PLD activation in HUVEC after stimulation with bFGF, although bFGF, in contrast to VEGF, evoked no generation of inositol phosphates (Ahmed et al, 1994). The demonstration of inositol lipid hydrolysis by VEGF is in agreement with previous studies (Brock et al, 1991), although the time course of induction is slower than those reported in the literature for other agonists (eg, bradykinin (Ahmed et al, 1994)). This is presumably because VEGF activates PLC-γ, whereas bradykinin activates PLC-β by a G-protein-linked mechanism.

The slow activation of inositol lipid hydrolysis by VEGF is likely to be accompanied by equally slow diacylglycerol generation. Thus, the activation of PKC may be controlled predominantly by the influx of calcium, as previously suggested for bFGF stimulation of PKC in these cells (Ahmed et al, 1994). Therefore, the reduction in PLD activity caused by lowering extracellular calcium and, thus, preventing calcium entry could be caused by an inhibition of PKC activity as suggested for regulation of PLD activity in fibroblasts (Cook et al, 1991).

Complete inhibition of VEGF-mediated increased [Ca^{2+}]i by extracellular EGTA has not been previously reported. This can be explained, at least in part, by the demonstration that the VEGF-stimulated intracellular generation of inositol phosphates is itself dependent on an influx of extracellular calcium (Fig. 6B). Although the calcium dependence of PLC has been previously suggested in some systems, subtypes of PLC with intrinsic calcium dependence have not been identified (Meldrum et al, 1991). The recent identification of a Ca^{2+}-activated tyrosine kinas could, however, suggest a mechanism for Ca^{2+}-dependent PLC-γ phosphorylation and, thus, activation.

Stimulated PLD activity is unlikely to be directly involved in the control of DNA synthesis. There are, however, indications that the enzyme plays a role in the regulation of cytoskeletal events, which may be important in mediating VEGF-stimulated angiogenic responses. Phosphatidate was suggested to stimulate actin stress fiber formation in IIC9 cells (Ha and Exton, 1993), and recent experiments have suggested that PLD activation is upstream of Rho activation (Collard, 1996) in an endothelial cell line (Cross et al, 1996). Recent work from Williger et al (1995) has reinforced the role of phosphatidate in controlling enzyme secretion, whereas photolysis of caged phosphatidic acid in metastatic fibrosarcoma cells was shown to mediate release of gelatinase A. This raises the possibility of a role for PLD in regulating cytoskeletal involvement in protease secretion and cellular motility (Cross et al, 1996), which are both processes fundamental to the angiogenic activity associated with solid tumors and with metastasis.

Determination of the physiologic implications of inhibiting VEGF-stimulated PLD activity is limited by the availability of specific PLD inhibitors, although semiselective inhibitors such as novel ketoepoxides (Pai et al, 1994) and demethoxyviridin (Bonser et al, 1991) are available. We are currently examining the effects of these agents on endothelial responses to VEGF and correlating with PLD inhibition to determine whether this enzyme constitutes a vulnerable and accessible nontumor target for selective intervention in cancer chemotherapy.

Materials and Methods

Medium 199, FCS, L-glutamine, EGTA, TPA, genestein, thrombin, perchloric acid, lithium chloride, and gelatin were purchased from Sigma Chemical Company (Poole, United Kingdom). bFGF was purchased from Advanced Protein Products (Brierley Hill, United Kingdom). VEGF and Roche 31.8220 were generous gifts from Zeneca Pharmaceuticals plc (Macclesfield, United Kingdom) and Roche Products (Welwyn Garden City, United Kingdom), respectively. PBS was purchased from Flowgen (Shenstone, United Kingdom), butanol was purchased from Fisons (Loughborough, United Kingdom), [^{3}H] palmitic acid and [^{3}H]myoinositol were purchased from Amersham International plc (Amersham, United Kingdom), type I collagenase was puchased from Lorne Diagnostics Ltd. (Twyford, United Kingdom), and Hanks' buffer was puchased from Gibco (Paisley, United Kingdom).

Cell Isolation and Culture

HUVEC were isolated from cords 1 to 2 hours old (Jaffe et al, 1973). The veins in cords 4 to 6 inches in length were cannulated and washed with 30 to 60 ml of PBS to remove blood clots. PBS was then replaced with 6 to 10 ml of type I collagenase (1 mg/ml in PBS) and incubated at 37°C for 10 minutes. The veins were rinsed with 10 ml of PBS, which was then collected. Cells were collected by centrifugation and then resuspended in 7 ml of M199 supplemented with 20% FCS, 1% L-glutamine, and 10 ng/ml of bFGF in 25-cm^2 flasks (Falcon, Cowley, United Kingdom) precoated with 2% gelatin. Cells were incubated at 37°C in a humidified atmosphere of air/CO_2 (19:1). Cells were split 1:3 every 7 days and were used before Passage 8.

Mitogenic Activity of VEGF

Confluent monolayers of HUVEC were trypsinized with EDTA-trypsin and plated at a density of 10^4 cells/ml^{-1} (200 μl/well) in gelatin-coated 96-well plates. After 24 hours in full medium, cells were incubated for a further 24 hours in media containing charcoal-stripped serum (10% v/v). Stimulation was initiated with agonist in medium M199 containing stripped serum (10% v/v). Cells were incubated at 37°C in a humidified atmosphere for 72 hours. After 67 hours, 3–4,5 dimethylthiazole-2,5 diphenyl tetrazolium bromide (MTT) was added to each well (final concentration, 500 μg/ml). Cell viability was assessed during the last 5 hours of culture by reduction of MTT to an insoluble formazan salt, monitoring by dissolution in dimethylsulfoxide, and measuring spectrophotometric absorption at 550 nm.

Assay for PLD Activity

For the assay of PLD-stimulated ^{3}H-labeled [^{3}H]PtdButOH accumulation, confluent monolayers of HUVEC were trypsinized with EDTA-trypsin and plated into gelatin-coated multiwell culture plates at 2×10^5 cells/well in 12-well plates or 10^5 cells/well in 24-well plates. Cells were incubated in serum-free M199 containing 4 μCi/ml of [^{3}H]palmitic acid for 24 hours at 37°C and were preincubated with butanol (30 mM, 5 minutes) before initiation of the reaction. Stimulation was initiated with agonist in M199 containing BSA (0.1% w/v). The reaction was terminated by rapid aspiration followed by the addition of 0.5 ml of ice-cold methanol, then washed with a further 0.2 ml, and the extracts were transferred to glass vials. Chloroform (0.7 ml) was added, and the samples were left to extract for 45 minutes. The phases were split by the

addition of water to a final ratio of 1:1:0.9 (methanol-:chloroform:water) followed by centrifugation. The aqueous phase was removed, and the lower phase was dried in a gyro-vac. A small quantity of unlabeled PtdButOH was added to the samples to enable determination of the position of the [^{3}H]PtdButOH peak with iodine. Radiolabeled products were separated by thin-layer chromotography using an organic phase of 2,2,4-trimethylpentane:ethyl acetate:acetic acid:water (5:11:2:10, v/v). The position of the PtdButOH spot was determined by iodine staining, and the spot was scraped, collected in vials with scintillation fluid (4 ml), and then counted for 1 minute after sublimation.

Measurement of Total Inositol Phosphates

Confluent monolayers of HUVEC were trypsinized with EDTA-trypsin and plated into gelatin-coated multiwell culture plates at 2×10^5 cells/well in 12-well plates or 10^5 cells/well in 24-well plates. Cells were incubated in serum-free M199 containing 3 μCi/ml [^{3}H]myoinositol for 24 hours at 37°C, washed twice in Hanks' buffer containing 0.1% BSA, and then incubated in buffer supplemented with LiCl (10 mM). Stimulation was initiated with the given concentration of agonist in buffer containing LiCl (10 mM) at 37°C. The reaction was terminated by aspirating the media and replacing it with ice-cold perchloric acid (5% w/v; 0.5 ml) for 30 minutes on ice to extract cellular ^{3}H-labeled inositol phosphates. Cell extracts were neutralized, and total inositol phosphate accumulation was determined as described by Black and Wakelam (1990). In certain experiments, cells were loaded with [^{3}H]myoinositol as above, then washed briefly in Hanks' buffer containing EGTA (1 mM) and reincubated in low-calcium (150 nM) buffer before stimulation with VEGF. Total accumulation of inositol phosphates was determined as before.

Intracellular Ca^{2+} Measurements

For [Ca^{2+}]i measurements, confluent monolayers of HUVEC were trypsinized with EDTA-trypsin and loaded with Fura-2 (2 μM, acetoxymethyl ester form) for 45 minutes at 37°C at a density of 10^7 cells/ml in complete media. Cells were then washed and resuspended in Hanks' buffer, pH 7.4, at 2×10^6 cells per ml.

Fura-2 fluorescence was measured from 1-ml samples of cell suspension (2×10^6 cells/ml) in a stirred cuvette using a Hitachi F-2000 fluorescence spectrophotometer (Yokohama, Japan). Excitation wave lengths of 340 and 380 nm were provided by a rotating filter wheel. [Ca^{2+}]i was calculated from the 340:380 nm fluorescence ratio according to th method of Grynkiewicz et al (1985). R_{max} was determined after addition of Triton X-100 (final concentration, 10 mM), and R_{min} was determined after the subsequent addition of EGTA (final concentration, 10 mM).

To determine response in the absence of extracellular [Ca^{2+}], cells were incubated with EGTA (10 mM, 5 minutes) before the addition of an agonist. R_{max} was determined by adding Triton X-100 (final concentration, 10 mM), and R_{min} was determined after the addition of $CaCl_2$ (final concentration, 100 mM).

Acknowledgements

We thank Zeneca Pharmaceuticals plc for kindly supplying recombinant human VEGF and Roche Products for the generous gift of Roche 31.8220.

References

Ahmed A, Plevin R, Shoaibi MA, Fountain SA, Ferriani RA, and Smith SK (1994). Basic FGF stimulates phospholipase D in endothelial cells in the absence of inositol lipid hydrolysis. Am J Physiol 266:C206–C212.

Black FM and Wakelam MJO (1990). Activation of inositol phospholipid breakdown by prostaglandin-F2-alpha without any stimulation of proliferation in quiescent NIH-3T3 fibroblasts. Biochem J 266:661–667.

Bonser RW, Thompson NT, Randall RW, Tateson JE, Spacey GD, Hodson HF, and Garland LG (1991). Demethoxyviridin and wortmannin block phospholipase C and phospholipase D activation in the human neutrophil. Br J Pharmacol 103: 1237–1241.

Brock TA, Dvorak HF, and Senger DR (1991). Tumor-secreted vascular permeability factor increases cytosolic Ca^{2+} and von Willebrand factor release in human endothelial cells. Am J Pathol 138:213–221.

Brown LF, Berse B, Jackman RW, Tognazzi K, Guidi AJ, Dvorak HF, Senger DR, Connolly JL, and Schnitt SJ (1995). Expression of vascular permeability factor (vascular endothelial growth factor) and its receptors in breast cancer. Hum Pathol 26:86–91.

Brown LF, Berse B, Jackman RW, Tognazzi K, Manseau EJ, Senger DR, and Dvorak HF (1993). Expression of vascular permeability factor (vascular endothelial growth factor) and its receptors in adenocarcinomas of the gastrointestinal tract. Cancer Res 53:4727–4735.

Collard JG (1996). Signalling pathways regulated by rho-like proteins: A possible role in tumour formation and metastasis. Int J Oncol 8:131–137.

Cook SJ, Briscoe CP, and Wakelam MJO (1991). Regulation of phospholipase D and its role in sn 1:2-diradylglycerol formation in bombesin and phorbol 12-myristate and 13-acetate-stimulated Swiss 3T3 cells. Biochem J 280:431–438.

Cook SJ and Wakelam MJO (1992). Epidermal growth factor increases sn-1,2-diacylglycerol levels and activates phospholipase D-catalysed phosphatidylcholine breakdown in Swiss 3T3 cells in the absence of inositol-lipid hydrolysis. Biochem J 285:247–253.

Cross MJ, Roberts S, Ridley AJ, Hodgkin MN, Stewart A, Claesson-Welsh L, and Wakelam MJO (1996). Stimulation of actin stress fibre formation mediated by activation of phospholipase D. Curr Biol 6:588–597.

Devries C, Escobedo JA, Ueno H, Houck K, Ferrara N, and Williams IT (1992). The fms-like tyrosine kinase, a receptor for vascular endothelial growth factor. Science 255:989–991.

Ferrara N (1995). The role of vascular endothelial growth factor in pathological angiogenesis. Breast Cancer Res Treat 36:127–137.

Grynkiewicz G, Poenie M, and Tsien RY (1985). A new generation of calcium indicators with greatly improved fluorescence properties. J Biol Chem 260:3440–3450.

Guo D, Jia Q, Song HY, Warren R, and Donner DB (1995). Vascular endothelial cell growth factor promotes tyrosine phosphorylation of mediators of signal transduction that contain SH2 domains. J Biol Chem 270:6729–6733.

Ha KS and Exton JH (1993). Activation of actin polymerisation by phosphatidic acid derived from phosphatidylcholine in IIC9 fibroblasts. J Cell Biol 123:1789–1796.

Jaffe EA, Nachman RL, Becker CG, and Minick CR (1973). Culture of human endothelial cells derived from umbilical veins. J Clin Invest 52:2745–2756.

Jiang H, Luo JQ, Urano T, Frankel P, Lu Z, Foster DA, and Feig LA (1995). Involvement of Ral GTPase in v-Src-induced phospholipase D activation. Nature 378:409–412.

Kim KJ, Li B, Winer J, Armanini M, Gillett N, Phillips HS, and Ferrara N (1993). Inhibition of vascular endothelial growth factor-induced angiogenesis suppresses tumour growth in vivo. Nature 362:841–846.

Klagsbrun M and Soker S (1993). VEGF/VPF: The angiogenesis factor found? Curr Biol 3:699–702.

Kuribara, H, Tago K, Yokozeki T, Sasaki T, Takai Y, Morii N, Narumiya S, Katada T, and Kanaho Y (1995). Synergistic activation of rat brain phospholipase D by ADP-ribosylation factor and rhoA p21, and its inhibition by clostridium botulinum C3 exoenzyme. J Biol Chem 270:25667–25671.

Lopez I, Burns DJ, and Lambeth JD (1995). Regulation of phospholipase D by protein kinase C in human neutrophils. J Biol Chem 270:19465–19472.

Meldrum E, Parker P, and Carozzi A (1991). The PtdIns-PLC superfamily and signal transduction. Biochim Biophys Acta 1092:49–71.

Millauer B, Shawver LK, Plate KH, Risau W, and Ullrich A (1994). Glioblastoma growth inhibited in vivo by a dominant negative flk-1 mutant. Nature 367:576–579.

Pai JK, Frank EA, Blood C, and Chu M (1994). Novel ketoepoxides block phospholipase D activation and tumor cell invasion. Anticancer Drug Dev 9:363–372.

Pepper MS, Ferrara N, Orci L, and Montesano R (1992). Potent synergism between vascular endothelial growth factor and fibroblast growth factor in the induction of angiogenesis in vitro. Biochem Biophys Res Commun 189:824–831.

Pepper MS, Ferrara N, Orci L, and Montesano R (1991). Vascular endothelial growth factor (VEGF) induces plasminogen activators and plasminogen activator inhibitor-1 in microvascular endothelial cells. Biochem Biophys Res Commun 181:902–906.

Plate KH, Breier G, Weich HA, and Risau W (1992). Vascular endothelial growth factor is a potential tumour angiogenesis factor in human gliomas in vivo. Nature 359:845–848.

Powis G (1994). Pharmacological intervention with signal transduction. In: Workman P, editor. New approaches in cancer pharmacology: Drug design and development, vol. 2. Berlin: Springer-Verlag, 39–54.

Senger DR, Galli SJ, Dvorak AM, Perruzzi CA, Harvey VS, and Dvorak HF (1983). Tumor cells secrete a vascular permeability factor that promotes accumulation of ascites fluid. Science 219:983–985.

Senger DR, Van de Water L, Brown LF, Nagy JA, Yeo KT, Yeo TK, Berse B, Jackman RW, Dvorak AM, and Dvorak HF (1993). Vascular permeability factor in tumour biology. Cancer Metast Rev 12:303–324.

Shweiki D, Itin A, Soffer D, and Keshet E (1992). Vascular endothelial growth factor induced by hypoxia may mediate hypoxia-initiated angiogenesis. Nature 359:843–845.

Takahashi Y, Kitadai Y, Buana CD, Cleary KR, and Ellis LM (1995). Expression of vascular endothelial growth factor and its receptor, KDR, correlates with vascularity, metastasis and proliferation of human colon cancer. Cancer Res 55:3964–3968.

Terman BI, Dougher-Vermazen M, Carrion ME, Dimitrov D, Armellino DC, Gospodarowicz D, and Böhlen P (1992). Identification of kdr tyrosine kinase as a receptor for vascular endothelial cell growth factor. Biochem Biophys Res Commun 187:1579–1586.

Waltenberger J, Claesson-Welsh L, Siegbahn A, Shibuya M, and Heldin CH (1994). Different signal transduction properties of KDR and Flt-1, two receptors for vascular endothelial growth factor. J Biol Chem 269:26988–26995.

Williger BT, Reich R, Neeman M, Bercovici T, and Liscovitch M (1995). Release of gelatinase A induced by photolysis of caged phosphatidic acid. FASEB J 9:A1369.

QP187.A1E
adams
NPL
428384

STIC-ILL

From: Holleran, Anne
Sent: Monday, January 20, 2003 11:57 AM
To: STIC-ILL
Subject: refs. for 09/868,968

Please send copies of the following papers:

1.	Hoyoku,	Anticancer Res. (1999) 19(5A): 3663-3664
2.	Chamson-Reig	Endocrinology (1999) 140(8): 3573-3580
3.	Lixin,	J. Medicinal Chemistry 91998) 41(18): 3303-3306
4.	Yorek,	American J. Physiology (1998) 274(1, part1): C58-C71
5.	Nazih-Sanderson	Biochimica et Biophysica Acta (1997) 1346(1): 45-60
6.	Wattenberg	Cancer Research (1996) 56(22): 5132-5135
7.	Caro	Infection and Immunity (1996) 64(8): 3438-3441
8.	Seymour	Laboratory Investigation (1996) 75(3): 427-437
9.	Brunn	Cancer Chemotherapy (1994) 35(1): 71-79
10.	Kopp	Cancer Research (1990) 50(20): 6490-6496
11.	Tanino	Japanese J. Experimental Medicine (1972) 42(6): 575-582
12.	Eagle	Biochmistry (1963) 2(5): 1125-1126
13.	Caro	Biochem. Mol. Med. (1997) 61: 214-228

10433213

9360051

Anne Holleran
AU: 1642
Tel: 308-8892
RM: 8e03

mailbox: 8e12

0013-7227/99/$03.00/0
Endocrinology

Vol. 140, No. 8
Printed in U.S.A.

Alterations in Intracellular Messengers Mobilized by Gonadotropin-Releasing Hormone in an Experimental Ovarian Tumor*

ASTRID CHAMSON-REIG, OMAR P. PIGNATARO, CARLOS LIBERTUN, AND VICTORIA A. R. LUX-LANTOS

Instituto de Biología y Medicina Experimental-CONICET, 1428 Buenos Aires, Argentina

ABSTRACT

Cells derived from an experimental luteinized ovarian tumor are more sensitive to GnRH endocrine action than control luteal cells. In an attempt to understand the possible causes of the differential sensibility to GnRH action, we examined the number and affinity of GnRH receptors and the second messenger response to GnRH stimulation in both tissues. For GnRH receptor studies membranes were obtained from 4- to 6-week-old ovarian tumors (luteoma) and ovaries from prepubertal rats treated with 25 IU PMSG and 25 IU hCG (SPO) and were incubated with [^{125}I]Buserelin. The number of GnRH receptors were increased in luteoma compared with that in SPO ovaries; dissociation constants were similar in both tissues. GnRH stimulation of second messenger release was assessed in cells obtained from luteoma and SPO ovaries by collagenase treatment. Buserelin (100 ng/ml) induced a significant 35% calcium increase in SPO cells, as determined by the fura-2 method; in luteoma cells no response was observed after buserelin stimulation, although a calcium transient was induced by thapsigargin (0.5 μM), an inhibitor of Ca^{2+}-adenosine triphosphatase associated with the endoplasmic reticulum. The effect of buserelin on inositol phosphates was evaluated after incubation of luteoma and SPO cells with [^{3}H]myo-inositol for 48 h. Buserelin induced a 400% increase in inositol trisphosphate in SPO cells. Again, luteoma cells did not respond to buserelin stimulation, although NaF (10 mM), an activator of G proteins coupled to phospholipase C, induced an 800% increase in inositol trisphosphate. Although the number of GnRH receptors is augmented in luteoma cells, justifying an increased endocrine response, neither inositol phosphates nor intracellular calcium were released by a GnRH analog, indicating the uncoupling of GnRH receptors from phospholipase C. These data provide evidence that the transformation of the ovary into a luteoma implies the acquisition of novel characteristics in the GnRH receptor second messenger-generating system. (*Endocrinology* **140:** 3573–3580, 1999)

IN PREVIOUS studies we have reported that intrasplenic ovarian tumors, which develop in response to the high gonadotropin levels characteristic of this model (1–3), regress significantly under a GnRH analog treatment, principally due to desensitization of the pituitary (4). Nevertheless, a direct effect of GnRH agonists on this ovarian tumor was also described, as it possesses GnRH receptors, and GnRH analogs inhibit the LH-induced progesterone secretion *in vitro* (5). In fact, the inhibitory effect elicited by GnRH on steroidogenesis was more intense in tumor cells than in control luteal cells from superovulated prepubertal rats (SPO) under the experimental conditions studied. Differences in GnRH action between both kinds of cells could be due to a variety of factors, including receptor number or affinity and second messenger mobilization.

GnRH is primarily recognized for its regulation of LH and FSH release from the pituitary. However, it is also thought to be an important paracrine/autocrine regulator in the gonads. A GnRH-like peptide and GnRH receptors have been isolated from ovarian extracts, and transcription from the genes has also been confirmed in this tissue (6–10). The identification of ovarian GnRH receptors and evidence of direct effects of the decapeptide on steroidogenesis (11–13) lend credence to its putative role as an intraovarian hormone. With regard to the mechanism of action of this peptide, it has been shown that activation of GnRH receptors in ovarian cells, like that in pituitary cells, is associated with G protein-mediated activation of phospholipase C (PLC) (11, 14, 15). Rapid incorporation of [^{32}P]orthophosphate into phosphatidic acid and phosphatidylinositols and hydrolysis of phosphatidylinositol (PI) mono- and bis-phosphates with rapid formation of inositol mono-, bis-, and tris-phosphates (InsP, $InsP_2$, and $InsP_3$) and diacylglycerol (DAG) have been described in ovarian tissue. Inositol-1,4,5-trisphosphate ($InsP_3$), acting on $InsP_3$-specific receptors at the endoplasmic reticulum, induces a rapid increase in intracellular Ca^{2+} ($[Ca^{2+}]_i$), although actions at the plasma membrane have also been described. In addition to its now classic effects through activation of phospholipase C, GnRH may exert its action through phospholipase A_2 and phospholipase D stimulation (15).

The present set of experiments was designed to evaluate both GnRH receptor number and affinity and second messenger response to GnRH stimulation comparatively in luteoma and control luteal cells.

Received November 5, 1998.

Address all correspondence and requests for reprints to: Dr. Carlos Libertun, Instituto de Biología y Medicina Experimental, Vuelta de Obligado 2490, 1428 Buenos Aires, Argentina. E-mail: libertun@dna.uba.ar.

* The data in this paper are from a thesis to be submitted for the degree of Doctor of Philosophy at the University of Buenos Aires (Buenos Aires, Argentina). Portions of this work have been presented in abstract form at the meeting of the Argentine Society of Clinical Investigation, Mar del Plata, Argentina, November 1997. This work was supported by the University of Buenos Aires, Agencia Nacional de Promocion Cientifica y Tecnologica and Consejo Nacional De Investigaciones Cientificas y Tecnicas (CONICET) (Buenos Aires, Argentina).

Materials and Methods

Adult female virgin Sprague Dawley rats (200–250 g) from the Instituto de Biología y Medicina Experimental colony were housed in groups in an air-conditioned room, with lights on from 0700–1900 h. They were given free access to laboratory chow and tap water. At the end of the experimental procedures, animals were killed by decapitation according to protocols for animal use approved by the institutional animal care and use committee (IBYME-CONICET) that follows NIH guidelines.

Tumor-bearing animals were bilaterally ovariectomized, and one ovary was implanted into the spleen 4–6 weeks before the experiments (luteoma), as previously described (3–5).

Control animals were 23- to 25-day-old female rats injected with 25 IU PMSG (Novormon, Syntex, Buenos Aires) and 25 IU hCG (Endocorion, Elea, Buenos Aires) 48 h later. These animals were used 5 days after hCG injection (SPO).

For GnRH receptor studies only, a second control group was used: 23- to 25-day-old female prepubertal rats without any treatment (PP). This group was included in receptor studies because it has been shown that prepubertal ovaries possess the maximal amount of ovarian GnRH receptors (16, 17); therefore, it served as a control of receptor levels for the experimental groups (luteoma and SPO).

GnRH receptors

Iodination of tracer ([^{125}I]Buserelin) and receptor assays were performed as described previously (5). Briefly, for saturation analysis, membranes from ovaries from SPO and PP rats or luteoma were obtained and incubated with 5–8 × 10^4 cpm [^{125}I]GnRH agonist. Ligand concentrations were near saturating, representing about 85% receptor occupancy. Nonspecific binding was determined by addition of 1 × 10^{-6} M unlabeled GnRH agonist and represented 5–8% of the total iodinated tracer. For Scatchard analysis, membranes were incubated with increasing concentrations of the labeled analog (5,000–120,000 cpm). In all cases tubes were incubated for 120 min on ice, and the reaction was terminated by centrifugation at 13,000 rpm for 20 min at 4 C. The supernatants were aspirated and discarded, and the pellets were counted in a γ-spectrometer.

Luteal cells

Animals were operated on as described above to induce the development of the luteoma and were left undisturbed for 4–6 weeks. Cells from ovarian tumors as well as from 23- to 25-day-old SPO were isolated with collagenase, as described previously (4, 5). Cells were then used either the same day for calcium measurements or plated in plastic 24-multiwell plates coated with rat tail collagen (~750,000 cells/ml in DMEM-Ham's F-12 with 2.2 g/liter sodium bicarbonate, 10% FCS, Nystatin, and gentamicin) for inositol phosphate studies. Note the similitude between both cell types, as observed by light microscopy in fresh cell cultures (10-fold; Fig. 1).

Intracellular Ca^{2+} measurements

Intracellular calcium was measured as described previously (18). Briefly, fura-2/AM (tetracetoxymethylesther fura-2) was used as a fluorescent indicator. The pellet of luteal cells of each experimental group (luteoma and SPO) was redispersed and incubated in the presence of 2 μM fura-2/AM for 45 min at 37 C in an atmosphere of 5% CO_2. Cells were then washed twice and prepared at a density of 2 × 10^6 cells/ml. Fluorescence was measured in a spectrofluorometer (Jasco Corp., Tokyo, Japan) provided with the accessory CA-261 to measure Ca^{2+} with continuous stirring, thermostat adjusted to 37 C, and injection chamber. Intracellular Ca^{2+} levels were registered every second by exposure to alternating 340- and 380-nm light beams, and the intensity of light emission at 505 nm was measured. Drugs (5 μl) were injected into the chamber at 2 min (concentration in chamber, 100 ng/ml buserelin, 1 × 10^{-12} M hCG, or 0.5 μM thapsigargin). The preparation was calibrated determining maximal fluorescence induced by 0.1% Triton X-100 (F_{max}) and minimal fluorescence (F_{min}) in the presence of 5 mM EGTA. $[Ca^{2+}]_i$ was calculated according to the method of Grynkiewicz (19). Basal values were considered to be those measured during the first minute of the experiment. Resulting graphs were scanned, processed, and quantified using Ungraph 2.0 and Excel 5.0 software. Results were normalized with respect to average basal levels. Experiments were repeated three to six times.

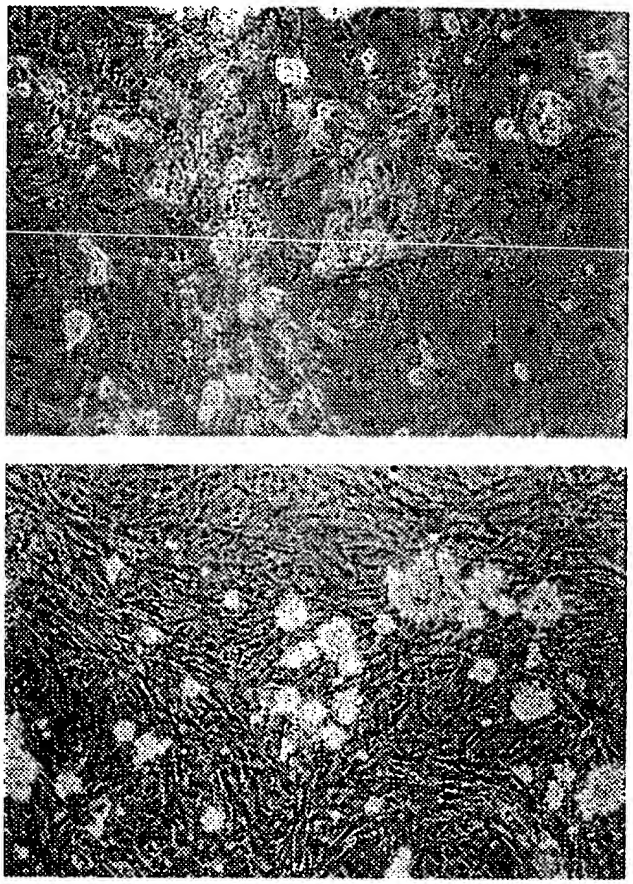

FIG. 1. Light microscopy photomicrographs of luteoma (*upper panel*) and superovulated prepubertal ovarian cells (*lower panel*) after 72 h in culture (magnification, ×10).

Measurement of inositol phosphates

Inositol phosphates were measured as described previously (20) with minor modifications. Briefly, 1 day after plating, the medium in the wells was changed to fresh medium containing 4 μCi/ml [^{3}H]myo-inositol and incubated for 48 h before the experiment. At the end of the labeling period, the cells were washed twice with DMEM-Ham's F-12 with 2.2 g/liter sodium bicarbonate containing 0.1% BSA (buffer 1). Cells were then incubated in buffer 1 with 20 mM LiCl for 15 min. Thereafter, stimuli (10 μl) were added (final concentrations in the well, 1 and 100 ng/ml Buserelin and 10 mM NaF), and cells were further incubated for 30 min. After the incubation, the cells were placed on ice, treated with 0.5 M $HClO_4$, and scraped. Well contents were transferred to tubes and centrifuged. The pellets were kept for DNA measurement. The neutralized supernatants (0.72 M KOH and 0.6 M $HKCO_3$) were chromatographed on Dowex (Bio-Rad Laboratories, Inc., Hercules, CA) columns (formate form) to elute InsP, $InsP_2$, and $InsP_3$. Two-milliliter aliquots of each wash were mixed with 6 ml Optiphase Hisafe 3 (Wallac, Turku, Finland) and counted in a liquid scintillation counter. Experiments were repeated three to five times.

Statistical analysis

Scatchard analysis of binding data was performed using a computer curve-fitting program (Ligand) for a single class of binding sites. Changes in receptor number among groups were analyzed using one-

way ANOVA followed by Tukey's test. In intracellular calcium studies, the amount of calcium released was assessed by the area under the curve between 2 and 3 min or 2 and 4.30 min, depending on the stimulus; differences in areas were analyzed by multiple variance analysis for paired samples, followed by Tukey's test. For inositol phosphate studies, differences among groups were analyzed by multiple variance analysis for paired samples, followed by Tukey's test. In all cases $P < 0.05$ was considered significant.

Drugs

[D-Ser(tBu)^6-des-Gly^{10}]GnRH-*N*-ethylamide (Buserelin), a GnRH agonist, was a gift from Hoechst (Buenos Aires, Argentina). PMSG (Novormon) was a gift from Syntex (Buenos Aires, Argentina), and hCG (Endocorion) was purchased from Elea (Buenos Aires, Argentina). NaF, myo-inositol, LiCl, fura-2/AM, and thapsigargin were purchased from Sigma Chemical Co. (St. Louis, MO). ^{125}Iodine and [2-N-^{3}H]myo-inositol (20 Ci/mmol) were obtained from NEN Life Sciences Products (Boston, MA).

Results

GnRH receptors in ovarian tissues from luteoma-bearing rats, prepubertal female rats, and SPO rats

According to Scatchard analysis ovarian tissues showed a single class of high affinity binding sites (Fig. 2, *upper panel*). K_d values were similar among the groups (PP, 0.054 ± 0.020 nM; SPO, 0.048 ± 0.039 nM; luteoma, 0.047 ± 0.032 nM).

Significant differences in GnRH receptor numbers were observed among all ovarian tissues ($P < 0.001$; Fig. 2, *lower panel*). Ovaries of PP animals had the largest number of GnRH receptors, followed by the luteoma group and finally by the ovaries of SPO rats.

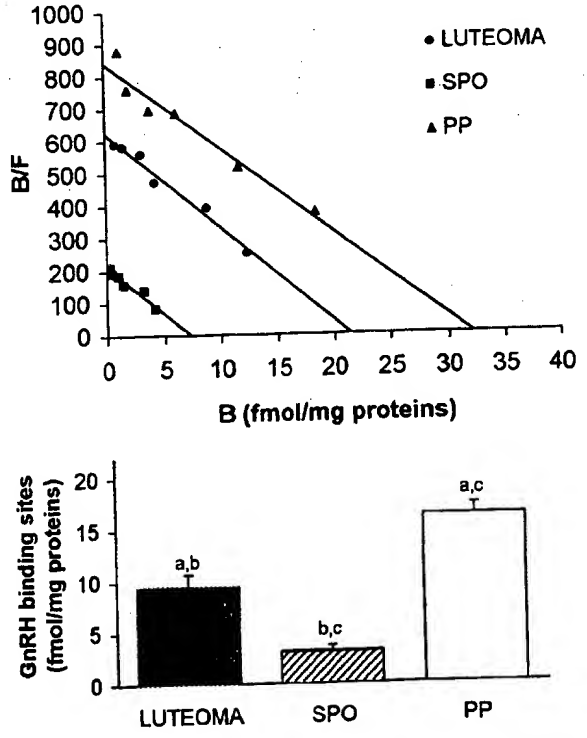

FIG. 2. GnRH receptors in ovarian tissues. *Upper panel*, Scatchard analysis of GnRH binding to membranes of ovarian tumors (LUTEOMA), prepubertal ovaries (PP), and superovulated prepubertal ovaries (SPO). One experiment representative of three is shown. *Lower panel*, Number of GnRH receptors in the different tissues determined by saturation analysis (n = 8 for each tissue). a, Significantly different from SPO; b, significantly different from PP; c, significantly different from LUTEOMA.

$[Ca^{2+}]_i$ mobilization in ovarian cells from luteoma and ovaries from SPO rats

Changes in intracellular calcium induced by different stimuli were monitored in luteoma and SPO cells. No differences were observed in basal calcium levels between the groups (basal $[Ca^{2+}]_i$, 171.6 ± 23.5 and 194.5 ± 18.1 nM in luteoma and SPO cells, respectively; n = 5). As expected, Buserelin induced a significant and classical release of $[Ca^{2+}]_i$ in SPO cells. In contrast, no mobilization of calcium was observed in luteoma cells (Fig. 3 and Table 1). hCG, an agent proposed to activate PLC in the ovary, was also able to induce a significant increase in $[Ca^{2+}]_i$ levels in SPO cells, although of less magnitude than that induced by Buserelin, both at concentrations that induce maximal endocrine responses (Table 1). Again, luteoma cells were unresponsive (Fig. 4). Thapsigargin, an inhibitor of Ca^{2+}-adenosine triphosphatase associated with the endoplasmic reticulum, induced calcium release in both cell types (Fig. 5), although the levels achieved were significantly higher in luteoma than in SPO cells [area under the plateau from 2.05–4.55 min: luteoma, 2195 ± 371.3 (7%); SPO, 1187 ± 195.3 (6%); $P < 0.05$].

Inositol phosphates in cell cultures from luteoma and ovaries from SPO rats

No significant differences in basal total inositol phosphates, including InsP, $InsP_2$, and $InsP_3$, were observed between luteoma- and SPO-derived cells. In SPO cells, Buserelin (100 ng/ml) and NaF (10 mM) induced significant increases in total inositol phosphates ($P < 0.01$; Fig. 6). Buserelin in concentrations as low as 1 ng/ml was still able to significantly increase inositol phosphate levels in SPO cells, although to a lesser degree than 100 ng/ml Buserelin. This indicated a concentration-dependent effect [1 ng/ml Buserelin, 4210 ± 380 cpm; 100 ng/ml Buserelin, 5970 ± 590 cpm;

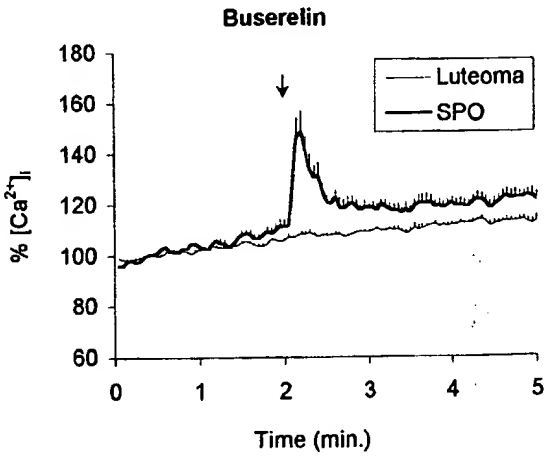

FIG. 3. $[Ca^{2+}]_i$ mobilization induced by Buserelin (100 ng/ml in chamber) in luteoma and SPO cells. *Curves* represent the average of five experiments (percent increase with respect to basal levels), and *lines on top* represent the SE for each point. Basal levels are cited in the text. Buserelin was administered at 2 min.

TABLE 1. Areas (percentages) under the peak of intracellular calcium curves induced by different stimuli in dispersed luteoma and SPO cells from 2.05–3.05 min

	Control	Buserelin (100 ng/ml)	hCG (1×10^{-12} M)
Luteoma	63.6 ± 5.7	52.5 ± 15.5[a]	51.4 ± 13.3[a]
SPO	71.3 ± 24.4	319.8 ± 35.1[b,c]	233.3 ± 40[c]

Multiple ANOVA for repeated measures indicates interaction $P < 0.01$. For this and the next table, cells treated with different stimuli come from the same batch of cells. Number of experiments, 4.

[a] Significantly different from SPO cells, $P < 0.05$ or less.

[b] Significantly different from hCG in SPO cells, $P < 0.05$ or less.

[c] Significantly different from control in each cell type, $P < 0.05$ or less.

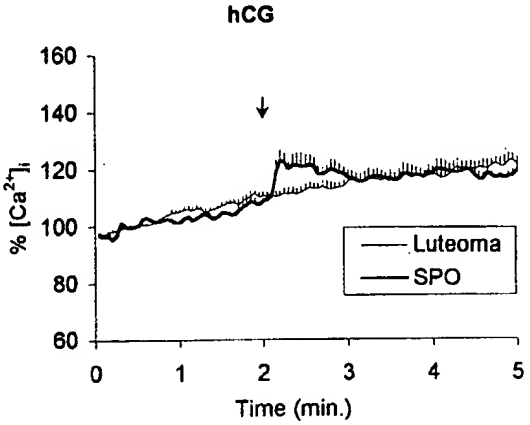

FIG. 4. $[Ca^{2+}]_i$ mobilization induced by hCG (1×10^{-12} M) in luteoma and SPO cells. *Curves* represent the average of four experiments. hCG was administered at 2 min.

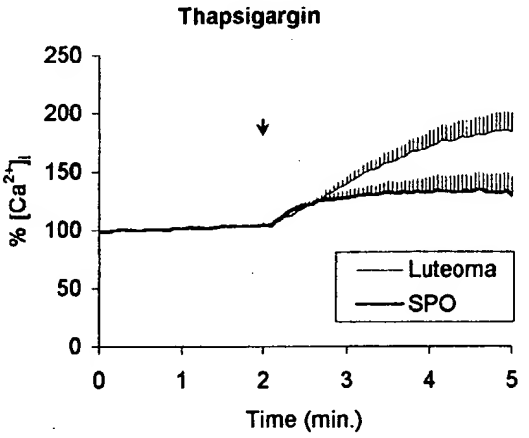

FIG. 5. $[Ca^{2+}]_i$ mobilization induced by thapsigargin (0.5 μM) in luteoma and SPO cells. *Curves* represent the average of six or seven experiments. Thapsigargin was administered at 2 min.

n = 3; by one-way ANOVA of control, 1 ng/ml Buserelin, and 100 ng/ml Buserelin followed by Student-Newman-Keuls test: 1 ng/ml Buserelin *vs.* 100 ng/ml Buserelin, $P < 0.05$]. In contrast, in luteoma cells only NaF was able to significantly augment total inositol phosphate levels ($P < 0.05$). The percent increase induced by NaF was significantly higher in SPO than in luteoma cells (SPO, 950 ± 132%; luteoma, 700 ± 106%; $P < 0.05$). When the effects of the different stimuli were analyzed on separate inositol phosphates (InsP, $InsP_2$, and $InsP_3$) formed from the hydrolysis of phosphatidylinositols in both kinds of cells, it was observed that in SPO cells both Buserelin and NaF significantly stimulated the increase of all three inositol phosphates (Fig. 7). Again, a concentration-dependent response to Buserelin (1 and 100 ng/ml) was observed in InsP, $InsP_2$, and $InsP_3$ in control cells (not shown), like that observed in total inositol phosphates. In luteoma cells, NaF significantly affected the three inositol phosphates analyzed, whereas Buserelin had no significant effect on any of them. Interestingly, for Buserelin the highest percent increase over basal levels in the different inositol phosphates was noted in $InsP_2$, whereas for NaF, which stimulated the G protein directly, the maximal increase was observed in $InsP_3$ (Table 2). Moreover, the percent increase in $InsP_3$ induced by NaF in both cell kinds was very similar (Table 2). Although no significant differences in basal levels of total inositol phosphates, InsP, $InsP_2$, or $InsP_3$ were observed between luteoma and SPO cells, intracellular free [^{3}H]inositol levels were significantly higher in SPO cells (Fig. 8). This difference could not be accounted for by differences in [^{3}H]inositol incorporation (luteoma, 300,346 ± 27,934 cpm; SPO, 349,742 ± 17,802 cpm; n = 3; P = NS), which was not significantly different between the groups, or by differences in cell number at the end of the experiments, as these varied maximally by 25% in favor of SPO, as assessed by DNA measurement in the pellets after cell lysis (not shown). After 30-min incubation with the different stimuli, a significant decrease in free [^{3}H]inositol was only observed after Buserelin treatment in SPO cells (Fig. 8). Decreases in free inositol in response to PLC-activating agents have been reported previously (21). It is interesting to note that NaF, which

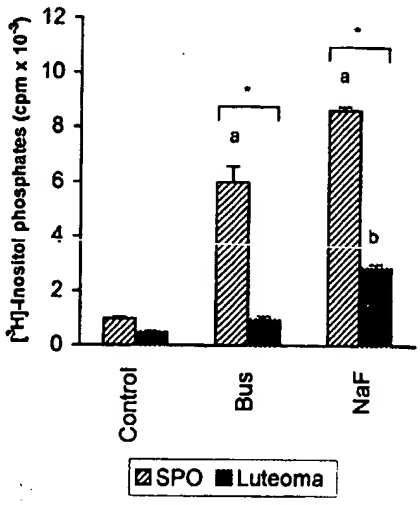

FIG. 6. Effect of 30-min stimulation with Buserelin (Bus; 100 ng/ml) and NaF (10 mM) on total inositol phosphates (counts per min/1 × 10^{-3}) in luteoma and SPO cells in primary culture. Cells were labeled with 4 μCi [^{3}H]inositol and preincubated with LiCl (20 mM). Results represent the average of five experiments. Multiple ANOVA of repeated measures indicates a significant interaction ($P < 0.01$). For this and the following figures, the *asterisk* indicates a significant difference between cell types for a given stimulus. a, Significantly different from control levels in SPO cells. b, significantly different from control levels in luteoma cells. In all cases, $P < 0.05$ or less.

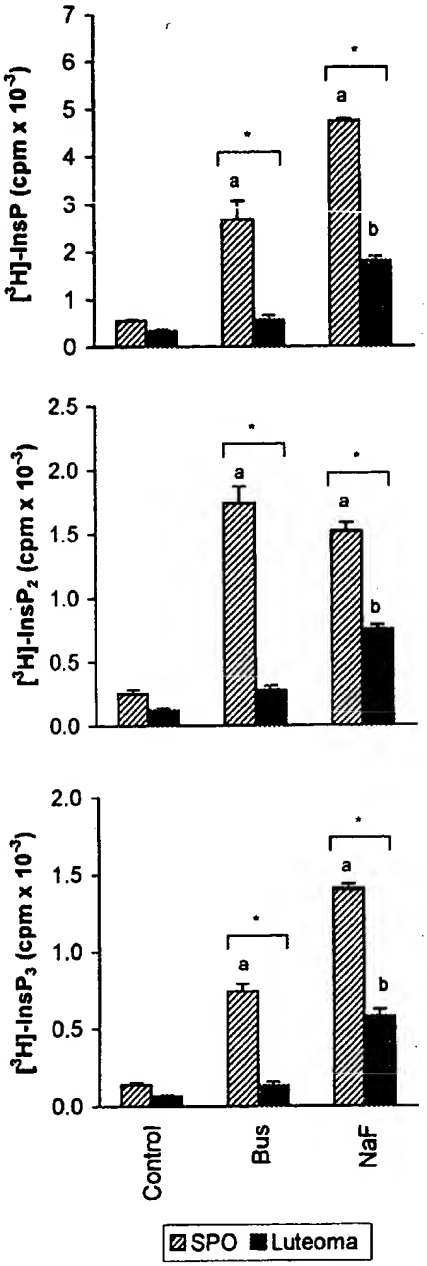

FIG. 7. Effects of Buserelin (Bus; 100 ng/ml) and NaF (10 mM) on InsP (*upper panel*), $InsP_2$ (*middle panel*), and $InsP_3$ (*lower panel*) in luteoma and SPO cells in primary culture. Conditions were the same as those described in Fig. 6. Results represent the average of three experiments. Multiple ANOVA of repeated measures indicates a significant interaction ($P < 0.01$ or less) for each inositol phosphate.

elicited the largest amount of inositol phosphates, did not alter free [^{3}H]inositol in either cell type.

To determine whether the difference in basal free [^{3}H]inositol between the two cell types could be due to differential incorporation of this compound into the various phosphatidylinositols in the plasma membranes, these were measured, as in previous works (22, 23), after extraction with methanol/chloroform of the membrane

TABLE 2. Percent increase in InsP, $InsP_2$, and $InsP_3$ with respect to control levels (100%) in cultured luteoma and SPO cells after a 30-min incubation with different stimuli

	InsP (%)	$InsP_2$ (%)	$InsP_3$ (%)
SPO			
Buserelin	489 ± 78[a,b]	736 ± 118[a,b]	537 ± 56[a,b]
NaF	862 ± 81[a,b]	638 ± 90[b]	1037 ± 78[b]
Luteoma			
Buserelin	165 ± 15	227 ± 25	205 ± 29
NaF	528 ± 39[b]	625 ± 159[b]	925 ± 89[b]

Data were analyzed by multiple ANOVA for repeated measures for each inositol phosphate.

[a] Levels significantly different from luteoma cells, $P < 0.05$ or less.

[b] Significantly different from control in each cell type, $P < 0.05$ or less.

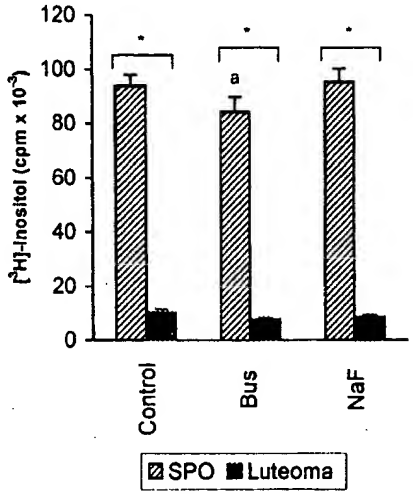

FIG. 8. Free [^{3}H]inositol levels in luteoma and SPO cells. Experimental procedures are detailed in Figs. 6 and 7. Results represent the average of five experiments. Multiple ANOVA of repeated measures indicates a significant interaction ($P < 0.01$).

pellet by TLC. A representative experiment shows that the incorporation of [^{3}H]inositol into PI was specifically augmented in luteoma cells with respect to that in SPO cells (luteoma, 35.1 ± 1.1%; SPO, 21.9 ± 1.0% of radioactivity incorporated into membrane lipids; $P < 0.05$). This 60% increase in [^{3}H]inositol incorporated into PI could be the explanation for the low levels of free inositol observed in luteoma cells.

Discussion

In previous works we had established the participation of GnRH in the control of the endocrine function of these experimental luteoma, indicating a direct effect on the tumor in addition to its effect through gonadotropin modulation (4, 5). Luteoma cells were more sensitive to the GnRH-induced inhibition of progesterone elicited by a LH stimulus than control luteal cells under those experimental conditions. This difference prompted us to study the receptors and mechanisms of action of the decapeptide in more detail in luteoma and control luteal tissue.

GnRH receptors have been described in ovarian tissue (7, 9, 16), and we had already determined their presence in experimental luteoma (5). Significant differences in receptor

number, although not in K_d values, were observed among the tested tissues. Ovarian GnRH receptor number was significantly greater in prepubertal animals than in prepubertal superovulated animals subjected to gonadotropin stimulation. This is in agreement with previous results (16, 17) and parallels the observations in the pituitary, where receptors have been described to be maximal previous to puberty onset (18, 24). Furthermore, receptor number was significantly higher in luteoma tissue than in ovaries from PMSG-hCG-treated prepubertal rats, although both were under the influence of very high gonadotropin levels. This difference in receptor number could justify a higher sensitivity of luteoma cells to GnRH action. It is important to take into account that GnRH receptor number per mg tissue does not increase when an estrous ovary turns into a luteoma (5). In these ovarian tumors, receptor levels are maintained even in the presence of very high gonadotropin levels, marking a difference from control ovaries from prepubertal rats, in which receptors abruptly fall after PMSG-hCG treatment.

Subsequently, the effect of GnRH on the increase in classical second messengers elicited by this peptide, inositol phosphates, and calcium (14, 15, 25) was analyzed to establish whether the increase in receptor number was coupled to an increase in second messenger response. Buserelin, in a dose that was maximal to exert its endocrine action, induced a typical calcium response in control SPO cells, in agreement with results from other laboratories (26–28). Surprisingly, no response was observed in tumor cells. Furthermore, a maximal hCG stimulus was also able to induce a calcium transient in SPO cells, although of lower intensity than that induced by Buserelin. The effect of LH (hCG) on calcium mobilization is controversial. Although the classical mechanism of action of LH implies stimulation of adenylate cyclase and cAMP production (15), the regulation of steroidogenesis by LH may be exerted through the stimulation of multiple pathways. The activation of PLC and intracellular calcium increases have been involved in the action of gonadotropins in the ovary in several species, including the mouse, swine, hen, and cow (29–32). In other species, such as sheep and rats, LH did not induce calcium transients in the ovary (21, 33, 34), although increases in $InsP_3$ formation after LH treatment were observed in these species (35, 36). In our experimental conditions, hCG induced significant calcium increases in rat SPO cells in a variety of concentrations (1×10^{-12} to 1×10^{-9} M; not shown). Again, no effect on intracellular calcium was observed in tumor cells under hCG stimulation. As shown above, we were unable to induce any calcium transients in luteoma cells with the stimuli tested. To evaluate the possibility that luteoma cells were unresponsive to GnRH or hCG but were still able to respond to other calcium-inducing agents, cells were tested in the presence of thapsigargin. Thapsigargin is a specific inhibitor of the endoplasmic reticulum calcium-adenosine triphosphatase (37) and therefore induces increases in cytosolic calcium due to calcium leakage, a mechanism independent of PLC activation. This drug has been shown to induce calcium release in rat ovarian cells (27, 38). In our case, both kinds of cells responded to 0.5 μM thapsigargin with calcium increases, although calcium levels attained in luteoma cells were significantly higher than those in SPO cells. It is interesting to note that although the thapsigargin-sensitive calcium stores in luteoma cells were augmented with respect to those in control cells, they were insensitive to GnRH stimulation. This resistance to increase intracellular calcium levels might be an adaptation of the luteoma cells to maintain low calcium levels, as increases in intracellular calcium, elicited by GnRH or $PGF_{2\alpha}$, have been proposed to induce cell death in ovarian tissue (39–41), which would hinder tumor growth. The use of other pharmacological agents acting on calcium metabolism will allow us to determine whether the impairment of calcium release after specific stimulation is a generalized phenomenon in these cells.

The failure of luteoma cells to respond to GnRH with a calcium transient is not an isolated observation, as it is in agreement with our results in phospholipid hydrolysis. Although both cell types had similar basal levels of inositol phosphates, the GnRH agonist and NaF induced significant increases in inositol phosphates in SPO cells, but only NaF did so in tumor cells. NaF is an activator of G proteins coupled to PLC by substituting for endogenous guanosine triphosphate (42). Therefore, the activation of phospholipid hydrolysis induced by this agent in luteoma cells implies that PLC is active. Moreover, when expressed as a percentage of control levels, the amount of $InsP_3$ formed was identical in luteoma and SPO cells under NaF stimulation. The lack of a significant amount of $InsP_3$ formation in response to Buserelin in luteoma cells correlates with the lack of calcium mobilization observed in these cells under this stimulus. In control SPO cells, Buserelin induced a concentration-dependent increase in all three inositol phosphates, as expected because calcium was also released by this treatment.

Taken together, these results suggest an uncoupling of GnRH and LH membrane receptors from PLC in luteoma cells, as evidenced by the lack of either calcium or inositol phosphate (or both) responses. This implies that the inhibition exerted by GnRH on LH-induced progesterone secretion in these cells, observed in former studies (4, 5), is probably not mediated by the classical GnRH activation of PLC as has been suggested for control luteal cells (14, 15, 21, 25, 26, 41). Alternative mechanisms for GnRH action in the ovary have been proposed. In addition to the generation of the calcium-mobilizing inositol phosphate(s) and protein kinase C (PKC) activator DAG, GnRH has also been reported to cause accumulation of arachidonic acid in ovarian cells (43–45) through PLC or PLA_2 stimulation (43, 46). It has also been suggested that PLA_2-induced increases in arachidonic acid may increase progesterone levels (47); on the other hand, an increase in PLA_2 activity caused a loss in progesterone secretion in late pregnancy (45). GnRH activation of phospholipase D, with a resultant increase in phosphatidic acid, has also been described (48). Among other effects, phosphatidic acid can be converted into DAG without a concomitant increase in $InsP_3$, and DAG has been implicated in PKC activation (49), which, in turn, is postulated to be responsible for the inhibition of LH-induced progesterone secretion (13). Several examples from the literature show that a receptor can be uncoupled from one second messenger-generating system while still being active on another. Davis (42) showed that although the phorbol ester 12-*O*-tetraphorbol 12-myristate 13-acetate, an activator of PKC, inhibited the actions of LH

receptor stimulation on phospholipid turnover, it was without effect on receptor-induced activation of cAMP and progesterone accumulation in bovine luteal cells. Another example was presented by McCann and Flint (50), who showed that treatment of sheep luteal tissue with pertussis toxin inhibited $PGF_{2\alpha}$ action on PLC, whereas the inhibitory effect of $PGF_{2\alpha}$ on LH-stimulated adenylate cyclase was conserved. Therefore, it is possible that although GnRH receptors might be uncoupled from PLC in luteoma cells, they might still be coupled to other second messenger-generating systems, such as PLA_2 or phospholipase D, to produce their antigonadotropic effects. Further studies will be needed to determine which pathway(s) is involved.

Although [^{3}H]inositol incorporation was similar in both cell types, a highly significant difference in free [^{3}H]inositol levels was observed. These levels were approximately 10 times higher in SPO cells than in luteoma cells, marking an interesting alteration in inositol metabolism in tumor cells. A representative experiment shows an important increase in membrane phosphatidylinositol in luteoma cells compared with that in control luteal cells, which could explain this difference. Unusual metabolism of phosphoinositides in tumor cells has been reported previously, as in MA-10 Leydig tumor cells (22, 23). The particular metabolism of phosphoinositides in luteoma cells will be the subject of future research.

In summary, our data show that luteoma cells, which develop under high constant gonadotropin stimulation, possess GnRH receptors that are not down-regulated in this particular endocrine milieu. Furthermore, they are uncoupled from their classic second messenger-generating system, PLC. Metabolism of inositol into phospholipids is also notably altered in luteoma cells. These data provide evidence that the transformation of the ovary into a luteoma implies the acquisition of novel characteristics in the GnRH receptor second messenger-generating system.

References

1. **Biskind M, Biskind G** 1944 Development of tumors in the rat ovary after transplantation into the spleen. Proc Soc Exp Biol Med 55:176–179
2. **Fels E, Moguilevky JA, Libertun C** 1968 Intrasplenic ovarian implants. Studies in androgenized rats. Acta Physiol Lat 18:132–135
3. **Lux VAR, Tesone M, Larrea GA, Libertun C** 1984 High correlation between prolactinemia, 125-I hLH binding and progesterone secretion by an experimental luteoma. Life Sci 35:2345–2352
4. **Lux-Lantos VAR, Thyssen SM, Chamson A, Libertun C** 1995 Effect of a gonadotropin releasing hormone analog on an experimental ovarian tumor: direct and indirect actions. Life Sci 57:291–300
5. **Chamson-Reig A, Lux-Lantos VAR, Tesone M, Libertun C** 1997 GnRH receptors and GnRH endocrine effects on luteoma cells. Endocrine 6:165–171
6. **Clayton RN, Harwood JP, Catt JK** 1979 Gonadotropin-releasing hormone analogue binds to luteal cells and inhibits progesterone production. Nature 282:90–92
7. **Pieper DR, Richards JS, Marshall JC** 1981 Ovarian gonadotropin-releasing hormone (GnRH) receptors: characterization, distribution, and induction by GnRH. Endocrinology 108:1148–1155
8. **Aten RF, Polan ML, Bayless R, Behrman HR** 1987 A gonadotropin-releasing hormone (GnRH)-like protein in human ovaries: similarity to the GnRH-like ovarian protein of the rat. J Clin Endocrinol Metab 64:1288–1293
9. **Peng C, Fan NC, Ligier M, Väänänen J, Leung PCK** 1994 Expression and regulation of gonadotropin-releasing hormone (GnRH) and GnRH receptor messenger ribonucleic acids in human granulosa-luteal cells. Endocrinology 135:1740–1746
10. **Olofsson JI, Conti CC, Leung PCK** 1995 Homologous and heterologous regulation of gonadotropin-releasing hormone receptor gene expression in preovulatory rat granulosa cells. Endocrinology 136:974–980
11. **Stojilkovic SS, Reinhart J, Catt KJ** 1994 Gonadotropin-releasing hormone receptors: structure and signal transduction pathways. Endoc Rev 15:462–499
12. **Behrman HR, Preston SL, Hall AK** 1980 Cellular mechanism of the antigonadotropic action of luteinizing hormone-releasing hormone in the corpus luteum. Endocrinology 107:656–664
13. **Hsueh AJW, Jones PBC** 1981 Extrapituitary actions of gonadotropin-releasing hormone. Endocr Rev 2:437–461
14. **Leung PCK, Wang J** 1989 The role of inositol lipid metabolism in the ovary. Biol Reprod 40:703–708
15. **Leung PCK, Steele GL** 1992 Intracellular signaling in the gonads. Endocr Rev 13:476–498
16. **Harwood JP, Clayton RN, Chen TT, Knox G, Catt KJ** 1980 Ovarian gonadotropin-releasing hormone receptors. II. Regulation and effects on ovarian development. Endocrinology 107:414–421
17. **Jones PBC, Conn PM, Marian J, Hsueh AJW** 1980 Binding of gonadotropin-releasing hormone (GnRH) receptors: characterization, distribution, and induction by GnRH. Life Sci 27:2125–2132
18. **Lacau-Mengido IM, Gonzalez Iglesias A, Lux-Lantos VAR, Libertun C, Becu-Villalobos D** 1998 Ontogenic and sexual differences in pituitary GnRH receptors and intracellular Ca^{2+} mobilization induced by GnRH. Endocrine 8:177–183
19. **Grynkiewicz G, Poenie M, Tsien RY** 1985 A new generation of Ca^{2+} indicators with greatly improved fluorescence properties. J Biol Chem 260:3440–3450
20. **Ascoli M, Pignataro OP, Segaloff DL** 1989 The inositol phosphate/diacylglycerol pathway in MA-10 Leydig tumor cells. J Biol Chem 264:6674–6681
21. **Davis JS, West LA, Farese RV** 1986 Gonadotropin-releasing hormone (GnRH) rapidly stimulates the formation of inositol phosphates and diacylglycerol in rat granulosa cells: further evidence for the involvement of Ca^{2+} and protein kinase C in the action of GnRH. Endocrinology 118:2561–2571
22. **Pignataro OP, Ascoli M** 1990 Epidermal growth factor increases the labeling of phosphatidylinositol 3,4-bisphosphate in MA-10 leydig tumor cells. J Biol Chem 265:1718–1723
23. **Pignataro OP, Ascoli M** 1990 Studies with insulin and insulin-like growth factor-I show that the increased labeling of phosphatidylinositol-3,4-bisphosphate is not sufficient to elicit the diverse actions of epidermal growth factor on MA-10 Leydig tumor cells. Mol Endocrinol 4:758–765
24. **White SS, Ojeda SR** 1981 Changes in ovarian LHRH receptor content during the onset of puberty in the female rat. Endocrinology 108:347–349
25. **Lahav M, West LA, Davis JS** 1988 Effects of prostaglandin $F_{2\alpha}$ and a gonadotropin-releasing hormone agonist on inositol phospholipid metabolism in isolated rat corpora lutea of various ages. Endocrinology 123:1044–1052
26. **Rodway MR, Baimbridge KG, Yuen BH, Leung PCK** 1991 Effect of prostaglandin $F_{2\alpha}$ on cytosolic free calcium ion concentrations in rat luteal cells. Endocrinology 129:889–895
27. **Anderson L, Hillier SG, Eidne KA, Miro F** 1996 GnRH-induced calcium mobilisation and inositol phosphate production in immature and mature rat ovarian granulosa cells. J Endocrinol 149:449–456
28. **Currie WD, Li W, Baimbridge KG, Yuen BH, Leung PCK** 1992 Cytosolic free calcium increased by prostaglandin $F_{2\alpha}$ ($PGF_{2\alpha}$), gonadotropin-releasing hormone, and angiotensin II in rat granulosa cells and $PGF_{2\alpha}$ in human granulosa cells. Endocrinology 130:1837–1843
29. **Gudermann T, Birnbaumer M, Birnbaumer L** 1992 Evidence for dual coupling of the murine luteinizing hormone receptor to adenylyl cyclase and phosphoinositide breakdown and Ca^{2+} mobilization. J Biol Chem 267:4479–4488
30. **Flores JA, Veldhuis JD, Leong DA** 1991 Angiotensin II induces calcium release in a subpopulation of single ovarian (granulosa) cells. Mol Cell Endocrinol 81:1–10
31. **Asem EK, Molnár M, Hertelendy F** 1987 Luteinizing hormone-induced intracellular calcium mobilization in granulosa cells: comparison with forskolin and 8-bromo-adenosine 3′,5′-monophosphate. Endocrinology 120:853–859
32. **Davis JS, Weakland LL, Farese RV, West LA** 1987 Luteinizing hormone increases inositol trisphosphate and cytosolic free Ca^{2+} in isolated bovine luteal cells. J Biol Chem 262:8515–8521
33. **Wiltbank MC, Guthrie PB, Mattson MP, Kater SB, Niswender GD** 1989 Hormonal regulation of free intracellular calcium concentrations in small and large ovine luteal cells. Biol Reprod 41:771–778
34. **Wang J, Baimbridge KG, Leung PCK** 1989 Changes in cytosolic free calcium ion concentrations in individual rat granulosa cells: effect of luteinizing hormone-releasing hormone. Endocrinology 124:1912–1917
35. **Jacobs AL, Homanics GE, Silver WJ** 1991 Activity of phospholipase C in ovine luteal tissue in response to $PGF_{2\alpha}$, PGE_2 and luteinizing hormone. Prostaglandins 41:495–500
36. **Davis JS, Weakland LL, Coffey RG, West LA** 1989 Acute effects of phorbol esters on receptor-mediated IP_3, cAMP, and progesterone levels in rat granulosa cells. Am J Physiol 256:E368–E374
37. **Putney JWJr, ird GStJ** 1993 The inositol phosphate-calcium signaling system in nonexcitable cells. Endocr Rev 14:610–631
38. **Pepperell JR, Behrman HR** 1990 The calcium-mobilizing agent, thapsigargin, inhibits progesterone production in rat luteal cells by a calcium-independent mechanism. Endocrinology 127:1818–1824
39. **Billig H, Furuta I, Hsueh AJW** 1994 Gonadotropin-releasing hormone directly induces apoptotic cell death in the rat ovary: biochemical and *in situ* detection

of deoxyribonucleic acid fragmentation in granulosa cells. Endocrinology 134:245–252
40. **Sawyer HR, Niswender KD, Braden TD, Niswender GD** 1990 Nuclear changes in ovine luteal cells in response to $PGF_{2\alpha}$. Dom Anim Endocrinol 7:229–238
41. **Niswender GD, Juengel JL, McGuire WJ, Belfiore CJ, Wiltbank MC** 1994 Luteal function: the estrous cycle and early pregnancy. Biol Reprod 50:239–247
42. **Davis JS** 1992 Modulation of luteinizing hormone-stimulated inositol phosphate accumulation by phorbol esters in bovine luteal cells. Endocrinology 131:749–757
43. **Minegishi T, Leung PCK** 1985 Luteinizing hormone-releasing hormone stimulates arachidonic acid release in rat granulosa cells. Endocrinology 117:2001–2007
44. **Kol S, Ruutiainen-Altman K, Ben-Shlomos I, Payne DW, Ando M, Adashi EY** 1997 The rat ovarian phospholipase A_2 system: gene expression, cellular localization, activity characterization, and interleukin-1 dependence. Endocrinology 138:322–331
45. **Wu XM, Carlson JC** 1990 Alterations in phospholipase A_2 activity during luteal regression in pseudopregnant and pregnant rats. Endocrinology 127:2464–2468
46. **Kawai Y, Clark MR** 1986 Mechanism of action of gonadotropin releasing hormone on rat granulosa cells. Endocr Res 12:195–209
47. **Wang J, Leung PCK** 1988 Role of arachidonic acid in luteinizing hormone-releasing hormone action: stimulation of progesterone production in rat granulosa cells. Endocrinology 122:906–911
48. **Liscovitch M, Amsterdam A** 1989 Gonadotropin-releasing hormone activates phospholipase D in ovarian granulosa cells. J Biol Chem 264:11762–11767
49. **Guin M, Pignataro OP, Jimenez de Asua L** 1993 Early cell cycle diacylglycerol (DAG) content and protein kinase C (PKC) activity enhancement potentiates prostaglandin $F_{2\alpha}$ ($PGF_{2\alpha}$) induced mitogenesis in Swiss 3T3 cells. FEBS Lett 316:68–72
50. **McCann TJ, Flint APF** 1993 Use of pertussis toxin to investigate the mechanism of action of prostaglandin $F_{2\alpha}$ on the corpus luteum in sheep. J Mol Endocrinol 10:79–85

STIC-ILL

NO

From: Holleran, Anne
Sent: Monday, January 20, 2003 11:57 AM
To: STIC-ILL
Subject: refs. for 09/868,968

4283811

Please send copies of the following papers:

1.	Hoyoku,	Anticancer Res. (1999) 19(5A): 3663-3664
2.	Chamson-Reig	Endocrinology (1999) 140(8): 3573-3580
3.	Lixin,	J. Medicinal Chemistry 91998) 41(18): 3303-3306
4.	Yorek,	American J. Physiology (1998) 274(1, part1): C58-C71
5.	Nazih-Sanderson	Biochimica et Biophysica Acta (1997) 1346(1): 45-60
6.	Wattenberg	Cancer Research (1996) 56(22): 5132-5135
7.	Caro	Infection and Immunity (1996) 64(8): 3438-3441
8.	Seymour	Laboratory Investigation (1996) 75(3): 427-437
9.	Brunn	Cancer Chemotherapy Pharmacol (1994) 35(1): 71-79
10.	Kopp	Cancer Research (1990) 50(20): 6490-6496
11.	Tanino	Japanese J. Experimental Medicine (1972) 42(6): 575-582
12.	Eagle	Biochmistry (1963) 2(5): 1125-1126
13.	Caro	Biochem. Mol. Med. (1997) 61: 214-228

9560027

7987980

Anne Holleran
AU: 1642
Tel: 308-8892
RM: 8e03

mailbox: 8e12

Cancer Chemother Pharmacol (1994) 35: 71–79

ORIGINAL ARTICLE

G. Brunn · A. H. Fauq · S. Chow · A. P. Kozikowski
A. Gallegos · G. Powis

Cellular pharmacology of D-3-azido-3-deoxy-*myo*-inositol, an inhibitor of phosphatidylinositol signaling having antiproliferative activity

Received: 29 December 1993 / Accepted: 6 May 1994

Abstract D-3-Azido-3-deoxy-*myo*-inositol (3AMI) is an inhibitor of the growth of v-*sis*-transformed NIH 3T3 cells but not of wild-type NIH 3T3 cells, whose effects may be mediated through the phosphatidylinositol-3′-kinase pathway. We studied some properties of the cellular pharmacology of 3AMI using high-specific-activity [^{3}H]-3AMI. The uptake of [^{3}H]-3AMI by wild-type NIH 3T3 and v-*sis* NIH 3T3 cells was similar. [^{3}H]-3AMI was a substrate for phosphatidylinositol synthetase, with the maximal velocity (V_{max}) being 1.0 nmol min^{-1} mg^{-1} and the Michaelis constant (K_m) being 23 m*M*. Corresponding values obtained for [^{3}H]-*myo*-inositol as a substrate were 5.5 nmol min^{-1} mg^{-1} and 3.2 m*M*. [^{3}H]-3AMI was incorporated into the cellular inositol lipids of v-*sis* NIH 3T3 cells to a similar extent as that observed for [^{3}H]-*myo*-inositol but was not incorporated into the inositol lipids of wild-type NIH 3T3 cells. The [^{3}H]-3AMI incorporated by the v-*sis* NIH 3T3 cells was present in the phosphatidylinositol and phosphatidylinositol phosphate fractions but not in bisphosphorylated phosphatidylinositol. *myo*-Inositol antagonized the growth-inhibitory effects of 3AMI. The v-*sis* NIH 3T3 cells were found to be more sensitive than the wild-type NIH 3T3 cells to growth inhibition (without 3AMI) caused by the removal of *myo*-inositol from the medium. The results of the study suggest that 3AMI is an antimetabolite of *myo*-inositol. The relative sensitivity of v-*sis* NIH 3T3 and some other cells to 3AMI may be a reflection of increased *myo*-inositol requirements for the growth of these cells as compared with wild-type NIH 3T3 cells.

G. Brunn
Mayo Clinic and Foundation, Rochester, Minnesota, USA

A. H. Fauq · A. P. Kozikowski
Mayo Clinic, Jacksonville, Florida, USA

S. Chow
Karolinska Institutet, Stockholm, Sweden

A. Gallegos · G. Powis (✉)
Arizona Cancer Center, University of Arizona, 1515 North Campbell Avenue, Tucson, AZ 85724, USA

Key words 3AMI · Phosphatidylinositol · Inositol phosphates · Signaling

Abbreviations 3AMI, D-3-azido-3-deoxy-*myo*-inositol; 3AmMI, D-3-amino-3-deoxy-*myo*-inositol; PIPLC, phosphoinositide-selective phospholipase C; PtdIns(4,5)P_2, phosphatidylinositol(4,5)bisphosphate; Ins(1,4,5)P_3, *myo*-inositol(1,4,5)trisphosphate; Ins(1,3,4,5)P_4, *myo*-inositol(1,3,4,5)tetrakisphosphate; PKC, protein kinase C; PtdIns3′K, phosphatidylinositol-3′-kinase; PDGF, platelet-derived growth factor; EGF, epidermal growth factor; CDP-diglyceride, cytidine dipalmitoyl diphosphodiglyceride; DMEM, Dulbecco's modified Eagle's medium; PBS, Dulbecco's phosphate-buffered saline; HCS, heat-inactivated calf serum; IC_{50}, concentration required to cause 50% inhibition; PtdIns synthetase; phosphatidylinositol synthetase; DAG, diacylglycerol

Introduction

The cyclohexitol sugar *myo*-inositol occupies a key position in intracellular signaling pathways that mediate the effects of growth factors and mitogens on cell proliferation. Mitogenic peptides such as bombesin and vasopressin bind to cell-surface receptors [35, 41] and activate a guanine nucleotide-binding, (G) protein-regulated, phosphoinositide-selective phospholipase C (PIPLC-β) [45], causing the hydrolysis of phosphatidylinositol(4,5)-bisphosphate [PtdIns(4,5)P_2] to inositol (1,4,5)trisphosphate [Ins(1,4,5)P_3] and diacylglycerol (DAG) [6, 10, 24]. Growth-factor-receptor protein tyrosine kinases activate another PIPLC, PIPLC-γ, that also hydrolyzes PtdIns(4,5)P_2 [27]. Ins(1,4,5)P_3 releases Ca^{2+} from non mitochondrial intracellular stores, causing an increase in the cytosolic free Ca^{2+} concentration ($[Ca^{2+}]_i$), whereas DAG activates a Ca^{2+}- and phospholipid-dependent protein kinase C (PKC) [5, 36]. A subsequent series of events, probably involving phosphorylation of nuclear transcription factors by PKC, results in increased DNA synthesis [7].

$Ins(1,4,5)P_3$ can undergo further metabolism by inositol-3-kinase to give inositol(1,3,4,5)tetrakisphosphate [$Ins(1,3,4,5)P_4$] [20]. The role of Ins(1,3,4,5) in Ca^{2+} signaling remains controversial [29, 38, 44], but it may modulate Ca^{2+} mobilization by $(1,4,5)P_3$ [17] and facilitate the refilling of internal Ca^{2+} stores by external Ca^{2+} [20, 21], thus permitting the continued release of Ca^{2+} by $Ins(1,4,5)P_3$.

A second *myo*-inositol signaling pathway involves phosphorylation of the D-3 position of the *myo*-inositol ring of phosphatidylinositols (PtdIns) by phosphatidylinositol 3′-kinase (type I phosphatidylinositol kinase, PtdIns3K). PtdIns3K is phosphorylated by and associates with a number of growth-factor-receptor protein tyrosine kinases, including the platelet-derived growth factor (PDGF) receptor and the epidermal growth factor (EGF) receptor [4, 23] as well as oncogene protein tyrosine kinases [9, 16]. The PtdIns-3-phosphates formed are not substrates for hydrolysis by known PIPLCs and, thus, do not contribute to the inositol phosphate signaling pathway [42]. Evidence for the importance of PtdIns3K in mitogenesis comes from situations in which mutated tyrosine kinases fail to associate with and activate PtdIns3K. Polyoma middle-T mutants that associate with and activate $pp60^{c\text{-}src}$ tyrosine kinase but fail to activate PtdIns3K are nontransforming [23, 48]. Cells transfected with mutated PDGF receptors that retain protein tyrosine kinase activity but do not associate with or activate PtdIns3K fail to show a mitogenic response to PDGF, unlike cells transfected with the wild-type PDGF receptor [12]. The function of PtdIns-3-phosphates in mitogenesis is not known but they may be involved in cytoskeletal reorganization [14].

On the basis of the evidence that phosphorylation at the D-3 position of *myo*-inositol is important for intracellular signaling by mitogens and, perhaps, for cell transformation, we synthesized a series of D-3-deoxy-3-substituted *myo*-inositol analogues that inhibited the proliferation of wild-type and transformed NIH 3T3 cells in culture [25, 26, 39]. The most active of these analogues was 3AMI. We have now synthesized high-specific-activity [^{3}H]-3AMI and report on its cellular pharmacology.

Materials and methods

Compounds

3AMI was synthesized as previously described [39]. [^{3}H]-3AMI was synthesized according to the procedure described by Kozikowski et al. [25] and had a specific activity of 6 Ci/mmol. [2-^{3}H]-*myo*-Inositol (specific activity, 20 Ci/mmol) and [^{14}C-(U)]-glucose-6-phosphate (specific activity, 300 mCi/mmol) were purchased from American Radiolabeled Chemicals, Inc. (St. Louis, Mo.). [^{3}H]-PtdIns, [^{3}H]-PtdIns(4)P and [^{3}H]-PtdIns(4,5)P_2 standards for chromatography were purchased from Amersham Radiochemicals (Downers Grove, Ill.). Cytidine dipalmitoyl diphosphodigylceride (CDP-diglyceride) was purchased from Sedary Research Laboratories (London, Ontario, Canada). *myo*-Inositol, arg^8-vasopressin, and bradykinin were purchased from Sigma Chemical Co. (St. Louis, Mo.). PDGF (β-chain homodimer) was obtained from Bachem Inc. (Torrance, Calif.) and aequorin was supplied by Friday Harbor Laboratories (Friday Harbor, Wash.). Both Dulbecco's modified Eagle's medium (DMEM) containing 40 μ*M* *myo*-inositol and *myo*-inositol-free DMEM were purchased from Grand Island Biological Co. (Grand Island, N.Y.).

Cell lines

Wild-type mouse NIH 3T3 cells were obtained from the American Type Culture Collection (Rockville, Md.). v-*sis* NIH 3T3 cells and v-*erb* B NIH 3T3 cells [32] were provided by Dr. D. S. Aaronson (National Cancer Institute, Bethesda, Md.), and *mas* NIH 3T3 cells [49] were provided by Dr. D. Young (Cold Spring Harbor Laboratory, Cold Spring Harbor, N.Y.).

Cell-growth assays

Cells were maintained in bulk culture in DMEM supplemented with 10% heat-inactivated calf serum (HCS) and were passaged using 0.05% trypsin and 0.5 m*M* ethylenediaminetetraacetic acid (EDTA). Cell-growth assays were performed by plating 5×10^3 cells in 1.6-cm-diameter culture wells in 0.5 ml DMEM with 10% HCS and allowing the cells to attach to the culture surface for 24 h. The medium was removed and the cells were washed first with Dulbecco's phosphate-buffered saline (PBS) and then with DMEM with or without *myo*-inositol, as appropriate; finally, DMEM with or without *myo*-inositol and containing 10% dialyzed HCS as well as the *myo*-inositol analogues was added. After 3 days, attached cells were harvested with 0.05% trypsin and 0.5 mM EDTA and then counted using an automated cell counter (Coulter, Hialea, Fla.). The mean concentration of *myo*-inositol analogue required to cause 50% growth inhibition in treated cells as compared with nontreated cells (IC_{50}) was calculated from nonlinear least-squares regression analysis of the cell-proliferation concentration data [3]. The time course of the inhibition of cell growth was measured by plating 10^3–10^4 cells in 1.6-cm-diameter culture wells in DMEM with or without *myo*-inositol and containing 10% dialyzed HCS with or without 100 μ*M* 3AMI. Cells were harvested and counted every day for 7 days. At day 3, free-floating cells in the medium were collected, washed three times with DMEM, and replated in DMEM (with *myo*-inositol) and 10% dialyzed HCS. Cells were measured every day for an additional 4 days. All incubations were conducted in quadruplicate.

Biochemical measurements

The uptake of [^{3}H]-*myo*-inositol and [^{3}H]-3AMI by wild-type NIH 3T3 and v-*sis* NIH 3T3 cells over 2 h was measured as previously described [31]. The phosphatidylinositol synthetase (PtdIns synthetase)-catalyzed incorporation of *myo*-inositol, 3AMI, D-3-deoxy-3-fluoro-*myo*-inositol, and D-3-deoxy-3-amino-*myo*-inositol (3AmMI) into PtdIns was measured as described by Moyer et al. [33] using partly purified rat-brain PtdIns synthetase [40]. The incorporation of [^{3}H]-*myo*-inositol and [^{3}H]-3AMI into cellular phospholipids was measured by growing 5×10^5 wild-type NIH 3T3 or v-*sis* NIH 3T3 cells in 60-mm diameter culture dishes in *myo*-inositol-free DMEM and 10% dialyzed HCS together with 1 μCi (0.17 μ*M*) [^{3}H]-*myo*-inositol/ml or 1 μCi [^{3}H]-3AMI/ml for 48 h. The cells were harvested with 0.05% trypsin and 0.5 m*M* EDTA and extracted with chloroform:methanol:HCl (80:40:1, by vol.). The organic layer was removed and dried under N_2 and the residue was dissolved in 100 μl chloroform. An aliquot of the chloroform solution was counted by liquid scintillation and the remainder was applied to a silica-gel thin-layer chromatography (TLC) plate (Whatman LK6D, Maidstone, UK), which was developed using a solvent system of chloroform:methanol:H_2O:ammonium hydroxide (50:50:10:5, by vol.). The radioactivity on the plates was measured using a radio-TLC scanner (Model RS, Packard Instruments, Downers Grove, Ill.) and compared with standards of [^{3}H]-PtdIns, [^{3}H]-PtdIns(4)P, and [^{3}H]-PtdIns(4,5)P_2 run under the same conditions. The formation of [^{3}H]-*myo*-inositol phosphates was measured in wild-type NIH 3T3 cells and v-*sis* NIH 3T3 cells grown with 1 μCi (0.17 μ*M*) [^{3}H]-*myo*-inositol/ml or 1 μCi [^{3}H]-3AMI/ml for 48 h as

described above. The cells were washed four times with *myo*-inositol-free DMEM, incubated in 2 ml *myo*-inositol-free DMEM containing 15 m*M* LiCl for 10 min at 37 °C, and then stimulated with 3.3×10^{-9} *M* PDGF for 10 min at 37 °C. The incubation was terminated by the addition of 2 ml 10% perchloric acid at 4 °C. *myo*-Inositol phosphates (i.e., *myo*-inositol mono-, bis-, and trisphosphates) were isolated by anion-exchange chromatography as previously described [1].

The de novo synthesis of *myo*-inositol by wild-type NIH 3T3 cells and v-*sis* transformed NIH 3T3 cells was measured by a modification of the method of Li et al. [28] as the conversion of [^{14}C]-glucose-6-phosphate to [^{14}C]-*myo*-inositol-1-phosphate by *myo*-inositol-1-phosphate synthase, which is the rate-limiting step in *myo*-inositol biosynthesis [15]. Briefly, saponin-permeabilized cells were incubated for up to 1 h at 37 °C with 12 μ*M* [^{14}C]-glucose-6-phosphate, 0.8 m*M* nicotinamide adenine dinucleotide (NAD^+), and 5 m*M* LiCl. [^{14}C]-Glucose-6-phosphate and [^{14}C]-*myo*-inositol-1-phosphate were separated by high-performance liquid chromatography (HPLC) using a 25-cm, 7-μm, mixed-mode RP-18/anion-exchange column (Alltech Associates, Deerfield, Ill.) and 20 m*M* $(NH_4)H_2PO_4$ as the eluant, run at a flow rate of 1 ml/min and detected with a radioactive flow detector (Flo-One Beta, Packard Instruments, Downers Grove, Ill.). The retention times found for [^{14}C]-*myo*-inositol-1-phosphate and [^{14}C]-glucose-6-phosphate with this HPLC system were 9.8 and 11.1 min, respectively. The limit of detection of the assay under the conditions employed was calculated to be 6 pmol *myo*-inositol-1-phosphate formed per 10^6 cells per hour.

Changes in intracellular free Ca^{2+} concentration ($[Ca^{2+}]_i$) were measured using the Ca^{2+}-sensitive photoprotein aequorin. Wild-type NIH 3T3 cells and v-*sis* NIH 3T3 cells were loaded with aequorin by a low-Ca^{2+} centrifugation technique as previously described [37]. In all, 10^6 cells were plated in 35-mm culture dishes containing 2 ml DMEM with 10% dialyzed HCS. After incubation overnight to allow the cells to attach to the surface of the culture dish, the medium was replaced with DMEM without HCS for 3 h. Some cells were grown for 2 days with 100 μ*M* 3AMI in *myo*-inositol-free DMEM with 10% dialyzed HCS, loaded with aequorin, and then exposed to the same medium with 100 μ*M* 3AMI overnight prior to the measurement of $[Ca^{2+}]_i$. The culture dish was placed in a 37 °C thermostated holder over a photomultiplier tube, and the surface of the medium was flushed with a humidified atmosphere of 5% CO_2: 95% air. Arg^8-vasopressin (10^{-7} *M*) and bradykinin (2×10^{-7} *M*), were used to produce maximal increases in $[Ca^{2+}]_i$. At the end of the study, the cells were lysed with a solution of 1% Triton X-100 and 5 m*M* $CaCl_2$ and the total light signal was integrated. An estimate of $[Ca^{2+}]_i$ was obtained using the calibration method for aequorin previously reported by Allen and Blinks [2].

Results

Cell growth inhibition by myo-inositol deprivation and 3AMI

The growth of wild-type NIH 3T3 cells was unaffected by 3AMI concentrations of up to 33 m*M* (the highest concentration tested), with or without *myo*-inositol in the medium. In contrast, 3AMI inhibited the growth of v-*sis* NIH 3T3 cells with an IC_{50} of 53 μ*M* without *myo*-inositol in the medium. The results confirm our previous observation that in the absence of *myo*-inositol, v-*sis* NIH 3T3 cells are extremely sensitive to growth inhibition by 3-deoxy-3-substituted *myo*-inositols as compared with a wild-type NIH 3T3 cell line [39]. We therefore used the two cell lines to compare the cellular pharmacology of 3AMI. *myo*-Inositol reversed the growth-inhibitory effects of 3AMI on v-*sis* NIH 3T3 cells with an IC_{50} for *myo*-inositol of 2 μ*M*.

The time course of the growth inhibition of NIH 3T3 cells and v-*sis* NIH 3T3 cells by 3AMI is shown in Fig. 1 and is compared with the effects of *myo*-inositol deprivation on cell growth. The growth curve generated for wild-type NIH 3T3 cells without *myo*-inositol in the medium (Fig. 1A) was the same as that generated for wild-type cells in medium containing 40 μ*M* *myo*-inositol (results not shown), demonstrating that *myo*-inositol is not necessary for the growth of these cells over the period studied. In contrast, the growth of v-*sis* NIH 3T3 cells required *myo*-inositol in the medium. Without *myo*-inositol, the number of attached cells began to decline slowly after 3 days. About 50% of the total v-*sis* NIH 3T3 cells that detached in *myo*-inositol free medium could be collected at day 3, and when replated in *myo*-inositol-containing medium they proceeded to grow normally. The growth of wild-type NIH 3T3 cells over 7 days was not inhibited by 100 μ*M* 3AMI, either in the absence of *myo*-inositol (Fig. 1A) or in its presence (results not shown). In the presence of 100 μ*M* 3AMI, the number of attached v-*sis* NIH 3T3 cells declined drastically after only 2 days (Fig. 1B). Less than 10% of the detached cells could be collected from the medium at day 3. However, when these cells were replated in 3AMI-free medium with *myo*-inositol they grew at a normal rate.

Fig. 1 A, B Cell-growth inhibition caused by *myo*-inositol deprivation and by 3AMI. **A** Approximately 10^3 wild-type NIH 3T3 cells (○) or v-*sis* NIH 3T3 cells (●) were grown in *myo*-inositol-free DMEM and 10% dialyzed HCS. Adherent cells were counted every day. At day 3 the floating v-*sis* NIH 3T3 cells were collected and replated in the same medium containing 40 μ*M* *myo*-inositol (▽). **B** Approximately 10^4 wild-type NIH 3T3 cells (○) or v-*sis* NIH 3T3 cells ( ) were grown in *myo*-inositol-free DMEM containing 100 μ*M* 3AMI and 10% dialyzed HCS. Adherent cells were counted every 3 days. At day 3 the floating v-*sis* NIH 3T3 cells were collected, washed, and replated in same medium without 3AMI and with 40 μ*M* *myo*-inositol (▽). More cells were plated in **B** than in **A** so as to obtain sufficient floating cells to replate. Each point represents the mean value for triplicate determinations

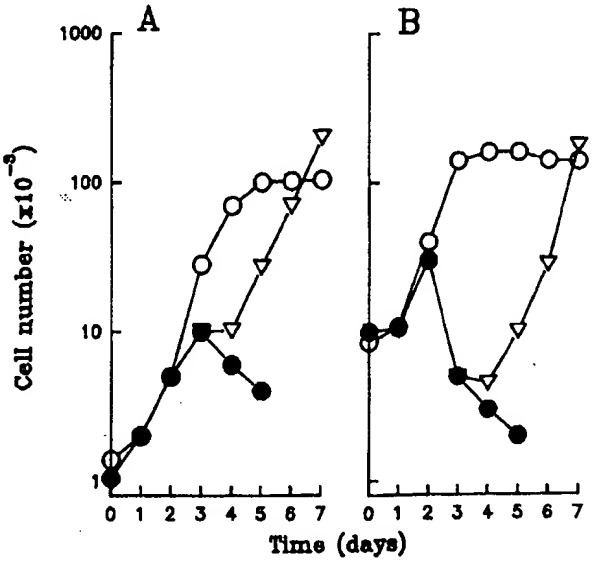

Table 1. Effect of LiCl on the cytotoxicity of D-3-substituted-3-deoxy *myo*-inositol analogues

	Without *myo*-inositol		With *myo*-inositol	
	NIH 3T3 IC_{50} (m*M*)	v-*sis* NIH 3T3 IC_{50} (m*M*)	NIH 3T3 IC_{50} (m*M*)	v-*sis* NIH 3T3 IC_{50} (m*M*)
3AMI	NT	0.08 ± 0.01	NT	NT
3AMI + 5 m*M* LiCl	ND	0.11 ± 0.00	ND	NT
3AmMI	0.13 ± 0.01	2.29 ± 0.25	4.54 ± 0.77	3.00 ± 0.30
3AmMI + 5 m*M* LiCl	0.10 ± 0.02	0.96 ± 0.11*	5.91 ± 1.07	3.18 ± 0.30

Cell growth was measured as described Materials and methods using 5 m*M* LiCl, a concentration that caused < 10% growth inhibition, and 3AMI or 3AmMI in various combinations with or without *myo*-inositol in the medium. Data represent IC_{50} values (± SD)
NT, Not toxic (< 10% inhibition of cell growth at 10 m*M*, the highest concentration tested); ND, not determined
* $P < 0.05$ versus the value obtained without LiCl

For further exploration of the relationship between the cell-growth inhibition produced by *myo*-inositol deprivation and by 3AMI, other NIH 3T3 cell lines were studied. We had previously observed that v-*erb* B NIH 3T3 cells were relatively resistant to 3AMI (IC_{50}, 29 m*M*), whereas *mas* NIH 3T3 cells were more sensitive (IC_{50}, 5 m*M*) [39]. These cells were studied for their *myo*-inositol requirement. The growth of v-*erb* B cells was not affected by the absence of *myo*-inositol in the medium for 7 days, whereas the growth of *mas* NIH 3T3 cells was inhibited by 57% (results not shown). Taken together, the results of these studies suggest that the effects of 3AMI in inhibiting cell growth are functionally like those of *myo*-inositol deprivation.

Synthesis of *myo*-inositol

Attempts were made to measure rates of [^{14}C]-*myo*-inositol-1-phosphate synthesis from [^{14}C]-glucose-6-phosphate in saponin-permeabilized wild-type NIH 3T3 cells and v-*sis* NIH 3T3 cells. However, we could not detect [^{14}C]-*myo*-inositol-1-phosphate synthesis by either cell line. The calculated limit of detectability for [^{14}C]-*myo*-inositol-1-phosphate synthesis in our assay was 6 pmol 10^{-6} cells h^{-1}. This is well below the levels of *myo*-inositol-1-phosphate biosynthesis (100 pmol/10^6 cells per 20 min) reported for retinal capillary pericytes using the same procedure [28].

Effects of LiCl on cell-growth inhibition

Because we could not detect *myo*-inositol biosynthesis by wild-type NIH 3T3 cells or v-*sis* NIH 3T3 cells, we studied the possibility that salvage or reutilization of *myo*-inositol formed from PtdIns would allow wild-type NIH 3T3 cells but not v-*sis* NIH 3T3 cells to grow in the absence of *myo*-inositol. To do this we studied the effects of LiCl, an inhibitor of *myo*-inositol phosphate phosphatases [34], on the cell-growth inhibition induced by 3AMI and by another 3-substituted *myo*-inositol, 3AmMI. We found no difference in the LiCl IC_{50} values (± SD) that inhibited the growth of wild-type NIH 3T3 cells (IC_{50}, 22.0 ± 2.1 μ*M* without *myo*-inositol in the medium; 20.0 ± 5.3 m*M* with *myo*-inositol) or v-*sis* NIH 3T3 cells (IC_{50}, 19.1 ± 3.2 m*M* without *myo*-inositol; 25.0 ± 4.7 m*M* with *myo*-inositol). A concentration of LiCl that caused less than 10% growth inhibition, 5 m*M*, was chosen for combination with the *myo*-inositol analogues. The growth inhibition induced by 3AMI or 3AmMI in either wild-type NIH 3T3 cells or v-*sis* NIH 3T3 cells was unaffected by this concentration of LiCl, with or without *myo*-inositol, except for a small potentiation in the cell-growth produced inhibition by 3AmMI in v-*sis* NIH 3T3 cells without *myo*-inositol (Table 1). Overall, the studies with LiCl do not support a role for *myo*-inositol salvage as a factor in the *myo*-inositol requirement for cell-growth or for differences in the growth inhibition induced by 3AMI or 3AmMI between wild-type NIH 3T3 cells and v-*sis* NIH 3T3 cells.

Cellular uptake of *myo*-inositol

The uptake of [^{3}H]-3AMI by wild-type NIH 3T3 cells exhibited a maximal rate (V_{max}) of 2.6 nmol 10^{-6} cell h^{-1} and a Michaelis constant (K_m) of 0.42 m*M*. We have previously reported that 3AMI is a competitive inhibitor of [^{3}H]-*myo*-inositol uptake by wild-type NIH 3T3 cells, with its inhibition constant (K_i) being 0.35 m*M* [39]. The uptake of [^{3}H]-*myo*-inositol by wild-type NIH 3T3 cells had a V_{max} of 2.8 nmol 10^{-6} cell h^{-1} and a K_m of 69 μ*M*. These values are similar to those previously reported for *myo*-inositol uptake by NIH 3T3 cells [43]. Uptake of [^{3}H]-3AMI by v-*sis* NIH 3T3 cells exhibited a V_{max} of 1.8 nmol 10^{-6} cell h^{-1} and a K_m of 0.35 m*M*, and the uptake of [^{3}H]-*myo*-inositol showed a V_{max} of 2.3 nmol 10^{-6} cell h^{-1} and a K_m of 53 μ*M*.

PtdIns synthetase

The ability of [^{3}H]-3AMI to act as a substrate for partly purified PtdIns synthetase with CDP-diglyceride as an acceptor is shown in Fig. 2. The V_{max} was 1.0 nmol min^{-1} mg^{-1} and the K_m, 23.0 m*M*. With [^{3}H]-*myo*-inositol as a substrate, the V_{max} was 5.5 nmol min^{-1} mg^{-1} and the K_m, 3.2 m*M*. The values obtained for *myo*-inositol as the

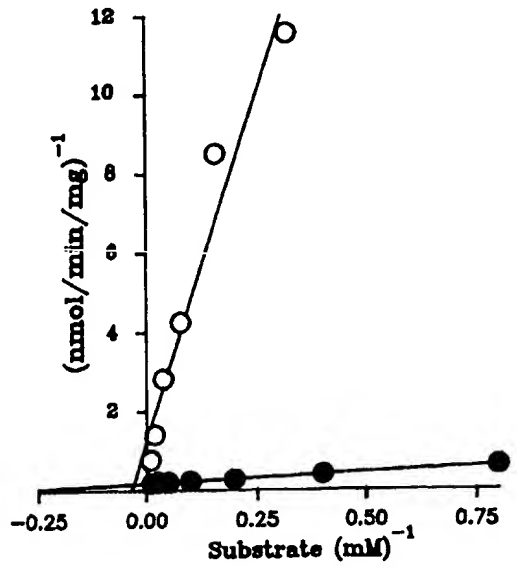

Fig. 2 3AMI and *myo*-inositol as substrates for PtdIns synthetase: Lineweaver-Burk plots of the incorporation of [^{3}H]-3AMI (○) and [^{3}H]-*myo*-inositol (●) into phospholipid when cells were incubated at various concentrations with rat-brain PtdIns synthetase and CDP-diglyceride for 30 min at 37 °C

substrate for PtdIns synthetase are similar to those previously reported [33]. We also studied the ability of some nonradiolabeled D-3-substituted 3-deoxy-*myo*-inositol analogues to act as inhibitors of PtdIns synthetase with [^{3}H]-*myo*-inositol serving as the substrate. The K_i values (together with the type of inhibition) were: D-3-fluoro-3-deoxy-*myo*-inositol, 37.2 m*M* (competitive); 3AmMI, 24.6 m*M* (noncompetitive); and 3AMI, 31.2 m*M* (noncompetitive).

Incorporation into cellular phospholipids

The incorporation of [^{3}H]-*myo*-inositol and [^{3}H]-3AMI into cellular phospholipids of wild-type and v-*sis* NIH 3T3 cells is shown in Table 2. Incorporation of [^{3}H]-*myo*-inositol into cellular phospholipids of wild-type NIH 3T3 cells was approximately twice that of v-*sis* NIH 3T3 cells. [^{3}H]-3AMI was incorporated into the cellular phospholipids of v-*sis* NIH 3T3 cells to a similar extent as that found for [^{3}H]-*myo*-inositol but was hardly incorporated into wild-type NIH 3T3 cells.

TLC analysis of the phospholipids is shown in Fig. 3. The majority of the radioactivity from [^{3}H]-*myo*-inositol chromatographed with PtdIns and lesser amounts, with PtdIns phosphates. The percentages of total radioactivity chromatographing with the standards in wild-type NIH 3T3 cells were PtdIns, 74%; PtdIns(4)P, 5%; PtdIns(4,5)P_2, 2%; and other peaks, 19%; those in v-*sis* NIH 3T3 cells were PtdIns, 85%; PtdIns(4)P, 6%; PtdIns(4,5)P_2, 3%; and other peaks, 6%. These values are similar to those reported by other workers for [^{3}H]-*myo*-inositol incorporation into PtdIns of fibroblasts [43]. [^{3}H]-3AMI, which was poorly incorporated into PtdIns by wild-type NIH 3T3 cells, had percentages of total radioactivity chromatographing with the standards as follows: PtdIns, 50%; PtdIns(4)P, 32%; PtdIns(4,5)P_2, 4%; and other peaks, 14%. In v-*sis* NIH 3T3 cells the percentages were: PtdIns, 91%; PtdIns(4)P, 8%; PtdIns(4,5)P_2, 0; and other peaks, 1%. Thus, it appears that although [^{3}H]-3AMI can be incorporated into PtdIns and PtdIns monophosphate by v-*sis* NIH 3T3 cells, it may not undergo further phosphorylation to PtdIns bisphosphates.

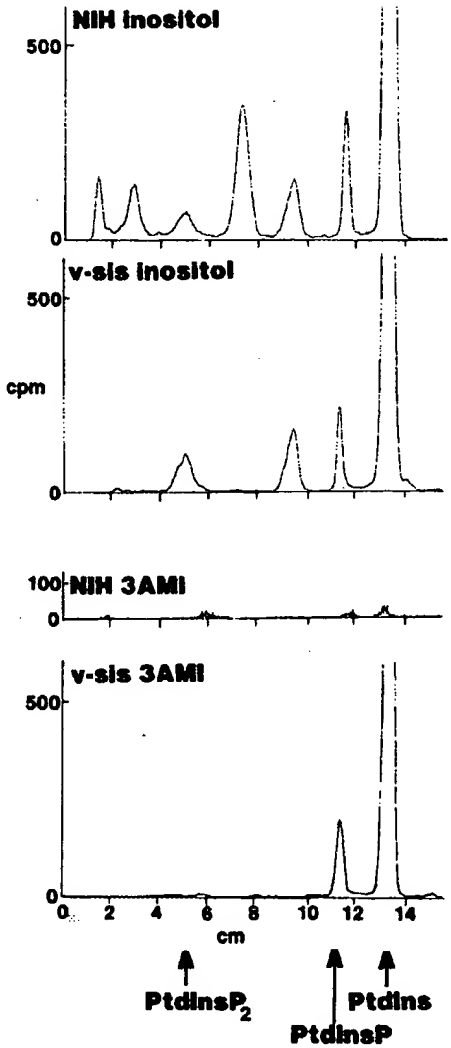

Fig. 3 Incorporation of [^{3}H]-*myo*-inositol and [^{3}H]-3AMI into phosphatidylinositols (PtdIns) of wild-type NIH 3T3 cells (*NIH*) and v-*sis* NIH 3T3 cells (*v-sis*). Cells were grown with 1 μCi [^{3}H]-*myo*-inositol or [^{3}H]-3AMI in *myo*-inositol-free DMEM and 10% dialyzed HCS for 48 h. Phospholipids were extracted from 2 × 10^6 cells with chloroform:methanol:HCl (80:40:1, by vol.) and subjected to TLC on silica gel with a solvent system of chloroform:methanol:H_2O:ammonium hydroxide (50:50:10:5, by vol.). Radioactivity was quantified using a radio-TLC scanner. The position of standards are shown by the *arrows*

Table 2. Incorporation of 3AMI into phosphatidylinositol and inositol phosphates of NIH 3T3 and v-*sis* NIH cells

Compound	Cell line	[^{3}H]-Phospholipid (pmol/10^6 cells)	[^{3}H]-Inositol phosphates	
			Without PDGF (fmol/10^6 cells)	With PDGF (fmol/10^6 cells)
myo-Inositol	NIH 3T3	8.00±0.36	198 ±57	581 ± 10*
	v-*sis* NIH 3T3	4.15±0.21	420 ±30	560 ±160
3AMI	NIH 3T3	0.29±0.02	6.8± 0.4	6.1± 0.8
	v-*sis* NIH 3T3	3.33±0.06	6.3± 4.0	6.2± 1.5

Wild-type NIH 3T3 and v-*sis* NIH 3T3 cells were grown with 1 μCi [^{3}H]-AMI/ml or 1 μCi [^{3}H]-*myo*-inositol/ml for 2 days. The incorporation of radioactivity into cellular phospholipids as well as the basal and (3.3×10^9 *M*) PDGF-stimulated inositol phosphate formation were measured. Data represent mean values for 3 separate determinations (±SE)

* $P < 0.01$ versus the nonstimulated value

Table 3. Effect of 3AMI on mitogen-stimulated $[Ca^{2+}]_i$ responses by NIH 3T3 and v-*sis* NIH 3T3 cells

Cell line	Without 100 μ*M* 3AMI		With 100 μ*M* 3AMI	
	Vasopressin $[Ca^{2+}]_i$ (μ*M*)	Bradykinin $[Ca^{2+}]_i$ (μ*M*)	Vasopressin $[Ca^{2+}]_i$ (μ*M*)	Bradykinin $[Ca^{2+}]_i$ (μ*M*)
NIH 3T3	0.55±0.10	0.56±0.04	0.50±0.16	0.58±0.06
v-*sis* NIH 3T3	0.72±0.13	1.20±0.15	0.37±0.30	1.33±0.17

Wild-type NIH 3T3 and v-*sis* NIH 3T3 cells were grown in *myo*-inositol-free DMEM with 10% HCS, with or without 100 μ*M* 3AMI for 3 days. At 24 h prior to the study, the cells were harvested, loaded with the Ca^{2+}-sensitive photoprotein aequorin, and allowed to reattach to the tissue-culture plates. Both control and drug-treated cells were exposed to the appropriate medium without HCS for 3 h prior to the addition of 10^{-7} *M* arg^8-vasopressin and 2×10^{-7} *M* bradykinin. Data are expressed as the maximal increase in $[Ca^{2+}]$ and represent mean values for 3–5 determinations (±SE). The resting $[Ca^{2+}]_i$ in the cells was 0.1 μ*M*

Formation of inositol phosphates

The formation of [^{3}H]-*myo*-inositol phosphates by wild-type NIH 3T3 cells and v-*sis* NIH 3T3 cells grown with [^{3}H]-*myo*-inositol or [^{3}H]-3AMI is shown in Table 2. PDGF stimulated [^{3}H]-inositol phosphate formation 2.9-fold in wild-type NIH 3T3 cells. The resting level of [^{3}H]-inositol phosphate formation in v-*sis* NIH 3T3 cells was over 2-fold that of wild-type NIH 3T3 cells and there was only a small, nonsignificant stimulation of [^{3}H]-inositol phosphate formation by PDGF. The v-*sis* NIH 3T3 cells are known to produce an autocrine PDGF-like factor [18] and to have low levels of PDGF receptors [19]. The resting levels of [^{3}H]-inositol phosphate formation were very low in both wild-type NIH 3T3 cells and v-*sis* NIH 3T3 cells exposed to [^{3}H]-3AMI, being less than 5% of those found for [^{3}H]-*myo*-inositol, and were not stimulated by PDGF.

Ca^{2+} signaling

Wild-type NIH 3T3 cells or v-*sis* NIH 3T3 cells grown in 100 μ*M* 3AMI for 3 days showed no effect in terms of the peak Ca^{2+} responses of the surviving cells to vasopressin and bradykinin (Table 3).

Discussion

We have previously reported that 3AMI is the most active of a series of growth-inhibitory D-3-substituted 3-deoxy-*myo*-inositol analogues [26, 39]. 3AMI selectively inhibits the growth of v-*sis* transformed NIH 3T3 cells, showing over a 1000-fold increased potency in the absence of exogenous *myo*-inositol for growth inhibition of v-*sis* NIH 3T3 cells as compared with wild-type NIH 3T3 cells. Providing a mechanistic basis for this remarkable selectivity was the reason for our study. To facilitate the investigation we synthesized high-specific-activity [^{3}H]-3AMI starting from the naturally occurring compound quebrachitol [25].

3AMI appears to be acting as a *myo*-inositol antimetabolite in inhibiting cell-growth. The effect of 3AMI on v-*sis* NIH 3T3 cell-growth was antagonized by *myo*-inositol with an IC_{50} of 2 μ*M*. This is considerably lower than the concentration of *myo*-inositol in serum, which is around 40 μ*M* [46]. Microinjection or scrape-loading of monodeoxyfluoro-*myo*-inositols into cells has shown that only the 3-fluoro- and 5-fluoro isomers inhibit serum-stimulated cell proliferation [11]. It has been suggested that cells that do not require *myo*-inositol for growth may be capable of synthesizing *myo*-inositol de novo [47]. However, we could not detect *myo*-inositol synthesis by either wild-type NIH 3T3 cells or v-*sis* NIH 3T3 cells. We also considered the possibility that wild-type NIH 3T3 cells might have a more efficient salvage pathway than v-*sis* NIH 3T3 cells for the reutilization of *myo*-inositol produced by the breakdown of PtdIns [6]. We used LiCl to inhibit *myo*-inositol phosphate phosphatases [34] but could not find any evidence of

differences in the salvage of *myo*-inositol as a factor in the *myo*-inositol requirement for growth between wild-type NIH 3T3 cells and v-*sis* NIH 3T3 cells. Despite our inability to demonstrate differences in *myo*-inositol synthesis or *myo*-inositol salvage between the cell types, the v-*sis* NIH 3T3 cells that showed the greatest sensitivity to 3AMI were also those that required *myo*-inositol for growth. It therefore remains possible that v-*sis* NIH 3T3 cells are sensitive to 3AMI because they have low levels of endogenous *myo*-inositol, whereas wild-type NIH 3T3 cells have higher levels of endogenous *myo*-inositol, which counteracts the effects of 3AMI as a *myo*-inositol antimetabolite.

Studies using [^{3}H]-3AMI showed that it was incorporated into the cellular phospholipids of v-*sis* NIH 3T3 cells to about the same extent as was [^{3}H]-*myo*-inositol. However, wild-type NIH 3T3 cells incorporated [^{3}H]-3AMI to less than 5% of the extent of [^{3}H]-*myo*-inositol incorporation. This difference could not be explained by the absence of an uptake mechanism for [^{3}H]-3AMI in the wild-type NIH 3T3 cells, which had a K_m value about 10-fold that found for *myo*-inositol, but was the same as that observed in v-*sis* NIH 3T3 cells, which incorporated [^{3}H]-3AMI into cellular phospholipids. Additionally, the difference could not be explained by the inability of [^{3}H]-3AMI to act as a substrate for PtdIns synthetase. This finding was important to establish because on the basis of work with 5-deoxy-5-substituted *myo*-inositols, Moyer et al. [33] had suggested, that PtdIns synthetase had strict structural requirements for *myo*-inositols as substrates and, thus, it might not have tolerated 3-deoxy-3-substituted *myo*-inositols. Johnson et al. [22] have reported that 3-modified *myo*-inositols are substrates for PtdIns synthetase. We found that the K_m of 3AMI for rat-brain PtdIns synthetase was about 10-fold that of *myo*-inositol. Unless mouse PtdIns kinase has properties very different from those of the rat enzyme, the inability of 3AMI to be incorporated into wild-type NIH 3T3 cell phospholipids is unlikely to lie at the level of PtdIns synthetase. Another explanation, although one that we could not confirm (see above), is that wild-type NIH 3T3 cells have sufficient *myo*-inositol, produced through either synthesis or salvage, to compete with 3AMI for incorporation into phospholipids.

Although 3AMI was incorporated into the PtdIns fraction of v-*sis* NIH 3T3 cells and could be phosphorylated to give PtdIns monophosphate, the PtdIns monophosphate was not further phosphorylated to PtdIns bisphosphate. Cosulich et al. [11] have recently reported that [^{3}H]-3-deoxy-3-fluoro-*myo*-inositol incorporated into the PtdIns of electropermeabilized thymoctyes also fails to form detectable PtdIns bisphosphates. This may explain why there was no formation of inositol phosphates in v-*sis* NIH 3T3 cells labeled with [^{3}H]-3AMI, either under resting conditions or on stimulation with PDGF. PDGF causes inositol phosphate formation through activation of PIPLC-γ [27]. The major substrate for PIPLC is PtdIns(4,5)P_2, and PtdIns monophosphates do not appear to be substrates for PIPLC under physiological conditions [30]. The inability of 3AMI to form PtdIns phosphates that lead to the production of inositol phosphates is probably attributable to the observation that the PtdIns is not phosphorylated past the monophosphate stage and thus fails to give rise to PtdIns phosphates that are substrates for PIPLC.

In wild-type NIH 3T3 cells and v-*sis* NIH 3T3 cells grown with 3AMI for 3 days, there was no alteration in the $[Ca^{2+}]_i$ responses to bradykinin and vasopressin. Both agonists are thought to cause an increase in $[Ca^{2+}]_i$ due to inositol phosphate formation through activation of PIPLC [13, 35]. It might be expected that $[Ca^{2+}]_i$ signaling would be decreased in the v-*sis* NIH 3T3 cells since there was no formation of inositol phosphates. It is possible that the increase in $[Ca^{2+}]_i$ caused by these agents is not due to the formation of inositol phosphates. There is evidence that bradykinin, at least, causes an increase in $[Ca^{2+}]_i$ through the release of arachidonic acid [8]. Alternatively, inositol phosphate production may not be affected by exposure of cells to 3AMI, despite its incorporation into PtdIns. Another possibility is that the cells surviving a 3-day exposure to 3AMI may be those that have unaffected inositol phosphate production and, thus, normal Ca^{2+} signaling. The majority of the cells were lost by this period of 3AMI treatment and could not be studied for their $[Ca^{2+}]_i$ response.

The mechanism of growth inhibition by 3AMI is unknown. The block of inositol phosphate and DAG formation through decreased PtdIns hydrolysis in 3AMI treated cells might be expected to lead to inhibition of cell-growth. It is known that blockage of increases in PKC activity in fibroblasts due to DAG produced in response to growth factors such as PDGF can prevent increased DNA synthesis [13]. However, the overall importance of the inositol phosphate and DAG signaling pathway to mitogenesis remains unclear at this time [12].

An alternative target for inhibition by 3AMI is the PtdIns3K pathway. 3-Substituted PtdIns and PtdIns monophosphates formed from 3AMI would not be substrates for PtdIns3K and might antagonize the effects of PtdIns-3-phosphates. The mechanisms by which PtdIns-3-phosphates cause mitogenesis is not known but may involve reorganization of the cytoskeleton. Cellular proliferation is known to be closely associated with changes in the actin network of the cytoskeleton, and a correlation between actin polymerization and the formation of PtdIns(3,4,5)P_3 has been reported [14]. It is noteworthy that we observed signs of changes in the cytoskeleton in 3AMI-treated fibroblasts, which became rounded and detached from the cell-culture surface. We also have preliminary evidence that a PtdIns prepared from 3-deoxy-3-fluoro-*myo*-inositol is an inhibitor of PtdIns3K (G. Powis and M. Berggren, unpublished observations). Thus, as well as acting as antimetabolites of PtdIns-3-phosphates, PtdIns derived 3-AMI might inhibit PtdIns3K.

In summary, we have confirmed that 3AMI exhibits a remarkable selectivity for growth inhibition of v-*sis* NIH 3T3 cells as compared with wild-type NIH 3T3 cells. 3AMI appears to be acting as an antimetabolite of *myo*-inositol. Wild-type NIH 3T3 cells can take up 3AMI but do not form PtdIns from 3AMI although it is a substrate for PtdIns synthetase. This could explain the observed lack of growth inhibition of wild-type NIH 3T3 cells by 3AMI. 3AMI is

taken up by v-*sis* NIH 3T3 cells and is incorporated into PtdIns and PtdIns monophosphate but does not form PtdIns bisphosphates. The block in the formation of inositol phosphates as well as a block in the formation of PtdIns-3-phosphates could explain the observed inhibition of cell growth by 3AMI in v-*sis* NIH 3T3 cells.

Acknowledgement This work was supported by NIH grant CA 61015

References

1. Abraham RT, Ho SN, Barna TJ, Mckean DJ (1987) Transmembrane signaling during interleukin 1-dependent T-cell activation. J Biol Chem 22: 2719
2. Allen DG, Blinks JR (1979) The interpretation of light signals from aequorin-injected skeletal and cardiac muscle cells: a new method of calibration. In: Ashley CC, Campbell AK (eds) Detection and measurement of free Ca^{2+} in cells. Elsevier-Holland, Amsterdam, p 159
3. Alley MC, Powis G, Appel PL, Kooistra KL, Lieber MM (1984) Activation and inactivation of cancer chemotherapeutic agents by rat hepatocytes cocultured with human tumor cell lines. Cancer Res 44: 549
4. Auger KR, Serunian LA, Soltoff SP, Libby P, Cantley LC (1989) PDGF-dependent tyrosine phosphorylation stimulates production of novel polyphosphoinositides in intact cells. Cell 57: 167
5. Berridge MJ (1983) Rapid accumulation of inositol trisphosphate reveals that agonists hydrolyse polyphosphoinositides instead of phosphatidylinositol. Biochem J 212: 849
6. Berridge MJ, Irvine RF (1989) Inositol phosphates and cell signaling. Nature 341: 197
7. Bohman D (1990) Transcription factor phosphorylation: a link between signal transduction and the regulation of gene expression. Cancer Cells 2: 337
8. Burch RM, Axelrod J (1987) Dissociation of bradykinin-induced prostaglandin formation from phosphatidylinositol turnover in Swiss 3T3 fibroblasts: evidence for G protein regulation of phospholipase A_2. Proc Natl Acad Sci USA 84: 6374
9. Cantley LC, Auger KR, Carpenter C, Duckworth B, Graziani A, Kapeller R, Soltoff S (1991) Oncogenes and signal transduction. Cell 64: 281
10. Cook SJ, Wakelam MJO (1989) Analyses of the water soluble products of phosphatidylcholine breakdown by ion-exchange chromatography. Biochem J 263: 581
11. Cosulich SC, Offer J, Smith GA, Hesketh R, Metcalfe JC (1993) Effects of fluorinated inositols on the proliferation of Swiss 3T3 fibroblasts. Biochem J 292: 719
12. Coughlin SR, Escobedo JA, Williams LT (1989) Role of phosphatidylinositol kinase in PDGF receptor signal transduction. Science 243: 1191
13. Dengler R, Faubner A, Müller-Esterl W, Roscher AA (1990) [Hyp^3]-bradykinin and [Hyp^3]-Lys bradykinin interact with B2-bradykinin receptors and stimulate inositol phosphate production in cultured human fibroblasts. FEBS Lett 262: 111
14. Eberle M, Traynor-Kaplan AE, Sklar LA, Norgauer J (1990) Is there a relationship between phosphatidylinositol trisphosphate and F-actin polymerization in human neutrophils? J Biol Chem 265: 16725
15. Eisenberg F Jr, Parthasarathy R (1987) Measurement of biosynthesis of *myo*-inositol from glucose 6-phosphate. Methods Enzymol 141: 127
16. Fukui Y, Kornbluth S, Jong S-M, Wang L-H, Hanafusa H (1989) Phosphatidylinositol kinase type I activity associates with various oncogene products. Oncogene Res 4: 283
17. Hansen CA, Mah S, Williamson JR (1986) Formation and metabolism of inositol 1,3,4,5-tetrakisphosphate in liver. J Biol Chem 261: 8100
18. Heldin C-H, Westermark B (1990) Platelet-derived growth factor: mechanism of action and possible in vivo function. Cell Regul 1: 555
19. Huang SS, Huang JS (1988) Rapid turnover of the platelet-derived growth factor receptor in *sis*-transformed cells and reversal by suramin. J Biol Chem 263: 12608
20. Irvine RF, Moore RM (1986) Microinjection of inositol 1,3,4,5-tetrakisphosphate activates sea urchin eggs by a mechanism dependent on external Ca^{2+}. Biochem J 240: 917
21. Irvine RF, Moore RM (1987) Inositol(1,4,5)tetrakisphosphate-induced activation of sea urchin eggs. Biochem Biophys Res Commun 146: 284
22. Johnson SC, Dahl J, Shih T-L, Schedler DJA, Anderson L, Benjamin TL, Baker DC (1993) Synthesis and evaluation of 3-modified 1D-*myo*-inositols as inhibitors and substrates of phosphatidylinositol synthase and inhibitors of *myo*-inositol uptake by cells. J Med Chem 36: 3628
23. Kaplan DR, Whitman M, Schaffhausen B, Pallas DC, White M, Cantley L, Roberts TM (1987) Common elements in growth factor stimulation and oncogenic transformation: 85 kd phosphoprotein and phosphatidylinositol kinase activity. Cell 50: 1021
24. Kikkawa U, Nishizuka Y (1986) The role of protein kinase C in transmembrane signaling. Annu Rev Cell Biol 2: 149
25. Kozikowski AP, Fauq AH, Aksoy IA, Seewald MJ, Powis G (1990) Synthesis of the first optically pure, fluorinated inositol 1,4,5-trisphosphate of *myo*-inositol stereochemistry and its effect on Ca^{2+} release in Swiss 3T3 cells. J Am Chem Soc 112: 7403
26. Kozikowski AP, Fauq AH, Powis G, Melder DC (1990) Efficient synthetic routes to fluorinated isosteres of inositol and their effects on cellular growth. J Am Chem Soc 112: 4528
27. Kriz R, Lin L-L, Sultzman L, Ellis C, Heldin C-H, Pawson T, Knopf J Phospholipase C isozymes: structural and functional similarities. Proto-oncogenes in cell development. Ciba Foundation Symposium. 150: 112
28. Li W, Zhou Q, Qin M, Tao L, Lous M, Hu T (1991) Reduced absolute rate of *myo*-inositol biosynthesis of cultured bovine retinal capillary pericytes in high glucose. Exp Cell Res 52: 569
29. Llano I, Marty A, Tanguy J (1987) Dependence of intracellular effects of GTP-2S and inositol trisphosphate on cell membrane potential and on external Ca^{2+} ions. Pflugers Arch 409: 499
30. Majerus PW, Ross TS, Cunningham TW, Caldwell KK, Jefferson AB, Bansal VS (1990) Recent insights in phosphatidylinositol signaling. Cell 63: 459
31. Markovits J, Linassier C, Fosse P, Couprie J, Pierre J, Jacquemin-Sablon A, Saucier JM, Le-Pecq JB, Larsen AK (1989) Inhibitory effects of the tyrosine kinase inhibitor genistein on mammalian DNA topoisomerase II. Cancer Res 49: 5111
32. Melchiori A, Carlone S, Allavena G, Aresu O, Parods S, Aarronson SA, Albinii A (1990) Invasiveness and chemotactic activity of oncogene transformed NIH/3T3 cells. Anticancer Res 10: 37
33. Moyer JD, Reizes O, Ahir S, Jiang C, Malinowski N, Baker DC (1989) Substrate properties of analogs of *myo*-inositol. Mol Pharmacol 33: 683
34. Nahorski SR, Potter BVL (1989) Lithium and the phosphoinositide cycle: an example of uncompetitive inhibition and its pharmacological consequences. Trends Pharmacol Sci 10: 139
35. Nånberg E, Rozengurt E (1988) Temporal relationship between inositol polyphosphate formation and increases in cytosolic Ca^{2+} in quiescent 3T3 cells stimulated by platelet-derived growth factor, bombesin and vasopressin. EMBO J 9: 2741
36. Nishizuka Y (1988) The molecular heterogeneity of protein kinase C and its implications for cellular regulation. Nature 334: 661
37. Olsen R, Santone K, Melder D, Oakes SG, Abraham R, Powis G (1988) An increase in intracellular free Ca^{2+} associated with serum free growth stimulation of Swiss 3T3 fibroblasts by epidermal growth factor in the presence of bradykinin. J Biol Chem 263: 18 030
38. Penner R, Matthews G, Neher E (1988) Regulation of calcium influx by second messengers in rat mast cells. Nature 334: 499

39. Powis G, Aksoy IA, Melder DC, Aksoy S, Eichinger H, Fauq AH, Kozikowski AP (1991) D-3-Deoxy-3-substituted *myo*-inositol analogues as inhibitors of cell-growth. Cancer Chemother Pharmacol 29: 95
40. Rao RJ, Strickland KP (1974) On the solubility, stability and partial purification of CDP-diacyl-*sn*-glycerol: inositol transferase from rat brain. Biochim Biophys Acta 348: 306
41. Rozengurt E (1989) Signal transduction pathways in mitogenesis. Br Med Bull 45: 515
42. Serunian LA, Haber MT, Fukui T, Kim JW, Rhee SG, Lowenstein JM, Cantley LC (1989) Polyphosphoinositides produced by phosphatidylinositol 3-kinase are poor substrates for phospholipases C from rat liver and bovine brain. J Biol Chem 264: 17 809
43. Sinha BK, Katki AG, Batist B, Cowan KH, Myers CE (1987) Adriamycin-stimulated hydroxyl radical formation in human breast tumor cells. Biochem Pharmacol 36: 793
44. Slack BE, Ball JE, Benos DJ (1986) Inositol-1,4,5-trisphosphate injection mimics fertilization potentials in sea urchin eggs. Am J Physiol 250: C340
45. Taylor SJ, Chae HZ, Rhee SG, Exton JH (1991) Activation of the β1 isozyme of phospholipase C by α subunits of the G_q class of G proteins. Nature 350: 516
46. Tietz NW, Finley PR, Pruden E (1988) Clinical guide to laboratory tests. Saunders, New York
47. Whiting PH, Palmano KP, Hawthorne JN (1979) Enzymes of *myo*-inositol and inositol lipid metabolism in rats with streptozotocin-induced diabetes. Biochem J 179: 549
48. Whitman M, Kaplan DR, Schaffhausen B, Cantley L, Roberts TM (1985) Association of phosphatidylinositol kinase activity with polyoma middle-T competent transformation. Nature 315: 239
49. Young D, Waitches G, Birchmeier C, Fasano O, Wigler M (1986) Isolation and characterization of a new cellular oncogene encoding a protein with multiple potential transmembrane domains. Cell 45: 711

STIC-ILL

Vol IV

From: Holleran, Anne
Sent: Monday, January 20, 2003 11:57 AM
To: STIC-ILL
Subject: refs. for 09/868,968

428380

Please send copies of the following papers:

1.	Hoyoku,	Anticancer Res. (1999) 19(5A): 3663-3664
2.	Chamson-Reig	Endocrinology (1999) 140(8): 3573-3580
3.	Lixin,	J. Medicinal Chemistry 91998) 41(18): 3303-3306
4.	Yorek,	American J. Physiology (1998) 274(1, part1): C58-C71
5.	Nazih-Sanderson	Biochimica et Biophysica Acta (1997) 1346(1): 45-60
6.	Wattenberg	Cancer Research (1996) 56(22): 5132-5135
7.	Caro	Infection and Immunity (1996) 64(8): 3438-3441
8.	Seymour	Laboratory Investigation (1996) 75(3): 427-437
9.	Brunn	Cancer Chemotherapy (1994) 35(1): 71-79
10.	Kopp	Cancer Research (1990) 50(20): 6490-6496
11.	Tanino	Japanese J. Experimental Medicine (1972) 42(6): 575-582
12.	Eagle	Biochmistry (1963) 2(5): 1125-1126
13.	Caro	Biochem. Mol. Med. (1997) 61: 214-228

mfk - 381. B523

Anne Holleran
AU: 1642
Tel: 308-8892
RM: 8e03

mailbox: 8e12

(2)
.18q 18L
1/22

dase. These facts indicate the virtual absence of acetylmuramic acid residues, unsubstituted by peptide, in these walls. The situation is thus quite different from the hydrolysis of walls of *M. lysodeikticus* by egg white lysozyme, which treatment alone resulted in liberation of a small percentage of di- and tetrasaccharide (Ghuysen and Salton, 1960; Ghuysen, 1960). The cell wall of *S. aureus* may therefore be a far more rigid structure than that of *M. lysodeikticus*. This fact could provide a further explanation for its resistance to egg white lysozyme.

References

Abrams, A. (1958), *J. Biol. Chem. 230*, 949.
Bellamy, L. J. (1958), The Infrared Spectra of Complex Molecules, London, Methuen, p. 178.
Brumfitt, W. (1959), *Brit. J. Exptl. Pathol. 40*, 441.
Brumfitt, W., Wardlaw, A. C., and Park, J. T. (1958), *Nature 181*, 1783.
Erwin, E. S., Marco, G. J., and Emory, E. M. (1961), *J. Dairy Sci. 44*, 1768.
Findlay, J., and Levvy, G. A. (1960), *Biochem. J. 77*, 170.
Ghuysen, J. M. (1960), *Biochim. Biophys. Acta 40*, 473.
Ghuysen, J. M., Leyh-Bouille, M., and Dierickx, L. (1962), *Biochim. Biophys. Acta 64*, 286.
Ghuysen, J. M., and Salton, M. R. J. (1960), *Biochim. Biophys. Acta 40*, 462.
Ghuysen, J. M., and Strominger, J. L. (1963), *Biochemistry 2*, 1110.
Hestrin, S. (1949), *J. Biol. Chem. 180*, 249.
Hough, L., Jones, J. K. N., and Wadman, W. H. (1950), *J. Chem. Soc. 1950*, 1702.
Ludowieg, J., and Dorfman, A. (1960), *Biochim. Biophys. Acta 38*, 212.
MacFadyen, D. A. (1945), *J. Biol. Chem. 158*, 107.
Mandelstam, M., and Strominger, J. L. (1961), *Biochem. Biophys. Res. Commun. 5*, 466.
Park, J. T., and Johnson, M. J. (1949), *J. Biol. Chem. 181*, 149.
Salton, M. R. J. (1957), *Bacteriol. Rev. 21*, 82.
Salton, M. R. J., and Ghuysen, J. M. (1960), *Biochim. Biophys. Acta 45*, 355.
Sanderson, A. R., Strominger, J. L., and Nathenson, S. G. (1962), *J. Biol. Chem. 237*, 3603.
Stoffyn, P. J., and Jeanloz, R. W. (1954), *Arch. Biochem. Biophys. 52*, 373.
Strominger, J. L. (1958), *Biochim. Biophys. Acta 30*, 645.
Strominger, J. L., Park, J. T., and Thompson, R. E. (1959), *J. Biol. Chem. 234*, 3263.
Suzuki, S., and Strominger, J. L. (1960), *J. Biol. Chem. 235*, 2768.
Trevelyan, W. E., Proctor, D. P., and Harrison, J. S. (1950), *Nature 166*, 444.

Failure of 10 Congeners of *myo*-Inositol to Support or to Inhibit the Growth of a Cultured Human Cell

H. Eagle* and G. E. McCasland

From the Department of Cell Biology, Albert Einstein College of Medicine, New York 61, and the Department of Medical Microbiology, Stanford University, Stanford, California

Received April 25, 1963

Ten congeners of *myo*-inositol failed to support the growth of a human cancer cell (KB) even at 10^{-4} g/ml, 1000 times the minimal effective concentration of *myo*-inositol itself. Eight compounds tested at 10^{-3} g/ml failed to inhibit the growth-promoting activity of *myo*-inositol at 2×10^{-6} g/ml, a ratio of analog to *myo*-inositol of 500:1.

Interest in the supporting or inhibiting effect of inositol congeners on human cell growth arises from the fact that ordinary (*myo*) inositol is one of the twenty-two organic compounds (including thirteen amino acids) which are necessary and sufficient for growth of cultured human cells. In the absence of *myo*-inositol, those defined components, supplemented with dialyzed serum, permit growth only on the addition of serum ultrafiltrate. Experiments in which ninety growth factors were examined showed that *myo*-inositol was able wholly to replace the ultrafiltrate, while none of the other eighty-nine factors, either separately or together, showed demonstrable activity (Eagle *et al.*, 1956).

Most cultured mammalian cells can synthesize only a fraction of their *myo*-inositol requirement from glucose (Eagle *et al.*, 1960). One cell line, a mouse fibroblast, not only produced enough for its own survival and growth but released sufficient inositol into the medium to permit the parabiotic growth of another and inositol-dependent line. Another cell, a variant of the Hela strain, synthesized marginal amounts, so that exogenous inositol became essential for survival only at inocula of less than 200,000–500,000/ml (Eagle and Piez, 1962). With most cultured mammalian cells, however, exogenous inositol was essential for survival and growth (Eagle *et al.*, 1956), presumably because of the loss of the newly synthesized material to the medium in amounts which exceeded the biosynthetic capacity of the cell (Eagle and Piez, 1962).

A number of recently synthesized inositol analogs and derivatives (McCasland *et al.*, 1954,1961, 1963a,b,c; Shoolery *et al.*, 1961) have now been tested both for their ability to support the growth of an inositol-requiring culture (human carcinoma strain KB) (Eagle, 1955), and for their possible antagonism to *myo*-inositol itself. The compounds are listed in Table I. None of these substituted for inositol in any concentration up to 10^{-4} g/ml, 100 times the maximally effective concentration of *myo*-inositol (Eagle *et al.*, 1956), and 1000 times the concentration (10^{-7} g/ml) with a partial growth-promoting action. Further, when eight of these compounds were used at 10^{-3} g/ml in conjunction

* Albert Einstein College of Medicine. Supported by a grant (E-4153) from the National Institute of Allergy and Infectious Diseases, National Institutes of Health, U. S. Public Health Service, and by a grant (G-17192) from the National Science Foundation.

with 2×10^{-6} g/ml of *myo*-inositol, a 500:1 ratio of analog to inositol, none showed a growth-inhibiting effect (cf. last column in Table I).

TABLE I

FAILURE OF TEN CONGENERS OF *myo*-INOSITOL[a] TO SUPPORT OR TO INHIBIT THE GROWTH OF A CULTURED HUMAN CELL

Compound Tested	Growth[b] in 5 Days when Added at 10^{-4} g/ml to Otherwise Inositol-free Medium	Antagonistic Action of 10^{-3} g/ml to *myo*-Inositol at 2×10^{-6} g/ml (amount of cellular growth[b] after 5 days)
DL-1-Deoxy-*epi*-inositol 	1.3[c]	13.6 ×
(+)-1-Deoxy-*allo*-inositol 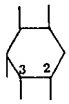	0.95	13.8 ×
(−)-2-Deoxy-*allo*-inositol 	1.16	—
(−)-3-Bromo-3-deoxy-L-inositol 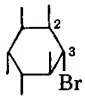	1.0	14.4 ×
(−)-3-Chloro-3-deoxy-L-inositol 	0.89	14.6 ×
(−)-1-Chloro-1-deoxy-*neo*-inositol 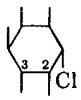	0.89	13.5 ×
(−)-1-Iodo-1-deoxy-*neo*-inositol 	1.27[c]	13.8 ×
DL(124/5) Stereoisomer of 1,2,4,5-cyclohexanetetrol 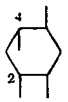	1.14	14.2 ×
meso(13/25) Stereoisomer of 1,2,3,5-cyclohexanetetrol 	0.94	3.84[d] ×
D(126/345) Stereoisomer of 5,6-dimercapto-1,2,3,4-cyclohexanetetrol 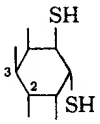	1.0	—
Control with *myo*-inositol alone	10^{-4} g/ml 12.9 10^{-5} g/ml 12.0 10^{-6} g/ml 11.2	14.0 ×

[a] The methods of cell cultivation, the medium used, and the measurement of cell growth by protein determination have been described in previous communications of Eagle *et al.* (1956, 1960, 1962). A human cancer cell (KB) culture was used throughout (Eagle, 1955). [b] Referred to inoculum as 1. [c] Insignificant amount of growth, often observed in inositol-free medium. [d] Questionable significance: growth with 10^{-5} g/ml of analog was 14.3 ×.

REFERENCES

Eagle, H. (1955), *Proc. Soc. Exptl. Biol. Med. 89*, 362.

Eagle, H., Agranoff, B. W., and Snell, E. E. (1960), *J. Biol. Chem. 235*, 1891.

Eagle, H., Oyama, V. I., Levy, M., and Freeman, A. (1956), *Science 123*, 845. See also *J. Biol. Chem. 226*, 191 (1957).

Eagle, H., and Piez, K. A. (1962), Amino Acid Pools, Amsterdam, Elsevier, pp. 694–705.

McCasland, G. E., Furuta, S., and Bartuska, V. (1963c), *J. Org. Chem. 28*, 2096.

McCasland, G. E., Furuta, S., Furst, A., Johnson, L. F., and Shoolery, J. N. (1963a), *J. Org. Chem. 28*, 456.

McCasland, G. E., Furuta, S., Johnson, L. F., and Shoolery, J. N. (1961), *J. Am. Chem. Soc. 83*, 2335.

McCasland, G. E., Furuta, S., Johnson, L. F., and Shoolery, J. N. (1963b), *J. Org. Chem. 28*, 894.

McCasland, G. E., and Horswill, E. C. (1954), *J. Am. Chem. Soc. 76*, 2373.

Shoolery, J. N., Johnson, L. F., Furuta, S., and McCasland, G. E. (1961), *J. Am. Chem. Soc. 83*, 4243.

STIC-ILL

Adams only $35.00

From: Holleran, Anne
Sent: Monday, January 20, 2003 11:57 AM
To: STIC-ILL
Subject: refs. for 09/868,968

Please send copies of the following papers:

1.	Hoyoku,	Anticancer Res. (1999) 19(5A): 3663-3664
2.	Chamson-Reig	Endocrinology (1999) 140(8): 3573-3580
3.	Lixin,	J. Medicinal Chemistry 91998) 41(18): 3303-3306
4.	Yorek,	American J. Physiology (1998) 274(1, part1): C58-C71
5.	Nazih-Sanderson	Biochimica et Biophysica Acta (1997) 1346(1): 45-60
6.	Wattenberg	Cancer Research (1996) 56(22): 5132-5135
7.	Caro	Infection and Immunity (1996) 64(8): 3438-3441
8.	Seymour	Laboratory Investigation (1996) 75(3): 427-437
9.	Brunn	Cancer Chemotherapy (1994) 35(1): 71-79
10.	Kopp	Cancer Research (1990) 50(20): 6490-6496
11.	Tanino	Japanese J. Experimental Medicine (1972) 42(6): 575-582
12.	Eagle	Biochmistry (1963) 2(5): 1125-1126
13.	Caro	Biochem. Mol. Med. (1997) 61: 214-228

Anne Holleran
AU: 1642
Tel: 308-8892
RM: 8e03

mailbox: 8e12

Article title	Isolation and partial characterisation of insulin-mimetic inositol phosphoglycans from human liver
Article identifier	107731509700152X
Authors	Caro_H_N Kunjara_S Rademacher_T_W Leon_Y Jones_D_R Avila_M_A Varela-Nieto_I
Journal title	Biochemical and Molecular Medicine
ISSN	1077-3150
Publisher	Academic Press USA
Year of publication	1997
Volume	61
Issue	2
Supplement	0
Page range	214-228
Number of pages	15
User name	Adonis
Cost centre	
PCC	$35.00
Date and time	Tuesday, January 21, 2003 11:41:30 PM

BIOCHEMICAL AND MOLECULAR MEDICINE 61, 214–228 (1997)
ARTICLE NO. MM972607

Isolation and Partial Characterisation of Insulin-Mimetic Inositol Phosphoglycans from Human Liver

H. N. Caro,* S. Kunjara,* T. W. Rademacher,*,[1] Y. León,† D. R. Jones,† M. A. Avila,† and I. Varela-Nieto†

*Molecular Medicine Unit, Department of Molecular Pathology, University College London Medical School, Windeyer Building, 46 Cleveland Street, London W1P 6DB, United Kingdom; and †Instituto de Investigaciones Biomédicas, Consejo Superior de Investigaciones Científicas, Arturo Duperier 4, 28029 Madrid, Spain

Received April 17, 1997

Extracts of human liver were found to contain activities which copurified and coeluted with the two major subtypes of mediators (type A and type P) isolated from insulin-stimulated rat liver. The putative type A mediator from human liver inhibited cAMP-dependent protein kinase from bovine heart, decreased phosphoenolpyruvate carboxykinase mRNA levels in rat hepatoma cells, and stimulated lipogenesis in rat adipocytes. The putative type P mediator stimulated bovine heart pyruvate dehydrogenase phosphatase. Both fractions were able to stimulate proliferation of EGFR T17 fibroblasts and the type A was able to support growth in organotypic cultures of chicken embryo cochleovestibular ganglia. Both activities were resistant to Pronase treatment and the presence of carbohydrates, phosphate, and free-amino groups were confirmed in the two fractions. These properties are consistent with the structure/function characteristics of the type A and P inositol-phosphoglycans (IPG) previously characterized from rat liver. Further, the ability of the human-derived mediators to interact with rat adipocytes and bovine-derived metabolic enzymes suggests similarity in structure between the mediators purified from different species. Galactose oxidase-susceptible membrane-associated glycosylphosphatidylinositols (GPI) have been proposed to be the precursors of IPG. GPI was purified from human liver membranes foll wed by treatment with galactose oxidase and redu tion with NaB^3H_4. Serial t.l.c. revealed three radiolabeled bands which comigrated with the putative GPI precursors found in rat liver. These galactose-oxidase-reactive lipidic compounds, however, were only partially susceptible to hydrolysis with phosphatidylinositol-specific phospholipase C from *Bacillus thuringiensis* and were resistant to glycosylphosphatidylinositol-specific phospholipase C from *Trypanosoma brucei*. These data indicate that IPG molecules with insulin-like biological activities ar present in human liver. © 1997 Academic Press

In mammals, insulin possesses a wide array of cellular effects, including the control of glucose homeostasis, the modulation of key enzymes of lipid and protein metabolism, positive and negative effects on the transcription of cell type-specific genes, and the modulation of cellular proliferation and differentiation postnatally and during development. In terms of metabolic control, the most important target tissues are the liver, adipose tissue, and skeletal muscle. Intracellular insulin responses are complex and exhibit tissue specificity. At the cellular level, insulin action starts with the activation of the endogenous tyrosine kinase activity of its receptor (1). This leads to the phosphorylation on tyrosine residues of a number of intracellular proteins. One of them, insulin receptor substrate-1 (IRS-1), following insu-

This work was supported by the Acción Integrada Hispano-Británica, by grants from the Medical Research Council, the Jules Thorn Trust, and the British Council to T.W.R. and Dirección General de Investigación, Ciencia y Tecnología (DGICYT), Comunidad de Madrid, and Europharma (Boehringer Ingelheim group) to I.V-N. H.N.C. and S.K. are supported by the Medical Research Council (UK). Y.L. and M.A.A. are supported by Ministerio de Educación y Ciencia (Spain) and D.R.J. by The Royal Society (UK) and the Consejo Superior de Investigaciones Científicas (Spain).

[1] To whom correspondence should be addressed. Fax: 0171-380-9497. E-mail t.rademacher@ucl.ac.uk.

1077-3150/97 $25.00

lin stimulation, serves as a link to a group of signaling proteins containing src-homology 2 domains (2). IRS-1 was thought to play a central role in the cellular responses to insulin and insulin-like growth factor-I (IGF-I) but recent gene knockout experiments indicate that much of the signaling by insulin and IGF-I receptors may be independent of IRS-1 (3). These findings suggest the existence of alternative pathways, one of them possibly being a second putative substrate for the insulin receptor, IRS-2 (4). In addition, insulin stimulation of glucose utilization and other metabolic effects seem to be independent of the activation of mitogen-activated protein kinase or mitogen-activated protein kinase kinase (reviewed in 5), two key kinases of the phosphorylation cascade pathway. The complexity of insulin actions suggests that a network of independent intracellular signaling pathways will be needed to achieve the appropriate specific response at the proper time.

The glycosylphosphatidylinositol (GPI) subgroup of glycolipids may play an important dual function in eukaryotic cells. GPIs serve as membrane anchors of covalently attached proteins which are found in the outer leaflet of the plasma membrane (6). They have also been proposed to be precursors to inositol phosphoglycan (IPG) second messengers (7). Following receptor ligation a putative phospholipase is activated and the cleavage of free GPI occurs, yielding IPG. It is at present not clear what structural features are in common between the free GPIs and the protein-associated GPIs. The role of IPG molecules as insulin mediators has been postulated on the basis of the unique ability of IPG to mimic the short- and long-term effects of this hormone (reviewed in 8). Moreover, mutant cells unable to synthesize GPI respond to insulin by tyrosine phosphorylation but they do not synthesize glycogen upon insulin stimulation (9). Insulin and IGF-I are members of a growing list of growth factors and extracellular stimuli which have been demonstrated to utilize free GPIs for at least part of their signal transduction mechanisms (reviewed in 8).

Different families of mammalian-derived IPG have been reported (10–12). At least two distinct types exist, denominated types A and P (13); the ratio of the types released is tissue-specific (14). The type A mediators are functionally and chemically distinct from the type P mediators (reviewed in 13,15). Briefly, type A mediators modulate a number of enzyme activities such as acetylCoA carboxylase (activates) (16), cAMP-dependent protein kinase (inhibits) (17), adenylate cyclase (inhibits) (18), and cAMP phosphodiesterases (stimulates) (19,20). In contrast type P mediators modulate the activity of insulin-dependent enzymes such as pyruvate dehydrogenase phosphatase (PDH-phosphatase) (stimulates), (12,21) and glycogen synthase phosphatase (stimulates) (22). The type A mediators mimic the lipogenic activity of insulin on adipocytes, whereas the type P mediators mimic the glycogenic activity of insulin in muscle (22,23). Both rat-derived type A and P mediators are mitogenic when added to EGFR T17 cells (14,26). In addition, IPG molecules modulate gene expression in an insulin-like manner (24,25). IPG molecules generated by treatment of rat liver membrane with PI-PLC can stimulate cell proliferation in the developing chick cochleovestibular ganglia (CVG) (27). Antibodies against IPG are able to block insulin action (28,29), which further supports the idea that release of IPG is a crucial event in insulin action. Alterations in IPG uptake and metabolism and an impaired insulin response in terms of GPI hydrolysis have been described in different experimental models of insulin resistance in rats (see Discussion).

Soluble IPG molecules have been extracted from a variety of tissues (for recent reviews, see 8,13). Despite these studies, evidence for the presence of soluble IPG mediators in a primary target organ for insulin action in humans has not been established. We describe here the isolation and partial characterization from human liver of two activities which copurify and coelute with the two subtypes of IPGs previously described (14,29) and the isolation and partial characterization of a putative IPG precursor, GPI. The two types of IPG reported here are shown to possess distinct chemical properties and insulin-like biological actions.

MATERIALS AND METHODS

Materials

Galactose oxidase, D-glucosamine, fluorescamine, D-galactose, bromophenol blue, activated charcoal, histone IIA, and cAMP-dependent protein kinase were obtained from Sigma (Poole, UK). GPI-PLC from *Trypanosoma brucei* was purchased from Oxford Glycosystems (Oxford, UK). Sodium borohydride NaB^3H_4 (5–20 Ci/mmol), [γ-^{32}P]ATP (3000 Ci/mmol), D-[U-^{14}C]glucose (3 mCi/mmol), [^{3}H]inositol phosphates (3 Ci/mmol), and [^{3}H]thymidine (40–60 Ci/mmol) were obtained from Amersham Int. (Amersham, UK). [α-^{32}P]dCTP (3000 Ci/mmol) and

En^{3}Hance were obtained from DuPont-New England Nuclear (Boston, MA). Sep-Pak C18 cartridges were obtained from Waters (Bedford, MA). Silica gel G60 thin-layer chromatography (t.l.c.) plates were obtained from Merck (Darmstadt, Germany). Ion exchange resins AG1-X8 (HO^-, 20–50 mesh), AG3-X4 (HO^-, 100–200 mesh), and AG50-X12 (H^+, 200–400 mesh) were obtained from Bio-Rad Laboratories (Hemel Hempstead, UK). Cell culture reagents were obtained from Biowhitaker (Verviers, Belgium). Fetal calf serum (FCS) was obtained from Gibco (Paisley, UK). Salts, organic solvents, and other reagents were of analytic grade or better.

Samples of human liver were obtained by hepatectomy before liver transplantation from a 56-year-old female patient suffering from primary biliary cirrhosis and from a 33-year-old male accident victim. The livers were surgically removed, immediately frozen in liquid nitrogen, and stored at −70°C until used.

Methods

Isolation of IPG. IPGs were purified following the protocol described previously (29), with some modifications. Briefly, each batch was prepared from approximately 90 g of frozen human or control rat liver. The frozen tissue was powdered under liquid nitrogen and placed directly into boiling 50 mM formic acid containing 1 mM ethylenediaminetetraacetic acid (EDTA) and 1 mM 2-mercaptoethanol (3 ml of buffer per gram (wet weight) of tissue). After a 1-min homogenization with a polytron mixer (Kinematica, Littau, Switzerland), the solution was further boiled for 5 min. The solution was then cooled on ice and centrifuged at 29,500*g* for 2 h at 4°C. The supernatant was treated with 10 mg/ml activated charcoal for 30 min with stirring at 4°C. The charcoal suspension was centrifuged at 29,500*g* for 1 h at 4°C and the clear supernatant recovered. The solution was then diluted 10-fold with distilled water, adjusted to pH 6.0 with 10% NH_4OH solution, and then gently shaken overnight at room temperature with AG1-X8 (formate form) resin (0.3 ml resin/ml solution). The resin was then poured onto a chromatography column (2.5 × 60 cm) and washed sequentially with water (2 bed volumes) and 1 mM HCl (2 bed volumes). Then material was eluted with 10 mM HCl (5 bed volumes) and finally with 50 mM HCl (5 bed volumes). Both fractions were adjusted to pH 4.0 with 10% NH_4OH solution before drying in a rotary evaporator. The dried fractions were redissolved in distilled water, lyophilized twice, and divided into five aliquots for both chemical and biochemical analyses. The n menclature for each preparati n was defined at this point following the criteria of (29): the material eluted from the column using 10 mM HCl was named IPG type P and that which eluted using 50 mM HCl was named IPG type A. For analyses, aliquots of each type of mediator were made by dissolving the amount of material obtained from 18 g (wet weight) of tissue in 200 μl of distilled water, appropriate buffers, or Hanks' salts (Seromed Laboratories, Berlin, Germany) and adjusted to pH 7.0 with 1 M KOH. Therefore, 10 μl of stock solution represents the amount of type A or P mediator recovered from 900 mg of starting tissue.

Chemical characterization of IPG. IPG was treated with pronase E as follows. Briefly, a stock solution of the enzyme (10 mg/ml) was preincubated at 60°C for 30 min in 100 mM Tris–HCl buffer, pH 8.0, to inactivate contaminating enzymes which may be present. Treatment was started by addition of Pronase solution (30 μl) to IPG samples in 200 μl of 100 mM Tris–HCl buffer, pH 8.0, at 37°C. After 2 h, the reaction was terminated by boiling for 3 min and then proteins were removed by acid precipitation.

For paper chromatography, IPG was dissolved in a minimum amount of distilled water and applied to Whatman 3MM chromatography paper (3 × 50 cm, origin at 8.5 cm). Descending paper chromatography was performed using *n*-butanol:ethanol:water (4:1:1, by volume) for a period of 9 h. After drying, the paper was cut every centimeter (−1 to +35 cm from the origin) and then the material associated in each fraction was eluted with water (60 μl, five washes). Each fraction was evaporated to dryness and redissolved either in water or in Hanks' salts (60 μl) and neutralized with 1 N KOH prior to the determination of free amino groups and phosphate content or to assay biological activities.

High-voltage paper electrophoresis (HVE) was performed on pooled material eluted from fractions −1 to +6 after paper chromatography. The material was redissolved in 50 μl of distilled water and applied to Whatman 3MM electrophoresis paper. Bromophenol blue and a mixture of [^{3}H]inositol phosphates were added as a marker and standards, respectively. Electrophoresis was performed for 30 min at 80 Vcm^{-1} in pyridine:acetic acid:water (3:1:387, by volume), pH 5.4. Subsequently, the paper was dried, fractions were cut every centimeter, and associated material was eluted with water as described above for paper chromatography. Neutral com-

pounds remained at the point of application, while negatively charged compounds moved toward the anode.

The interaction of IPGs with ion-exchange resins and Sep-Pak C18 cartridges was performed using dilutions of the aqueous stock solutions. After loading onto columns containing 600 μl of either AG3-X4 (HO^-) or AG50-X12 (H^+) or onto Sep-Pak C18 cartridges, elutable material was recovered with water (5 bed volumes). The solutions were concentrated to dryness, redissolved in 30 μl of Hanks' salts, and adjusted to pH 7.0 before being used for biological analysis.

Measurement of free amino groups was performed as described previously (30). Samples and standards (0–100 nmol of D-(+)-glucosamine hydrochloride) were dissolved in water (50 μl) before sequentially adding aqueous sodium borate (pH 9.0) and fluorescamine (prepared in dry acetone), yielding final concentrations of 140 mM and 0.75 mg/ml, respectively. Emission fluorescence at 475 nm was observed after excitation at 390 nm using a spectrofluorimeter (Kontron Instruments, Rotkreuz, Switzerland).

Total phosphate levels were assayed by an adaptation of (31). Samples and standards (0–100 nmol of disodium hydrogen phosphate) were evaporated to dryness and hydrolyzed with perchloric acid (70%, by volume) at 180°C for 30 min. After cooling to room temperature, distilled water (250 μl) was added. Ammonium molybdate and ascorbic acid were sequentially added, yielding final concentrations of 3 and 72 mM, respectively. Color development was achieved by heating the samples at 95°C for 15 min. Optical absorbance was measured at 655 nm.

The presence of carbohydrates and the absence of peptides was confirmed by anion exchange HPLC (Dionex) using pulsed amperometric detection and measuring the absorbance at 254 nm, respectively. Analysis was performed with the material obtained after paper chromatography purification.

Lipid isolation and analysis. Glycolipids were partially purified from human liver membranes following the method described in (11) with minor modifications (30). The membrane fraction was obtained by sequential centrifugation from 20 g of material. Total lipids were obtained by chloroform/methanol extraction followed by the removal of nonpolar lipids. GPI was separated from other phospholipids by sequential acid/base silica gel G60 t.l.c. (see below). Lipid migration was calibrated in parallel with phospholipid standards that were detected by staining with iodine. Lipids were extracted from the t.l.c. plate with methanol, dried, applied to a Sep-Pak C18 cartridge, eluted with methanol, and dried. The glycolipids were labeled by treatment with galactose oxidase followed by reduction with [^{3}H]sodium borohydride according to (32). The radiolabeled GPI was subjected to sequential acid/base t.l.c as above. The purified sample was resuspended in water, applied to a Sep-Pak C18 cartridge, and eluted with water (5 ml) and then with methanol (5 ml). The methanol fraction was collected, dried, and stored at −70°C until used. Approximately 5×10^4 cpm of radiolabeled GPI was spotted onto the origin of a silica gel G60 t.l.c. plate which was developed twice in an acidic solvent system [chloroform:acetone:methanol:acetic acid:water (50:20:10:10:5, by volume)] or in a basic solvent system [chloroform:methanol:ammonium hydroxide:water (45:45:3.5:10, by volume)]. Alternatively, labeled GPI molecules were further resolved by double-dimension t.l.c. as described in (26,33) or by using high-performance (HP)-t.l.c. plates developed in chloroform:methanol:ammonium hydroxide:water (40:45:3.5:15, by volume) as described (34). The plates were then sprayed with En^{3}Hance and the pattern of labeled glycolipids was analyzed by autoradiography.

Sensitivity to PLC was determined by incubation of [^{3}H-galactose]GPI with 1 unit of either PI-PLC from *Bacillus thuringiensis* or GPI-PLC from *T. brucei* for 15 h according to the manufacturer's instructions. Controls were performed by incubating [^{3}H-galactose]GPI samples in the reaction buffer without enzyme. At the end of the incubation, the reaction was terminated by loading the sample onto a Sep-Pak C18 cartridge. The water eluate (5 ml) was dried and the associated radioactivity determined by liquid scintillation counting. The methanol eluate (5 ml) was dried and labeled glycolipids were resolved on HP-t.l.c. plates as described above. Dried plates were impregnated with En^{3}Hance and subjected to autoradiography.

cAMP-dependent protein kinase activity assay. The ability of the IPG fractions to inhibit the activity of the cAMP-dependent protein kinase was assessed by using histone IIA as substrate as described previously (17). Briefly, the reaction mixture (100 μl) contained 25 mM Hepes buffer (pH 7.6), 10 μM MgATP (10^6 cpm of [γ-^{32}P]ATP), histone IIA (50 μg protein), and the catalytic subunit of the cAMP-dependent protein kinase (60 units/ml). Either buffer control (10 μl) or IPG stock solution in Hanks' salts

(10 μl) was added to the reaction mixture. After incubation at 37°C for 10 min, the reaction was stopped and proteins were precipitated with 10% TCA (500 μl). The incorporation of ^{32}P into proteins was determined by Cerenkov counting.

PDH phosphatase activity assay. The pyruvate dehydrogenase complex (PDC) and the PDH phosphatase were prepared from bovine heart as described (21) and stored at −80°C until use. The assay for PDH phosphatase, in the presence or the absence of insulin mediator, was based upon the initial rate of the activation of the inactivated phosphorylated PDH complex. The initial activity of the PDC was 8–13 units/ml (1 unit of enzyme produces 1 μmol NADH/min). After inactivation with ATP, this value was reduced to less than 1% of the original value. A two-stage assay was used to quantitate the phosphatase activity. A sample of inactivated PDC (50 μl) was preincubated at 30°C with 1 mg/ml fat-free bovine serum albumin, 10 mM $MgCl_2$, 0.1 mM $CaCl_2$, and 1 mM dithiothreitol in 20 mM potassium phosphate buffer, pH 7.0 (total volume 250 μl), for 3 min. At this time, 10 μl of the PDH phosphatase and 10 μl of IPG stock solution were added and the incubation was continued for a further 2 min. At the end of this time, 200 μl of the reaction mixture was removed and added to 100 μl of 300 mM NaF. The activated PDH was determined at the second stage spectrophotometrically by measuring the rate of production of the reduced form of NADH. One hundred microliters of the stopped reaction was added to 1 ml of reaction mixture containing 50 mM potassium phosphate buffer at pH 8.0, 2.5 mM of the oxidized form of NAD, 0.2 mM thiamine pyrophosphate (TPP), 0.13 mM coenzyme A, 0.32 mM dithiothreitol, and 2 mM sodium pyruvate. The production of NADH was followed using an absorbance at 340 nm for 5 min. One unit of IPG PDH activity is the amount required to increase the basal rate by 50%.

Activation of lipogenesis in rat adipocytes. The effect of both IPG subtypes on the activation of lipogenesis was tested in rat adipocytes isolated from the epididymal fat pads of young rats, following the procedure described by Rodbell (36). Briefly, adipocytes from two young rat (200 g weight each) epididymal fat pads were suspended in 8 ml of Krebs Ringer bicarbonate buffer. Two hundred and fifty microliters of the cell suspension was incubated at 37°C for 2 h in Krebs Ringer bicarbonate buffer containing 1% w/v albumin and 5 mM [U-^{14}C]glucose (1 μCi/sample) with, or without, insulin (1 nM) or IPG samples (10 μl from stock solution). The rate of incorporation of uniformly labeled glucose into fatty acids was used as a measure of lipogenesis (cpm incorporated/2 h). One unit of IPG lipogenic activity is the amount required to increase the baseline incorporation by 50%. One picomole of insulin produces a stimulation of approximately 300–400%, equivalent to 6–8 units of IPG based on the unit defined above.

RNA extraction and Northern analysis. H4IIE rat hepatoma cells were routinely grown in Dulbecco's modified Eagle's medium (DMEM) with 5% fetal bovine serum, 5% fetal calf serum (FCS), 2 mM L-glutamine, 100 units/ml penicillin, and 100 μg/ml streptomycin at 37°C in a water-saturated atmosphere containing 5% CO_2. Serum was removed for 20–24 h before experiments when the cells were approximately 70% confluent. Treatment with the different agonists was performed as previously described (25). IPG type A or P samples were assayed at a final dilution of 1/100. RNA from treated and control H4IIE cells was isolated by acid guanidinium thiocyanate–phenol–chloroform extraction (37). Total RNA (20 μg per sample) was separated by 1% agarose electrophoresis under denaturing conditions (1.1 M formaldehyde and 50% formamide) and transferred to nitrocellulose filters (Schleicher & Schuell, Keene, NH). Prehybridization and hybridization of the membranes were carried out under moderate stringency conditions (35% formamide at 42°C) for 5 and 24 h, respectively, using the Wahl buffer (38). Filters were hybridized with a 2.6-kb cDNA for rat cytosolic PEPCK (39). Probes were labeled with [α-^{32}P]dCTP by the random priming method (sp act 5–10 × 10^8 cpm/mg DNA) according to the manufacturer's instructions (Amersham Int.). Quantitation was performed by scanning densitometry of the X-ray film and of the ethidium bromide-stained agarose gel as loading control.

Measurement of cellular proliferation in fibroblasts. EGFR T17 fibroblasts were routinely grown in DMEM containing 10% FCS, 2 mM L-glutamine, 100 units/ml penicillin, and 100 μg/ml streptomycin at 37°C in a humidified atmosphere of 5% CO_2. The cells were subcultured when they reached 80% confluency. The EGFR T17 cells are NIH 3T3 fibroblasts transfected with the human epidermal growth factor receptor (40). To evaluate fibroblast cell proliferation, cells were plated into 96-well microtiter wells at a density of 10^4 cells per well in DMEM containing 10% FCS. After 24 h the medium was removed, the cells were washed twice with Hanks' salts, serum-

free medium was added, and the cells were incubated for a further 24-h period. At this point the cells were stimulated with serum, IPG preparations, or the appropriate controls. Eighteen hours later [^{3}H]thymidine (1 μCi/well) was added to each well for 4 h. At the end of this treatment, the cells were washed twice with Hanks' salts, trypsinized, and the radioactivity associated with cellular DNA was determined using a cell harvester (Skatron Instruments, Lier, Norway) and scintillation counting (OptiPhase "HiSafe" liquid scintillation cocktail, Wallac, Turku, Finland), as previously described (25).

Explants culture and measurement of cellular proliferation. CVG were isolated from 72-h chicken embryos as described previously (27). Chicken embryos were removed from eggs and placed in 35-mm petri dishes (NUNC, Roskilde, Denmark), in M199 medium containing Hanks' salts and used only if equivalent to stages 19 or 20. The explanted CVGs were cultured in 4-well multidishes (NUNC) in 0.25 ml of culture medium that consisted of serum-free Medium M199, Earle's salts, 2 mM L-glutamine, 25 mM Hepes, and antibiotics as above. Human IPG fractions were tested at a final dilution of 1/100. DNA synthesis was determined by culturing the CVG explants in medium containing [^{3}H]thymidine (10 μCi/ml) for 24 h. Incubations were carried out at 37°C in a humidified atmosphere containing 5% CO_2. The CVGs were individually rinsed three times with ice-cold phosphate-buffered saline. The explants were then extracted with 10% trichloroacetic acid and the incorporated radioactivity was determined by scintillation counting.

RESULTS

IPG Isolation and Chemical Characterization

Human liver was used for the isolation of IPGs using a protocol previously described for the isolation of IPGs from bovine liver (29) and rat tissues (14). Briefly, the extract was prepared by heat and acid treatment of a liver homogenate. After centrifugation and charcoal extraction, the solution was allowed to interact overnight with an anion exchange resin (AG1-X8, formate form). The resin was washed sequentially with water and dilute HCl. Two fractions were then obtained by elution with 10 mM HCl and 50 mM HCl and defined as human IPG type P and type A, respectively. These fractions were neutralized and lyophilized several times before being used. Both species of IPG showed positive identification for amino groups and phosphate moieties. To compare the biological effects of both IPG types, and due to the scarcity of data available on the chemical composition of IPG type P, identical aliquots of each fraction were prepared taking as a reference the starting wet weight of tissue as reported in (14).

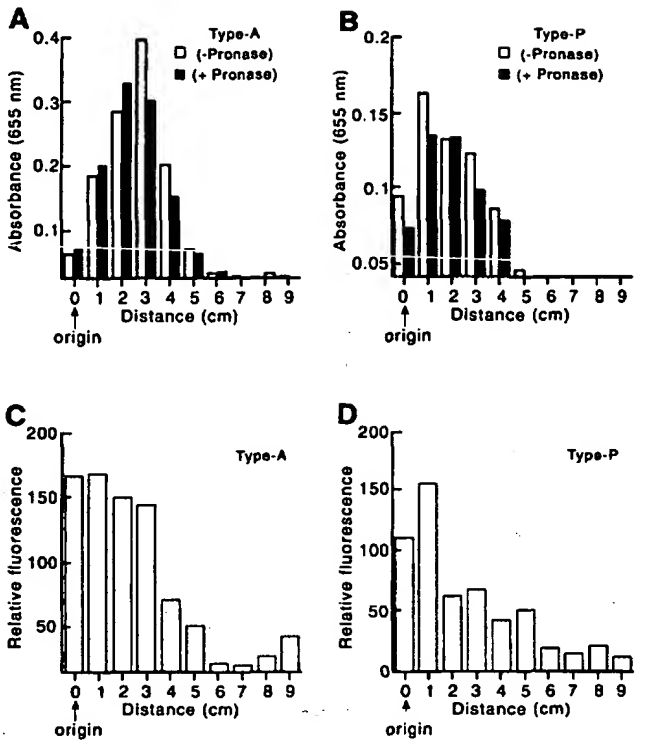

FIG. 1. Purification of IPG by descending paper chromatography. Descending paper chromatographic profiles of control- and Pronase E-treated IPG type A and type P, A and B, respectively, following analysis for phosphate content. (C and D) Free amino group analysis in the same chromatographic fractions. For clarity only the first 10 fractions are displayed in each panel. The profiles for Pronase-treated or untreated mediators were identical (C and D). The solvent front was at +35 cm.

Samples of both IPG types were purified by descending paper chromatography after treatment with Pronase E as described under Materials and Methods. Figures 1A and 1B show the chromatographic profiles for IPG type A and type P, respectively, following analysis for phosphate content. Compounds containing phosphate were found to migrate between the origin and approximately 5 cm (total length 43 cm, solvent front +35 cm). Pronase E treatment did not alter the chromatographic profile. The paper chromatograms were also analyzed for the presence of free amino groups, as shown in Figs. 1C and 1D. Compounds containing free amino groups were predominantly located between the ori-

gin and a migration distance of 5 cm, with a pattern similar to that found for the phosphate analysis. Treatment with Pronase did not alter the elution pattern (data not shown). Carbohydrates were detected in these fractions by pulsed amperometric detection when these samples were further analyzed by anion exchange HPLC (Dionex, data not shown).

The material eluted from the paper (from −1 to +6 cm) after descending chromatography was pooled and subjected to HVE at pH 5.4. Under these conditions, negatively charged compounds containing phosphate, carboxyl, or sulfate groups migrate toward the anode. Phosphate was detected at the origin and as a broad unresolved peak extending from 5 to 20 cm from the origin, as shown in Fig. 2A. The profiles for both types of human IPG were remarkably similar. The presence of phosphate at the origin indicates that compounds recovered in this position must have an equal number of positively charged moieties which neutralize the overall charge. The compounds which migrate might have an excess of negatively charged groups (i.e., phosphate) over the positively charged moieties (i.e., amino, metal). In order to study which fractions had biological activity we tested the uptake of [^{3}H]thymidine by EGFR T17 cells in response to the HVE fractions of both types of IPG. This assay has been used to estimate the relative abundance of the two mediators in several rat tissues since both type A and P mediators are active in the assay (14). Figure 2B shows the effect of IPG type P fractions post-HVE in the stimulation of [^{3}H]thymidine uptake by EGFR T17 cells. Figure 3A shows that the EGFR T17 cells respond in a dose-dependent manner to both the human type A and P IPG prior to HVE. Similar results were found for the human type A IPG after HVE. These data indicate that biological activity is still present after the Pronase treatment followed by the sequential purification through paper chromatography and HVE. The profile of the ability of IPG type P to stimulate [^{3}H]-thymidine incorporation into EGFR T17 cells following HVE mirrored the phosphate analysis profile shown in Fig. 2A, with activity present at the origin and in a broad band extending to a migration distance of 20 cm. Similar results were found with IPG type A (data not shown). The reference assay which defines IPG type P activity is the stimulation of PDH phosphatase (12,13). Figure 3B shows that the human liver type P IPG is able to induce a dose-dependent stimulation of PDH phosphatase. For comparison the dose response of purified rat type P IPG isolated from the same wet weight of rat liver as

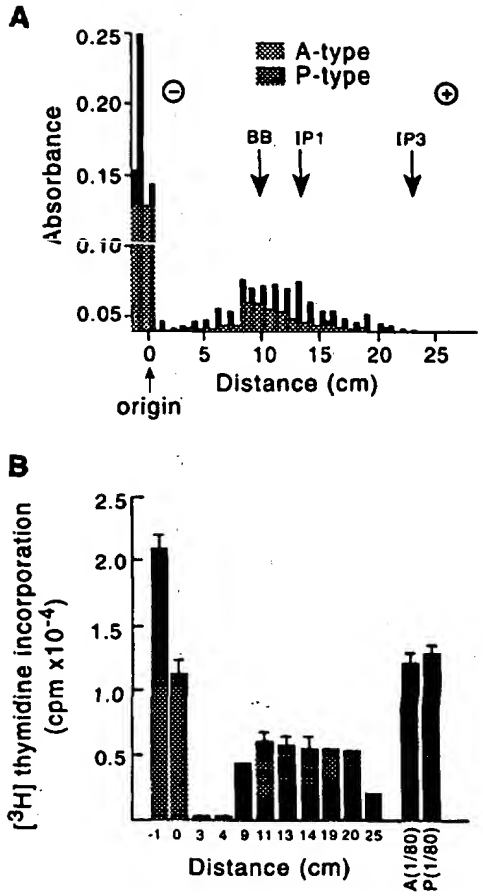

FIG. 2. *HVE of IPG type A and type P.* A representative electrophoretogram of IPG type A (hatched) and type P (black) HVE following detection of phosphate is shown in A. B (left) shows the effect of selected fractions of IPG type P on cell proliferation after the Pronase treatment, descending paper chromatography, and HVE purification steps. B (right) also shows the effect of the crude preparation of IPG type A and type P at a final dilution of 1/80 (see Materials and Methods) on [^{3}H]thymidine incorporation into EGFR T17 fibroblasts. The migration positions of bromophenol blue (BB), inositol monophosphate (IP1), and inositol di/tri-phosphate (IP3) are indicated by arrows.

human liver is shown. The HVE fractions used to assess [^{3}H]thymidine incorporation into EGFR T17 cells were assayed for their ability to stimulate PDH phosphatase. These parameters exhibited a high correlation of $r = 0.97$ ($P < 0.001$) (Fig. 4A). Figure 4B shows that there is also a strong correlation $r = 0.87$ ($P < 0.01$) between the phosphate content of the IPG type P fractions isolated from the HVE electrophoretogram and their ability to stimulate cellular proliferation. The correlation between phosphate content and PDH phosphatase stimulating activity was found to be $r = 0.73$ (data not sh wn).

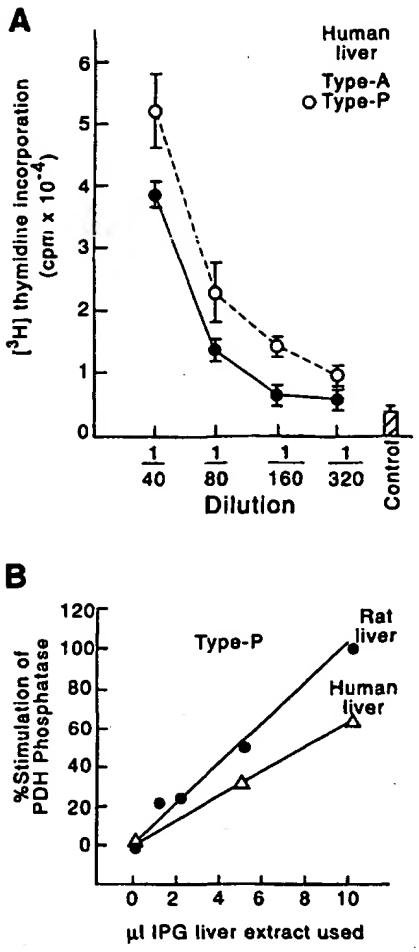

FIG. 3. Stimulation of EGFR T17 fibroblasts and PDH phosphatase. (A) Serial dilutions of stock human liver-derived type A and type P were assayed for their ability to stimulate proliferation. Control represents the proliferation of the fibroblasts in serum-free medium without addition of the IPG. (B) Stimulation of bovine heart-derived PDH phosphatase was linear for both human and rat liver-derived type P mediator. The amount of mediator used was by volume of stock (see Materials and Methods).

The behavior of IPGs in their interaction with two different ion exchange resins and a C18 reverse phase resin were determined by the ability of the aqueous eluates to induce [^{3}H]thymidine incorporation into EGFR T17 cells and is summarized in Table 1. In the case of the Sep-Pak C18 cartridge, about 80–85% of the biological activity of the IPG type A was recovered in the water eluate, whereas only a 50–60% of the activity of the IPG type P was recovered following the same protocol. These results suggest that the type A mediator is hydrophilic. In contrast, the type P mediator is either a mixture of hydrophilic and hydrophobic compounds, both having proliferative activity, or it exists in complex equilibria resulting in partitioning depending on its physical state. The A or P type mediators could not be recovered from either a cation exchange column (AG50-X12) or an anion exchange column (AG3-X4) following water elution, as assessed by [^{3}H]thymidine incorporation into EGFR T17 cells. This is in agreement with the presence of dual functional groups such as free amino and phosphate moieties within both types of human IPG molecules (see Fig. 1).

Both IPGs have been reported to have a variety of insulin-like effects in intact cells and *in vitro* assays of certain enzyme activities (reviewed in 15). Hence the next step was to assess whether human IPG types have distinct biological effects.

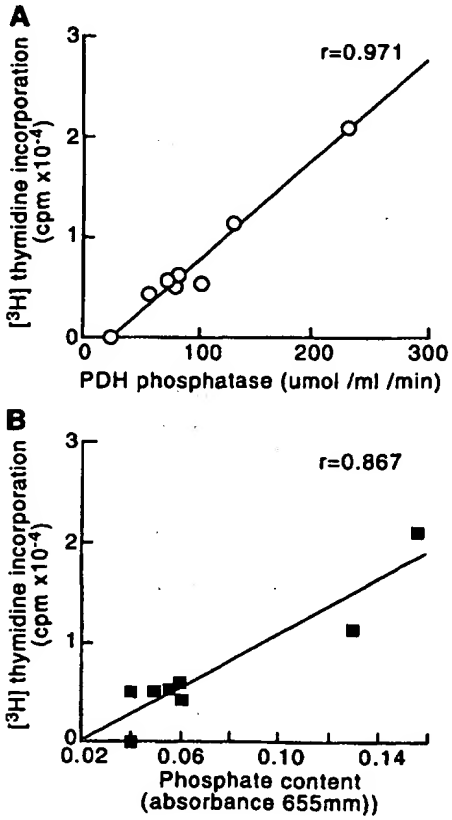

FIG. 4. The correlation among [^{3}H]thymidine incorporation, PDH phosphatase stimulating activity, and phosphate content of selected fractions from the HVE electrophoretogram. (A) HVE fractions (equal to those used in Fig. 2B) were assayed for their ability to stimulate PDH phosphatase. The correlation between both effects was of $r = 0.97$. B shows the correlation ($r = 0.87$) between the phosphate content and the stimulation by the same fractions of [^{3}H]thymidine incorporation into EGFR T17 fibroblasts.

TABLE 1
Interacti n f IPGs with Ion Exchange Resins and C-18 Reverse-Phase Matrix

Control (cpm)	209 ± 79
10% FCS (cpm)	46313 ± 10231
A-type (cpm)	33917 ± 6697
P-type (cpm)	36542 ± 2278
C-18 (% recovery)	
A-type	86
P-type	55
Blank (cpm)	1377 ± 317
AG3 (% recovery)	
A-type	11
P-type	1.5
Blank (cpm)	505 ± 61
AG50 (% recovery)	
A-type	1.5
P-type	2
Blank (cpm)	258 ± 144

Note. [^{3}H]Thymidine incorporation into the EGFR T17-transfected fibroblasts. A and P type mediators were eluted with water from the different supports. Final concentration of IPG was a 1/40 dilution of stock (see Materials and Methods). Similar results were obtained for dilutions of 1/80. All IPG stimulations were dose dependent. Partial recovery of the P type was consistently observed on C-18. No attempt was made to recover the bound material.

Insulin-like Biological Actions of IPG Types A and P

Inhibition of cAMP-dependent protein kinase. The ability of both IPG subtypes to inhibit the activity of the cAMP-dependent protein kinase was tested as already described (17). The addition of IPG type A or type P (stock solution diluted 1/10) caused a 78.5 ± 9.5 and 56.7 ± 16.4% inhibition, respectively, of the kinase activity (n = 4, in triplicate). Control incorporation of ^{32}P into washed histone IIA was approximately 75,000 c.p.m. This effect was dose dependent. When both fractions were assayed at a final dilution of 1/100 a significative inhibition of the kinase activity was achieved only with the type A fraction (50% inhibition type A, 11% inhibition type P). These data are in agreement with those reported for rat or bovine liver-derived IPGs (14,29), where the type A mediator fraction contains the predominant inhibitor activity against cAMP-dependent protein kinase.

Stimulation of PDH phosphatase. The ability of both fractions to stimulate the activity of bovine heart PDH was studied. Table 2 shows that human liver contained substantial PDH phosphatase stimulating activity in the type P eluate. The amount of activity recovered was similar to that recovered from rat liver in the absence of insulin stimulation (see Table 2). Insulin stimulation of rat liver results in a 2-fold increase in recoverable activity 2 min after insulin injection. IPG type A contained less PDH stimulating activity (2.8 fold less compared to IPG type P) which did not increase after insulin stimulation. The predominant insulin-sensitive PDH phosphatase stimulating activity was therefore present in the type P fraction, as already reported for rat and bovine liver (14,29).

Effect on lipogenesis. Both IPGs were tested for their ability to stimulate lipogenesis in isolated rat adipocytes. Table 2 shows that no lipogenic activity was found in the IPG type P from either human liver. This is consistent with the lack of lipogenic activity in the IPG type P from rat liver. In contrast, the IPG type A contained lipogenic activity. The normal human liver was found to contain the same amount of lipogenic activity as that found in type A IPG from insulin-stimulated rat liver. In contrast the diseased liver, obtained at the time of transplantation, was active but contained about fivefold less lipogenic activity than the normal human liver. This was the only differential activity found between the human liver samples.

Effect on PEPCK mRNA expression. The ability of the two human IPG subtypes to mimic the effects of insulin on the regulation of the expression of the gluconeogenic enzyme PEPCK was studied in rat H4IIE hepatoma cells. Incubation of the cells with 0.1 mM 8-bromo-cAMP (8-Br-cAMP) caused within 3–5 h a 3-fold induction over the steady-state levels of PEPCK mRNA (Fig. 5, lanes 2 and 3). As expected, the addition of 100 nM insulin after 3 h of preinduction with 8-Br-cAMP produced a 2-fold reduction in the levels of PEPCK mRNA within 2 h (Fig. 5, lane 4), its effect being dominant over that of 8-Br-cAMP. Under the same conditions, the addition of IPG type A (1/100 final dilution) reversed the stimulatory effect of the 8-Br-cAMP, showing a 2-fold reduction, while the same concentration of IPG type P had a negligible effect on the level of PEPCK mRNA (Fig. 5, lanes 5 and 6). These results indicate that human liver IPG type A had the same effect as rat liver IPG that was generated either by treatment of hepatoma cells with insulin or by PI-PLC hydrolysis of GPI (25).

Effects on CVG proliferation. The insulin family of growth factors has a central role in the control of cell proliferation during the early stages of inner ear development. Mitogenic effects of IGF-I appear to be coupled to the hydrolysis of GPI and the generation of a soluble IPG (27, 41). Studies were conducted to

TABLE 2

Bi activity of Mediators per Tissue Weight (milliunits/g liver)[a,b]

	PDH phosphatase (stimulating activity)	Lipogenesis (lipogenic activity)
Human liver type P[c]	1250, 1960 [N] (n = 2)	No activity [N]
	1487 ± 297 [D] (n = 3)	No activity [D]
Human liver type A	600,466 [N] (n = 2)	2640 ± 231 (n = 3)
	480 ± 280 [D] (n = 3)	551 ± 119 (n = 7)
Controls		
Rat liver type P (no insulin)[d]	2456 ± 364 (n = 6)	No activity
Rat liver type P (insulin-treated animals)[d]	3609 ± 265 (n = 5)	No activity
Rat liver type A (no insulin)[d]	1280, 2900 (n = 2)	1546, 1870 (n = 2)
Rat liver type A (insulin-treated animals)[d]	1693 ± 620 (n = 3)	2222 ± 447 (n = 3)

[a] Unit of activity: A unit of activity is defined as the amount causing a 50% activation in the basal level of the test system.

[b] In the lipogenesis assay, 1 nM insulin has an activity of 5160 ± 310 (n = 20) milliunits equivalent.

[c] The values for human liver are from two separate livers, normal [N] and diseased [D] (see Materials and Methods). Values are expressed as ± SEM for repeat extractions $n > 2$ of the same liver.

[d] For the rat liver data, the n value represents different independent extractions of separate liver preparations. Each lipogenesis assay was performed in triplicate. Two separate values are given, for sham-injected rats or for livers extracted 2 min after an injection of 50 munits of insulin. Both groups were starved overnight.

determine whether human IPG subtypes affected cell proliferation in the CVG obtained from 72-h chicken embryos. Explant cultures of CVG were maintained for 24 h under five different conditions: serum-free medium, medium containing 10% FCS, medium containing IPG prepared from rat liver by treatment with PI-PLC, and medium containing either human liver IPG type A or IPG type P (1/100 final dilution). Figure 6 shows a representative experiment of four independent experiments performed in triplicate. Measurements of [^{3}H]thymidine incorporation revealed that explant cultures of CVG incorporated greater amounts of [^{3}H]thymidine in the presence of either rat liver IPG or human liver IPG type A (Figs. 6b and 6c, respectively). In the case of human IPG type A, there was a 2.3 ± 0.1-fold increase over the control and a 2.9 ± 0.3-fold increase in the presence of rat liver IPG. Control samples incorporated an average of 1900 ± 110 cpm per explant. However, IPG type P had a negligible effect when assayed under the same conditions in parallel experiments (Fig. 6d).

[^{3}H]*Galactose–Glycolipid Purification and Characterization*

Putative GPI was purified from human liver microsomes and radiolabeled by treatment with galactose oxidase and NaB^3H_4. The rationale of this method is that galactose oxidase is able to oxidize galactose molecules which will be later reduced with [^{3}H]sodium borohydride, with tritium being incorporated into the exocyclic C-6 position of galactose/galactosamine. After labeling, the radioactive glycolipid was purified by sequential t.l.c. and the major radioactive peak (R_f 0.57) was eluted with methanol

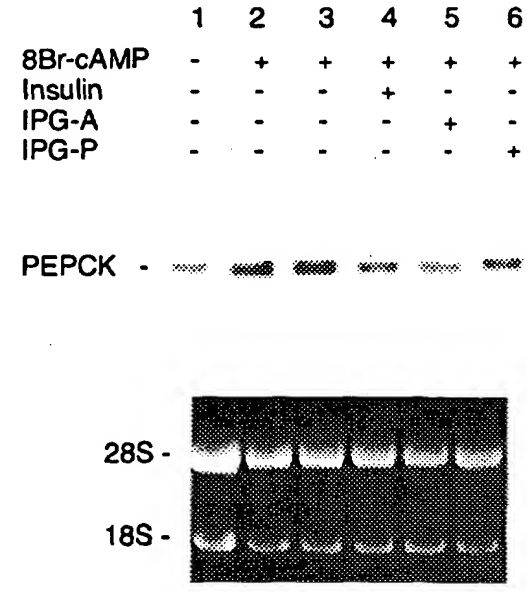

FIG. 5. Modulation of PEPCK mRNA levels by IPGs in H4IIE hepatoma cells. After 24 h of serum starvation, cultures of H4IIE cells were incubated in the absence (lane 1) or the presence of 8-Br-cAMP for 3 h (lane 2) or 5 h (lanes 3 to 6). Insulin (lane 4), IPG type A (lane 5), or IPG type P (lane 6) was added to the medium for the last 2 h of 8-Br-cAMP treatment. PEPCK mRNA levels were analyzed by Northern blotting. An autoradiogram of a typical experiment is shown alongside the ethidium bromide-stained agarose gel.

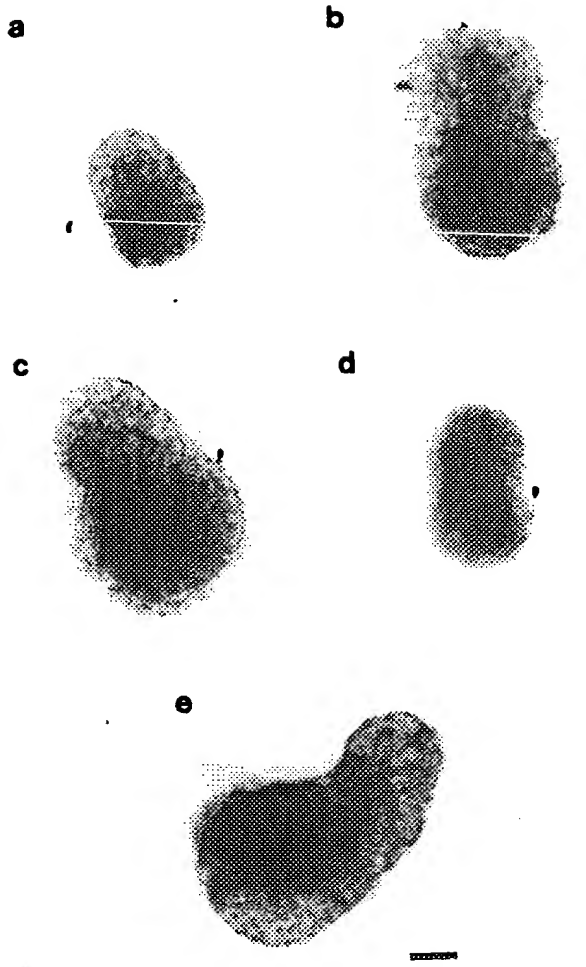

FIG. 6. Effect of human IPGs on the growth of CVG. Appearance of CVG obtained from 72-h (stage 19–20) chicken embryos following a 24-h culture in M-199 Medium alone (a) or M-199 containing rat liver IPG (b), human liver IPG type A (c), human liver IPG type P (d), or 10% FCS (e). Calibration bar, 100 μm.

and analyzed by t.l.c. Only one radioactive peak was detected at the origin of the acidic solvent t.l.c. plate (Fig. 7a). However, when the plate was developed in a basic solvent system (Fig. 7b) a wide band was observed. The ^{3}H-labeled glycolipid was then resolved on a HP-t.l.c. plate in a basic solvent system under conditions which yielded three main spots with R_f values of 0.72, 0.75, and 0.78 (Fig. 7c).

In order to study whether any components of the major radioactive peak (prior to separation by HP-t.l.c) had properties consistent with a GPI structure it was subjected to different PLC treatments. The ^{3}H-labeled glycolipid was resistant to hydrolysis by GPI-PLC from *T. brucei* (42) but was partially sensitive to hydrolysis by PI-PLC from *B. thuringiensis* (17.5% cleavage, $n = 3$).

DISCUSSION

This work shows that human liver contains IPG-like molecules. These IPGs exhibit similar chemical and biological characteristics to those purified from insulin-stimulated rat tissues (14). Both IPGs possess distinct insulin-like activities. Putative human IPG type P strongly stimulated PDH phosphatase, weakly inhibited cAMP-dependent protein kinase, but was inactive in stimulating lipogenesis. Putative human IPG type A inhibited cAMP-dependent protein kinase to a greater extent, decreased the expression of 8-Br-cAMP preinduced PEPCK in rat hepatoma cells, and stimulated lipogenesis in rat adipocytes. In addition, IPG type A mimicked IGF-I action in the developing chicken inner ear by inducing cellular proliferation in organotypic cultures of CVG. Both IPGs stimulated the proliferation of

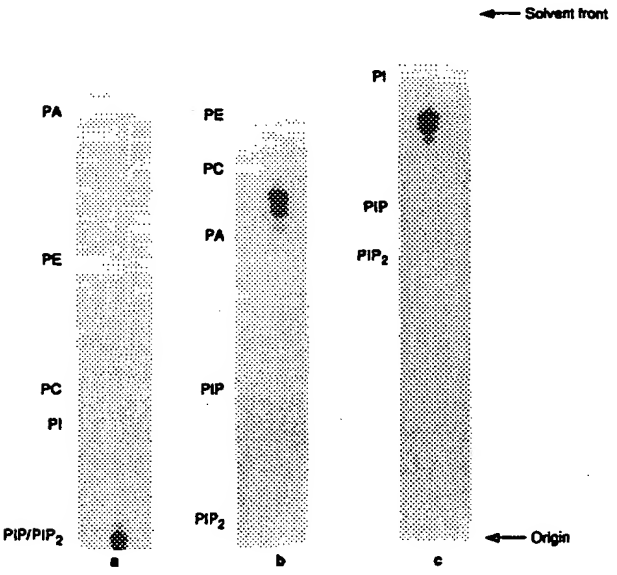

FIG. 7. Thin-layer chromatographic properties of [^{3}H]GPI. [^{3}H]GPI was applied to t.l.c. and HP-t.l.c. plates which were developed in various solvent systems (see Materials and Methods). Radioactivity on the plates was detected by autoradiography after spraying with En^{3}Hance. The panels show (a) migration of [^{3}H]-GPI in the acidic solvent system, (b) migration of [^{3}H]GPI in the basic solvent system, and (c) migration of [^{3}H]GPI in the basic solvent system specific for HP-t.l.c. Abbreviations used for authentic phospholipid standards: PIP_2, phosphatidylinositol-4,5-bisphosphate; PIP, phosphatidylinositol-4-phosphate; PI, phosphatidylinositol; PC, phosphatidylcholine; PE, phosphatidylethanolamine; PA, phosphatidic acid.

EGFR T17 cells. The nomenclature IPG type A denotes that this type is the predominant inhibitor of the cAMP-dependent protein kinase, while IPG type P denotes its unique ability to stimulate the PDH phosphatase (13,15). Our data are consistent with the presence of type A and type P insulin-mimetic IPGs in human liver. Further, the ability of the human-derived mediators to interact with bovine metabolic enzymes and rat adipocytes suggests similarity in structure between the mediators purified from different species.

The biological activities of the IPGs isolated from human liver were maintained after treatment with Pronase E. This indicates that their activity was not due to the presence of either protein or peptides in the preparation. The presence of phosphate, free amino groups, and carbohydrate in both IPG types agrees with the chemical composition reported for IPGs isolated from other sources (11, 12). The carbohydrate nature of the putative IPGs is supported by their behavior in the descending paper chromatography system used, which is characteristic of carbohydrate-containing compounds and resembles that obtained for the IPGs isolated from insulin-stimulated rat tissues (14). Further, anion exchange chromatography utilising pulsed amperometric detection indicated the presence of multiple carbohydrate species in the paper chromatography-purified type A and type P mediator fractions (data not shown). The presence of dual-charged moieties within the human IPGs was confirmed by their migration pattern in HVE and their interaction with ion exchange resins. The high correlation observed between phosphate content and the ability to stimulate cell proliferation (and PDH phosphatase stimulating activity for the type P mediator) strongly suggests that phosphate is a key component of both mediators. This result is in agreement with that reported for IPG purified from rat liver GPI by PI-PLC treatment (43).

In addition to the direct extraction methods (e.g., ref 29) or the release of IPG into medium following growth factor stimulation of intact cells (e.g., ref 44), IPG molecules with biological activity have also been obtained by treatment of membrane or purified glycolipid with preparations of *B. thuringiensis*- or *Staphylococcus aureus*-derived PI-PLC (e.g., ref 25). The extraction, purification, and labeling of glycolipid from human liver membranes was performed as described for rat and bovine liver (30). The chromatographic profile obtained was identical to that reported for the insulin-modulated GPI. Three main lipidic bands were observed similar to those found for human and murine T-lymphocytes (33,34) and murin EGFR T17 fibroblasts (26). The recovered glycolipid was completely resistant to GPI-PLC from *T. brucei,* suggestive of the absence of mannose residues linked to the hexosamine moiety which is the minimal structural motif needed in the GPI anchors to be substrates for the GPI-PLC (42). The glycolipid was partially cleaved by *B. thuringiensis*-derived PI-PLC, which would give an IPG containing a cyclic phosphate on the inositol residue.

To date no GPI-PLC activity has been recovered from mammalian tissues. Analysis of released GPI-anchored proteins from mammalian tissues has shown the absence of a cyclic phosphate moiety on the inositol, consistent with the action of a lipase with GPI-PLD activity (45). Recently an IPG inhibitor has been isolated from human serum which has been proposed to contain inositol with a cyclic phosphate residue since treatment with 10 mM HCl destroyed the bioactivity (46). However, this group is stable at this pH and other acid-labile constituents must account for the loss in biological activity (unpublished observations). It is not clear if preparations of the bacterial-derived PI-PLC are active due to the presence of contaminating GPI-PLD activities. The activity profile of the material released by the bacterial enzymes suggests that IPG with type A characteristics may predominate (43). It was not possible to directly address this issue in the present study due to the small amount of activity which could be recovered following PI-PLC treatment. This may have been due to the inefficiency of the *B. thuringiensis* PI-PLC per se or to a small amount of IPG lipidic precursor in the glycolipid preparations or the presence of the cyclic phosphate residue on released IPG. In addition, the precursor for IPG type-P has not yet been isolated, but since it may contain *chiro*-inositol it would not be a substrate for the PI-PLC. It has previously been proposed that the IPG contains non-N-acetylated hexosamine residues analogous to the GPI which forms the anchor of many membrane proteins (6,13). We were able to demonstrate that free amino groups correlated with the presence of bioactive material (Fig. 1). Results of nitrous acid deamination experiments (data not shown) were ambiguous due to inefficient and bias recoveries and to the observation that a fraction of the soluble type P mediator has hydrophobic characteristics, e.g., binds to the C-18 support (Table 1).

The importance of IPG in insulin signaling comes from both *in vitro* and *in vivo* data. Both insulin action and breakdown of GPI correlate with insulin

receptor levels (47). An antibody raised to an enzymatically (α-galactosidase) and chemically modified (mild acid). PI-PLC-solubilized form of the GPI-anchored VSG from *T. brucei* blocks some, but not all, of the effects of insulin (23, 28, 29) or other growth factors such as NGF (48). Mutant cells unable to make GPI respond to insulin by tyrosine phosphorylation, but without metabolic effects (9), and cells bearing kinase-deficient insulin receptors do not hydrolyse GPI following insulin stimulation (49).

Several diabetic animal models have biochemical alterations which are consistent with a role for IPG/GPI in insulin action and defects in this signaling system may contribute to the diabetic pathogenesis. For example, insulin-induced hydrolysis of GPI does not occur in adipocytes and is reduced in hepatocytes from spontaneously diabetic Goto-Kakizaki (GK) rats (50). Adipocyte glycerol-3-phosphate acyltransferase (G3PAT) is also not activated by insulin in intact and cell-free preparations (50). However, the type P mediator isolated from bovine liver is able to bypass the G3PAT defect and comparably activate G3PAT in cell-free adipocyte preparations from both the diabetic GK and the nondiabetic control rats (50). Insulin-stimulated hydrolysis of GPI in adipocytes from streptozotocin-diabetic rats has also been shown to be impaired (51,52).

In diabetic New Zealand obese (NZO) mice, adipocyte PDH is unresponsive to insulin stimulation. IPG isolated from insulin-stimulated NZO adipocytes is able to activate PDH in adipocytes from nondiabetic lean New Zealand chocolate (NZC) mice, but paradoxically causes a decrease in mediator production or activity in adipocytes of NZO mice (44). These results suggest that in NZO mice there is a postreceptor defect of insulin action at the level of pyruvate dehydrogenase activation (i.e., type P mediator). Changes in the IPG/GPI signaling system have also been reported in isolated hepatocytes in genetically obese (fa/fa) rats (53).

There is decreased urinary *chiro*-inositol (the proposed hydrolysis product of type P mediator) excretion in spontaneously diabetic (fat) rhesus monkeys (54), and *chiro*-inositol lowers plasma glucose in such monkeys and in streptozotocin-treated rats and activates glycogen synthase (55). These studies are all complicated by the recent report that the type P mediator contains pinitol rather than *chiro*-inositol (56). Intravenous infusion of the mediators in streptozotocin-treated rats decreases plasma glucose without a change in the serum insulin concentrations and i.p. injection results in glycogenic changes in the diaphragm, with the type P mediator being 50–100 times more active than the type A (54). A recent study has shown that infusion of the type P mediator normalizes plasma glucose in streptozotocin diabetic rats at a dose equivalent to insulin without inducing hypoglycemia (56).

In humans, postreceptor tissue insulin resistance of glucose metabolism is a feature of non-insulin-dependent diabetes mellitus (NIDDM) and many other disorders (46). The decreased urinary *chiro*-inositol secretion found in patients with type II diabetes (57,58) suggests a postreceptor defect in human patients similar to that of some of the above animal models, although not all studies have been able to confirm these observations (59). Insulin resistance could either result from an intrinsic defect in insulin signaling pathways or be caused by the presence of a circulating inhibitor of insulin action, or both. Defects in IPG-associated mediator pathways therefore are key targets for investigations on the pathogenesis of NIDDM, especially since a defect in glucose homeostasis is not evident in *GLUT4* knockout mice (60) and *IRS-1* knockout mice can still respond to insulin (3). The latter, however, may b the result of the presence of a second recently cloned IRS-signaling protein designated IRS-2 (4).

In summary, we report here for the first time the presence of two different IPG molecules, type A and type P, in human liver. These IPGs exhibit distinct insulin-like biological effects. In addition, human liver contains putative lipidic IPG precursors. Therefore, all the elements of the IPG signaling system exist in human liver, a target organ of insulin action. Further structural and functional studies are needed to assess the importance of liver-derived IPGs in insulin signaling in normal and pathological states, such as type II insulin-dependent diabetes.

ACKNOWLEDGMENTS

We thank Drs. P. McLean and A. L. Greenbaum of the Molecular Medicine Unit for their invaluable assistance with the lipogenic and PDH phosphatase assays and Dr. J. M. Mato for helpful criticisms and support. We thank Dr. S. Udenfriend for providing us with the PI-PLC, Dr. L. Beguinot for the EGFR T17 cells, and Drs. R. W. Hanson and J. P. García-Ruiz for the PEPCK probe.

REFERENCES

1. Rosen OM. After insulin binds. *Science* **237**:1452–1458, 1987.
2. White MF, Kahn CR. The insulin signaling system. *J Biol Chem* **269**:1–4, 1994.

3. Lienhard GE. Life without the IRS. *Nature* **372**:128–129, 1994.
4. Sun XJ, Wang LM, Zhang Y, Yenush L, Myers MG Jr, Glasheen E, Lane WS, Pierce JH, White MF. Role of IRS-2 in insulin and cytokine signalling. *Nature* **377**:173–177, 1995.
5. Denton RM, Tavaré JM. Does mitogen-activated-protein kinase have a role in insulin action? The cases for and against. *Eur J Biochem* **227**:597–611, 1995.
6. Thomas JR, Dwek RA, Rademacher TW. Structure, biosynthesis and function of glycosylphosphatidylinositols. *Biochemistry* **29**:5413–5422, 1990.
7. Gaulton GN, Pratt JC. Glycosylated phosphatidylinositol molecules as second messengers. *Semin Immunol* **6**:97–104, 1994.
8. Varela-Nieto I, León Y, Caro HN. Cell signalling by inositol phosphoglycans from different species. *Comp Biochem Physiol* **115B**(2):223–241, 1996.
9. Lazar DF, Knez JJ, Medof ME, Cuatrecasas P, Saltiel AR. Stimulation of glycogen synthesis by insulin in human erythroleukemia cells requires the synthesis of glycosylphosphatidylinositol. *Proc Natl Acad Sci USA* **91**:9665–9669, 1994.
10. Saltiel AR, Cuatrecasas P. Insulin stimulates the generation from hepatic membranes of modulators derived from an inositol glycolipid. *Proc Natl Acad Sci USA* **83**:5793–5797, 1986.
11. Mato JM, Kelly KL, Abler A, Jarett L. Identification of a novel insulin-sensitive glycophospholipid from H35 hepatoma cells. *J Biol Chem* **262**:2131–2137, 1987.
12. Larner J, Huang LC, Schwartz CF, Oswald AS, Shen TY, Kinter M, Tang GZ, Zeller K. Rat liver insulin mediator which stimulates pyruvate dehydrogenase phosphate contains galactosamine and *D-chiro* inositol. *Biochem Biophys Res Commun* **151**:1416–1426, 1988.
13. Rademacher TW, Caro HN, Kunjara S, Wang DY, Greenbaum AL, McLean P. Inositolphosphoglycan second messengers. *Braz J Med Biol Res* **27**:327–341, 1994.
14. Kunjara S, Caro HN, McLean P, Rademacher TW. Tissue specific release of inositolphosphoglycans. In Biopolymers and Bioproducts: Structure, Function and Applications (J. Svasti *et al.*, Eds.), Bangkok: Dokya, 1995, pp 301–306.
15. Romero G, Larner J. Insulin mediators and the mechanism of insulin action. *Advances in Pharmacol* **24**:21–50, 1993.
16. Saltiel AR, Doble A, Jacobs S, Cuatrecasas P. Putative mediators of insulin action regulate hepatic acetyl CoA carboxylase activity. *Biochem Biophys Res Commun* **110**:789–795, 1983.
17. Villalba M, Kelly KL, Mato JM. Inhibition of cyclic AMP-dependent proten kinase by the polar head group of an insulin-sensitive glycophospholipid. *Biochim Biophys Acta* **968**:69–76, 1988.
18. Malehoff CD, Huang L, Gillespie N, Villar-Palasi C, Schwartz CFW, Cheng K, Hewlett FL, Larner J. A putative mediator of insulin action which inhibits adenylate cyclase and adenosine-3,5-monophosphate dependent protein kinase: partial purification from rat liver site and kinetic mechanism of action. *Endocrinology* **120**:1327–1337, 1984.
19. Saltiel AR. Insulin generates an enzyme modulator from hepatic plasma membrane: regulation of cAMP phosphodiesterase, pyruvate dehydrogenase and adenylate cyclase. *Endocrinology* **120**:967–972, 1987.
20. Saltiel AR, Fox JA, Sherline P, Cuatrecasas P. Insulin-stimulated hydrolysis of a novel glycolipid generates modulators of cAMP phosphodiesterase. *Science* **233**:967–972, 1986.
21. Lilley K, Zhang C, Villar-Palasi C, Larner J, Huang L. Insulin mediator stimulation of pyruvate dehydrogenase phosphatases. *Arch Biochem Biophys* **296**:170–174, 1992.
22. Larner J, Roach PJ, Huang LC, Brooker G, Murad F, Hazen R. Hormonal control of glycogen metabolism. *Adv Exp Med Biol* **111**:103–112, 1979.
23. Huang LC, Fonteles MC, Houston DB, Zhang C, Larner J. Chiroinositol deficiency and insulin resistance. III. Acute glycogenic and hypoglycemic effects of two inositol phosphoglycan insulin mediators in normal and streptozotocin-diabetic rats in vivo. *Endocrinology* **132**:652–657, 1993.
24. Sato T, Villar Palasi C, Huang L, Tang G, Larner AC, Larner J. Insulin and a putative insulin metabolic mediator fraction from liver and muscle stimulate p33 mRNA accumulation by apparently different mechanisms. *Endocrinology* **123**:1559–1564, 1988.
25. Alvarez L, Avila MA, Mato JM, Castaño JG, Varela-Nieto I. Insulin-like effects of inositol phosphate-glycan on messenger RNA expression in rat hepatocytes. *Mol Endocrinol* **5**:1062–1068, 1991.
26. Clemente R, Jones D, Ochoa P, Romero G, Mato JM, Varela-Nieto I. Role of glycosyl-phosphatidylinositol hydrolysis as a mitogenic signal for epidermal growth factor. *Cell Signalling* **7**:411–421, 1995.
27. Varela-Nieto I, Represa J, Avila MA, Miner C, Mato JM, Giraldez F. Inositol phospho-oligosaccharide stimulates cell proliferation in the early developing inner ear. *Dev Biol* **143**:432–435, 1991.
28. Romero G, Gamez G, Huang LC, Lilley K, Luttrell L. Anti-inositolglycan antibodies selectively block some of the actions of insulin in intact BC3H1 cells. *Proc Natl Acad Sci USA* **87**:1476–1480, 1990.
29. Nestler JE, Romero G, Huang LC, Zhang CG, Larner J. Insulin mediators are the signal transduction system responsible for insulin's actions on human placental steroidogenesis. *Endocrinology* **129**:2951–2956, 1991.
30. Varela-Nieto I, Alvarez L, Mato JM. In Handbook of Endocrine Research Techniques: Intracellular Mediators of Peptide Hormone Action: Glycosylphosphatidylinositol/Inositol Phosphoglycan System (de Pablo F, Scanes C, Weintraub BD, Eds.). San Diego: Academic Press, 1993, pp 391–406.
31. Bartlett GR. Phosphorous assay in column chromatography. *J Biol Chem* **234**:466–468, 1958.
32. Alvarez JF, Sánchez-Arias JA, Guadaño A, Estévez F, Varela I, Felíu JE, Mato JM. Transport in isolated rat hepatocytes of the phospho-oligosaccharide that mimics insulin action. *Biochem J* **274**:369–374, 1991.
33. Avila MA, Clemente R, Varela-Nieto I. A phosphatidylinositol-linkage-deficient T-cell mutant contains insulin-sensitive glycosyl-phosphatidylinositol. *Biochem J* **282**:681–686, 1992.
34. Gaulton GN. Differential regulation of glycosylated phos-

phatidylinositol subtypes by insulin. *Diabetes* **40**:1297–1304, 1991.

35. Guther ML, de Almeida ML, Yoshida N, Ferguson MA. Structural studies on the glycosylphosphatidylinositol membrane anchor of *Trypanosoma cruzi* 1G7-antigen. *J Biol Chem* **239**:375–380, 1992.
36. Rodbell M. Metabolism of isolated fat cells. *J Biol Chem* **239**:375–380, 1964.
37. Chomczynski P, Sacchi N. Single-step method of RNA isolation by acid guanadinium thiocyanate-phenol-chloroform extraction. *Anal Biochem* **162**:156–159, 1987.
38. Wahl GM, Stern M, Stark G. Efficient transfer of large DNA fragments from agarose gels to diazobenzyloxy-methyl-paper and rapid hybridization by using dextran sulfate. *Proc Natl Acad Sci USA* **76**:3683–3687, 1979.
39. Warren YH, Monahan JE, Short J, Short M, Bruzel A, Wynshaw-Boris A, Meisner HM, Samolds D, Hanson RW. Isolation and characterization of the gene encoding for cytosolic phosphoenolpyruvate carboxylase (GTP) from the rat. *Proc Natl Acad Sci USA* **80**:3656–3660, 1983.
40. Velu TJ, Beguinot L, Vass WC, Willingham MC, Merlino GT, Pastan I, Lowry DR. Epidermal growth factor-dependent transformation by a human EGF receptor proto-oncogene. *Science* **238**:1408–1410, 1987.
41. León Y, Vazquez E, Sanz C, Vega JA, Mato JM, Giraldez F, Represa J, Varela-Nieto I. Insulin-like growth factor-I regulates cell proliferation in the developing inner ear, activating glycosyl-phosphatidylinositol hydrolysis and Fos expression. *Endocrinology* **136**:3494–3503, 1995.
42. Morris JC, Sheng PL, Shen T-Y, Mensa-Wilmot K. Glycan requirements of glycosylphosphatidylinositol phospholipase C from *Trypanosoma brucei*. *J Biol Chem* **270**:2517–2524, 1995.
43. Merida I, Corrales FJ, Clemente R, Ruiz-Albusac JM, Villalba M, Mato JM. Different phosphorylated forms of an insulin-sensitive glycosyl-phosphatidylinositol from rat hepatocytes. *FEBS Lett* **236**:251–255, 1988.
44. Macaulay SL, Larkins RG. Impaired insulin action in adipocytes of New Zealand obese mice: A role for postbinding defects in pyruvate dehydrogenase and insulin mediator activity. *Metabolism* **37**:958–965, 1988.
45. Mukasa R, Umeda M, Endo T, Kobata A, Inoue K. Characterization of glycosylphosphatidylinositol (GPI)-anchored NCAM on mouse skeletal muscle cell line C2C12: The structure of the GPI glycan and release during myogenesis. *Arch Biochem Biophys* **318**:182–190, 1995.
46. Galasko GT, Bao Y, Broomfield SJ, Hooper NM, Turner AJ, Larner J. Circulating factors and insulin resistance. I. A novel myoinositol 1,2-cyclic phosphate phosphoglycan insulin antagonist from human plasma is elevated in noninsulin-dependent diabetes mellitus. *J Clin Endocrinol Metab* **80**:2419–2429, 1995.
47. Macaulay SL, Clark S, Larkins RG. Correlation of insulin receptor level with both insulin action and breakdown of a potential insulin mediator precursor; studies in CHO cell-lines transfected with insulin receptor cDNA. *Biochim Biophys Acta* **1134**:53–60, 1992.
48. Represa J, Avila MA, Miner C, Giraldez F, Romero G, Clemente R, Mato J, Varela-Nieto I. Glycosyl-phosphatidylinositol/inositol phosphoglycan: A signaling system for the low-affinity nerve growth factor receptor. *Proc Natl Acad Sci USA* **88**:8016–8019, 1991.
49. Villalba M, Alvarez JF, Russell DS, Mato JM, Rosen OM. Hydrolysis of glycosyl-phosphatidylinositol in response to insulin is reduced in cells bearing kinase-deficient insulin receptors. *Growth Factors* **2**:91–97, 1990.
50. Farese RV, Standaert ML, Yamada K, Huang LC, Zhang C, Cooper DR, Wang Z, Yang Y, Suzuki S, Toyota T, Larner J. Insulin-induced activation of glycerol-3-phosphate acyltransferase by a chiro-inositol-containing insulin mediator is defective in adipocytes of insulin-resistant, type II diabetic, Goto-Kakizaki rats. *Proc Natl Acad Sci USA* **91**:11040–11044, 1994.
51. Macaulay SL, Larkins RG. Isolation of insulin-sensitive phosphatidylinositol-glycan from rat adipocytes. Its impaired breakdown in the streptozotocin-diabetic rat. *Biochem J* **271**:427–435, 1990.
52. Sánchez-Arias JA, Sánchez-Gutierrez JC, Guadaño A, Alvarez JF, Samper B, Mato JM, Feliú JE. Impairment of glycosyl-phosphatidylinositol-dependent insulin signaling system in isolated rat hepatocytes by streptozotocin-induced diabetes. *Endocrinology* **131**:1727–1733, 1992.
53. Sánchez-Gutierrez JC, Sánchez-Arias JA, Valle JC, Guadaño A, Samper B, Mato JM, Feliú JE. Insulin resistance in genetically obese (*fa/fa*) rats: Changes in the glycosyl-phosphatidylinositol signaling system in isolated hepatocytes. *Endocrinology* **134**:1485–1492, 1994.
54. Ortmeyer HK, Bodkin NL, Lilley K, Larner J, Hansen BC. Chiroinositol deficiency and insulin resistance. I. Urinary excretion rate of chiroinositol is directly associated with insulin resistance in spontaneously diabetic rhesus monkeys. *Endocrinology* **132**:640–645, 1993.
55. Ortmeyer HK, Huang LC, Zhang L, Hansen BC, Larner J. Chiroinositol deficiency and insulin resistance. II. Acute effects of D-chiroinositol administration in streptozotocin-diabetic rats, normal rats given a glucose load, and spontaneously insulin-resistant rhesus monkeys. *Endocrinology* **132**:646–651, 1993.
56. Fonteles MC, Huang LC, Larner J. Infusion of pH 2.0 D-*chiro*-inositol glycan insulin putative mediator normalizes plasma glucose in streptozotocin diabetic rats at a dose equivalent to insulin without inducing hypoglycaemia. *Diabetologia* **39**:731–734, 1996.
57. Kennington AS, Hill CR, Craig J, Bogardus C, Raz I, Ortmeyer HK, Hansen BC, Romero G, Larner J. Low urinary chiro-inositol excretion in non-insulin-dependent diabetes mellitus. *N Engl J Med* **323**:373–378, 1990.
58. Suzuki S, Kawasaki H, Satoh Y, Ohtomo M, Hirai M, Hirai A, Hirai S, Onoda M, Matsumoto M, Hinokio Y. Urinary chiro-inositol excretion is an index marker of insulin sensitivity in Japanese type II diabetes. *Diabetes Care* **17**:1465–1468, 1994.
59. Ostlund RE Jr, McGill JB, Herskowitz I, Kipnis DM, Santiago JV, Sherman WR. D-chiro-inositol metabolism in diabetes mellitus. *Proc Natl Acad Sci USA* **90**:9988–9992, 1993.
60. Katz EB, Stenbit AE, Hatton K, DePinho R, Charron MJ. Cardiac and adipose tissue abnormalities but not diabetes in mice deficient in GLUT4. *Nature* **377**:151–155, 1995.

STIC-ILL

NPL

428383

From: Holleran, Anne
Sent: Monday, January 20, 2003 11:57 AM
To: STIC-ILL
Subject: refs. for 09/868,968

Please send copies of the following papers:

1.	Hoyoku,	Anticancer Res. (1999) 19(5A): 3663-3664
2.	Chamson-Reig	Endocrinology (1999) 140(8): 3573-3580
3.	Lixin,	J. Medicinal Chemistry ~~91998)~~ 1998 41(18): 3303-3306
4.	Yorek,	American J. Physiology (1998) 274(1, part1): C58-C71
5.	Nazih-Sanderson	Biochimica et Biophysica Acta (1997) 1346(1): 45-60
6.	Wattenberg	Cancer Research (1996) 56(22): 5132-5135
7.	Caro	Infection and Immunity (1996) 64(8): 3438-3441
8.	Seymour	Laboratory Investigation (1996) 75(3): 427-437
9.	Brunn	Cancer Chemotherapy (1994) 35(1): 71-79
10.	Kopp	Cancer Research (1990) 50(20): 6490-6496
11.	Tanino	Japanese J. Experimental Medicine (1972) 42(6): 575-582
12.	Eagle	Biochmistry (1963) 2(5): 1125-1126
13.	Caro	Biochem. Mol. Med. (1997) 61: 214-228

agk - RS 403. A1J2

Anne Holleran
AU: 1642
Tel: 308-8892
RM: 8e03

mailbox: 8e12

Journal of Medicinal Chemistry

Volume 41, Number 18 August 27, 1998

Communications to the Editor

3-Deoxy-D-*myo*-inositol 1-Phosphate, 1-Phosphonate, and Ether Lipid Analogues as Inhibitors of Phosphatidylinositol-3-kinase Signaling and Cancer Cell Growth

Lixin Qiao,[†] Fajun Nan,[†] Mark Kunkel,[‡] Alfred Gallegos,[‡] Garth Powis,*[,‡] and Alan P. Kozikowski*[,†]

Drug Discovery Program, Georgetown University Medical Center, 3970 Reservoir Road NW, Washington, D.C., 20007, and Arizona Cancer Center, 1515 North Campbell Avenue, Tucson, Arizona 85724

Received April 27, 1998

Growth factors and certain oncogenes activate a range of phospholipid-mediated signal transduction pathways resulting in cell proliferation. Phosphatidyl *myo*-inositol (PI) occupies a unique position in that it can undergo reversible phosphorylation at multiple sites to generate five different phosphoinositides,[1] while its metabolites regulate two pathways important for cell proliferation: the inositol phosphate/diacylglycerol signaling pathway[2,3] and the phosphatidylinositol 3-phosphate (PI-3-kinase) pathway.[4,5] In the first pathway, PI-specific phospholipase C (PI-PLC) hydrolyses a minor membrane phospholipid, $PI(4,5)P_2$, to give the water-soluble $Ins(1,4,5)P_3$ and a lipophilic diacylglycerol (DAG). $Ins(1,4,5)P_3$ interacts specifically with membrane receptors to release Ca^{2+},[6] a key event in cellular signal transduction, while DAG is an endogenous activator of protein kinase C (PKC).[7] $Ins(1,4,5)P_3$ is metabolized by either hydrolysis of the phosphate at position 5 giving $Ins(1,4)P_2$ or phosphorylation at position 3 giving $Ins(1,3,4,5)P_4$. $Ins(1,4)P_2$ is not active as a Ca^{2+}-mobilizing agent and is subsequently degraded by other phosphatases. However, it has been suggested that $Ins(1,3,4,5)P_4$ may play a role in refilling the intracellular Ca^{2+} stores with extracellular Ca^{2+}.[8] Together, the increase in $[Ca^{2+}]$ and the increased activity of PKC lead to a sequence of events that culminate in DNA synthesis and cell proliferation.

In the second pathway, PI-3-kinase has been found associated with almost every growth factor receptor or oncogene transformation.[9] PI-3-kinase phosphorylates PI at position 3 of the *myo*-inositol ring to give a class of PIs that are poor substrates for hydrolysis by PI-PLC, e.g., $PI(3,4)P_2$ and $PI(3,4,5)P_3$. The exact mechanism by which 3-phosphorylated PIs modulate cell growth is not known, but they appear to be important modulators of protein interaction and enzyme activity through binding to specific sites on proteins. For example, binding of $PI(3,4)P_2$, $PI(4,5)P_2$, or $PI(3,4,5)P_3$ to pleckstrin-homology (PH) domains on enzymes such as AKT (protein kinase B) leads to enzyme activation, whereas the Src-homology-2 (SH2) domain that mediates protein tyrosine phosphate binding binds specifically $PI(3,4,5)P_3$.[10] Some studies have also provided evidence that PKC is activated by $PI(3,4)P_2$ and $PI(3,4,5)P_3$,[11-13] while adapter protein-2 (AP-2) is the only protein with high affinity and isomer-specific binding to PI(3)P.[14] Thus, inhibition of the production of such lipids produced by PI-3-kinase can result in inhibition of many acute cellular responses. The fungal metabolite wortmannin, an inhibitor of PI-3-kinase,[15] has shown antitumor activity in animal models but is relatively toxic and nonspecific and inhibits a variety of other related kinases.

Our studies have been directed toward the synthesis of 3-substituted *myo*-inositol derivatives to selectively block the effects of *myo*-inositol-derived second messengers on cell proliferation and transformation while leaving other aspects of *myo*-inositol signaling unaffected. This strategy may offer a basis for the selective control of cancer cell growth without disrupting the function of normal cells. Our approach has been to synthesize PI analogues modified on the inositol ring and then to improve the antiproliferative activity of the most promising analogues by making additional changes in the diacylglycerol moiety. We have found that 1D-3-deoxyphosphatidyl-*myo*-inositol (**1**)[16] (Chart 1) and its 3-fluoro derivative **2**[17] at relatively high concentrations

[†] Georgetown University Medical Center.
[‡] Arizona Cancer Center.

S0022-2623(98)00254-4 CCC: $15.00
Published on Web 08/08/1998

Chart 1

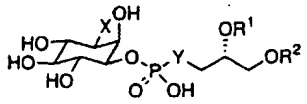

1 X = H; Y = O; $R^1 = R^2$ = palmitoyl
2 X = F; Y = O; $R^1 = R^2$ = palmitoyl
3 X = H; Y = CH_2; $R^1 = R^2$ = palmitoyl
4 X = H; Y = O; R^1 = Me; $R^2 = C_{18}H_{37}$-*n*
5 X = H; Y = CH_2; R^1 = Me; $R^2 = C_{18}H_{37}$-*n*
6 X = OH; Y = O; R^1 = Me; $R^2 = C_{18}H_{37}$-*n*

Scheme 1

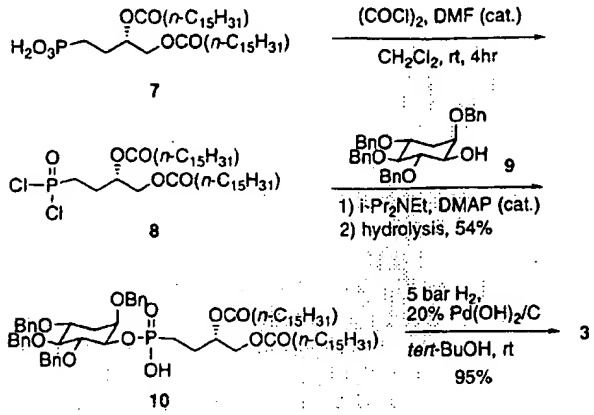

inhibit colony formation by HT-29 human colon carcinoma cells, with IC_{50} values of 35 and 37 μM, respectively. We hypothesize that the relatively low potency of these compounds may be due to their hydrolysis by phospholipases including PI-PLC, and the DAG produced by hydrolysis can activate PKC and may lead to tumor cell proliferation.

To decrease the susceptibility of the 3-deoxy-PI analogues to phospholipase hydrolysis, we adopted two separate synthetic strategies. First, we synthesized a phosphonate derivative (**3**), in which the *sn*-3 oxygen of the DAG is replaced by methylene group, rendering this compound resistant to hydrolysis by PI-PLC and maintaining relatively high concentration as an antimetabolite in the PI-3-kinase signaling pathway (Scheme 1). Second, we synthesized ether lipid analogues of 3-deoxy-PI. The ether lipid analogue **4** is of synthetic interest not only because of its greater stability to phospholipases but also due to the known antitumor activity of some members of its family.[18] Ether lipids such as 1-*O*-octadecyl-2-*O*-methylglycerophosphocholine (edelfosine) are inhibitors of PI-PLC with IC_{50}'s in the low micromolar range.[19] Thus we expected that the 3-deoxy-PI ether lipid would not be a substrate for PI-PLC. A further advantage of the ether lipids is that they have shown intrinsic antitumor activity against a variety of tumor types. Some ether lipid analogues that have undergone clinical trial as antitumor agents are inhibitors of PI-3-kinase.[20] They affect several aspects of lipid intracellular signaling, and their antitumor activity may arise from a combination of effects on the signaling pathway. 1-*O*-Octadecyl-2-*O*-methylphosphatidylinositol (**6**), however, has not shown good antitumor activity.[21]

For the synthesis of the phosphonate analogue **3** (Scheme 1), the dichloride **8** was prepared from (*S*)-3,4-bis(palmitoyloxy)butylphosphonic acid (**7**)[22] with oxalyl chloride in the presence of a catalytic amount of DMF at room temperature. The inositol component, 1D-2,4,5,6-tetra-*O*-benzyl-3-deoxy-*myo*-inositol (**9**), was obtained as reported before.[23] Phosphorylation of **9** with **8** in the presence of a base afforded monoester chloride intermediate which was transformed into **10** by hydrolysis, a reaction which proceeded in a surprisingly sluggish manner. After purification by preparative TLC, catalytic hydrogenation of **10** using $Pd(OH)_2/C$ in *tert*-butyl alcohol[24] provided the target phosphonate **3** in good yield.

Scheme 2

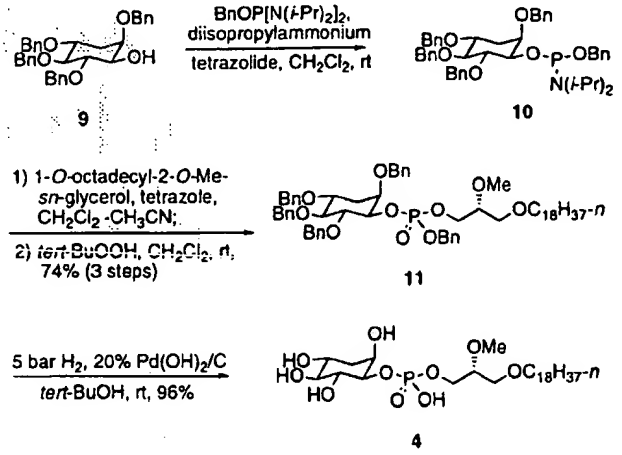

Scheme 3

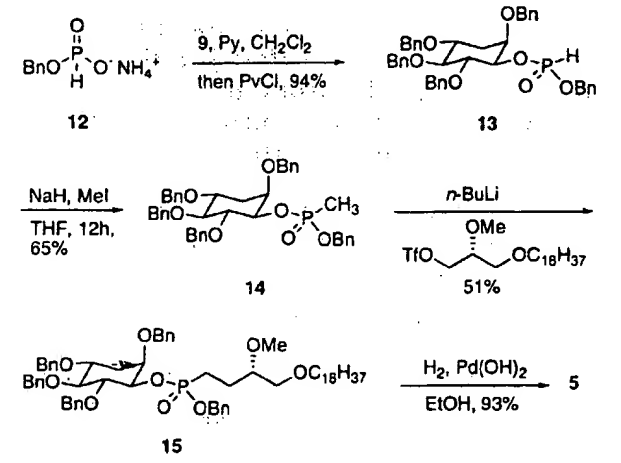

We also tested the hypothesis that an ether lipid analogue would be a more potent inhibitor of cell growth. Compound **4** was synthesized with 1-*O*-octadecyl-2-*O*-methyl-*sn*-glycerol instead of dipalmitoylglycerol through similar steps as in the synthesis of **1**[23] (Scheme 2). Phosphonate **5** was also synthesized to prevent PI-PLC hydrolysis. Synthesis of compound **5** was effected through *H*-phosphonate methodology[25] using ammonium *O*-benzyl-*H*-phosphonate (**12**) (Scheme 3), which is readily available by hydrolysis of dibenzyl phosphite with ammonium hydroxide.[26] The phosphorylation of **9** was complete within 10 min after addition of pivaloyl chloride into a dichloromethane solution of **9**, **12**, and pyridine at room temperature. Subsequent alkylation of *H*-phosphonate **13** with MeI provided methyl phosphonate **14**,[27] the anion of which was then

Table 1. Effects of Compounds 1–5 on PI-PLC and PI-3-kinase Activity and Growth Inhibition of HT-29 in Vitro

	IC_{50} (μM)		
compd	PI-PLC	PI-3-K	growth inhibition HT-29
1	N/A[b]	>250[a]	35[a]
2	8	30	37
3	N/A[b]	N/A[b]	10
4	19.9	2.5	2.1
5	10	5.3	45

[a] Reported in ref 16. [b] N/A, not active, with <20% inhibition at 100 μM.

Table 2. Antitumor Activity of 1 and 4 against HT-29 Human Colon in Scid Mice

compd dose (mg/kg)	schedule[a]	tumor vol[b] on day 10 (cm^3)	T/C (%)	P[c]
control		0.27 ± 0.04		
1				
500	ip, qd 4–5	lethal		
250	ip, qd 4–7	0.30 ± 0.06	111.1	NS
4				
150	ip, qd 4–7	0.09 ± 0.07	33.3	<0.05
100	ip, qd 4–7	0.32 ± 0.09	118.0	NS
50	ip, qd 4–7	0.28 ± 0.05	103.7	NS

[a] e.g., 250 mg/kg ip, qd 4–7 means that the 250 mg/kg dose was given as an intraperitoneal injection each day from days 4 to 7 (4 daily injections) after the tumors were implanted. [b] Tumor volume values are the mean for 8 mice per group with SE. [c] The *P* column is the significance value for a Student's test comparing the tumor volumes in the treated group to the tumor volumes in the control group; 0.05 is usually the maximum value for significance. NS, not significant, meaning that these studies were not repeated.

coupled with the triflate of 1-*O*-octadecyl-2-*O*-methyl-*sn*-glycerol to provide the fully protected precursor **15**.[28] Final hydrogenation furnished the desired phosphonate **5**.

Biological Activity. In vitro inhibition of bovine PI-PLC[19] and of bovine brain p110/p85 PI-3-kinase[16] was measured as previously described.[16] Inhibition of colony formation in soft agarose of HT-29 colon carcinoma cells with continuous 7-day drug exposure was measured as described.[16]

The most important result is the finding that replacement of the diacylglycerol moiety with an ether lipid group results in an over 15-fold increase in growth inhibition activity (compare **1** and **4**). Although replacement of phosphate by phosphonate increases the growth inhibiting activity of 3-deoxy-PI by almost 3-fold (compare compounds **1** and **3**), it decreases the growth inhibiting activity of the 3-deoxy ether lipid analogue (compare **4** and **5**). These compounds are only weak inhibitors of PI-PLC compared to 1-*O*-octadecyl-2-*O*-methylglycerophosphocholine which has an IC_{50} under the same assay conditions of around 1 μM.[29] The 3-deoxy ether lipid PIs were relatively potent inhibitors of PI-3-kinase with IC_{50} values of 2–5 μM. *O*-Octadecyl-2-*O*-methylglycerophosphocholine has previously been found to be an inhibitor of PI-3-kinase with an IC_{50} of 35 μM, while *myo*-inositol-containing analogue **6** is a much weaker inhibitor with an IC_{50} of 90 μM.[30] Thus, the presence of a 3-deoxy-*myo*-inositol moiety appears to impart PI-3-kinase inhibiting activity to the compounds.

Preliminary studies of in vivo antitumor activity were conducted in *scid* (severe combined immunodeficient) mice implanted subcutaneously with 10^7 HT-29 human colon adenocarcinoma cells. Injection of compounds 1 and 4 was begun 4 days after tumor inoculation in groups of 8 mice as 4 daily intraperitoneal injections of the compounds suspended in 3% EtOH, 3% Tween 20, 0.9% NaCl. Tumor volume was measured with calipers on day 10. As shown in Table 2, compound 1 was lethal at a daily dose of 500 mg/kg and exhibited no antitumor activity at one-half this dose. Compound 4 was not toxic at the highest dose tested of 150 mg/kg/day and inhibited tumor growth by 67%. There was no antitumor activity at doses of 100 and 50 mg/kg/day.

In summary, we present the synthesis and the bioactivity of several rationally designed phosphatidylinositol analogues. Further studies of these compounds in animals using other tumor xenografts will be reported in due course.

Acknowledgment. This work was supported by the National Institute of Health Grants No. CA61015 and CA42286.

References

(1) Potter, B. V. L.; Lampe, D. Chemistry of Inositol Lipid Mediated Cellular Signaling. *Angew. Chem., Int. Ed. Engl.* **1995**, *34*, 1933–1972.
(2) Berridge, M. J.; Irvine, R. F. Inositol Phosphates and Cell Signaling. *Nature (London)* **1989**, *341*, 197–205.
(3) Berridge, M. J. Inositol Trisphosphate and Calcium Signaling. *Nature (London)* **1993**, *361*, 315–325.
(4) Carpenter, C. L.; Cantley, L. C. Phosphoinositide Kinases. *Curr. Opin. Cell Biol.* **1996**, *8*, 153–158.
(5) Shepherd, P. R.; Reaves, B. J.; Davidson, H. W. Phosphoinositide 3-Kinases and Membrane Traffic. *Trends Cell Biol.* **1996**, *6*, 92–97.
(6) Streb, H.; Irvine, R. F.; Berridge, M. J.; Schulz, I. release of Ca^{2+} from a Nonmitochondrial Intracellular Store in Pancreatic Acinar Cells by Inositol-1,4,5-trisphosphate. *Nature (London)* **1983**, *306*, 67–69.
(7) Wender, P. A.; Gribbs, C. M. In *Advances in Medicinal Chemistry*; Maryanoff, B. E., Maryanoff, C. A., Eds.; JAI Press: Greenwich, CT, 1992; Vol. 1, pp 1–53.
(8) Irvine, R. F. 'Quantal' Ca^{2+} Release and the Control of Ca^{2+} entry by Inositol Phosphates – A Possible Mechanism. *FEBS Lett.* **1990**, *263*, 5–9.
(9) Toker, A.; Cantley, L. C. Signaling through the lipid products of phosphoinositide-3-OH kinase. *Nature (London)* **1997**, *387*, 673–676.
(10) Rameh, L. E.; Chen, C.-S.; Cantley, L. C. Phosphatidylinositol-(3,4,5)P_3 interacts with SH2 domains and modulates PI-3-kinase association with tyrosine-phosphorylated proteins. *Cell* **1995**, *83*, 821–830.
(11) Palmer, R. H.; Dekker, L. V.; Woscholski, R.; Good, J. A. L.; Gigg, R.; Parker, P. J. Activation of PRK1 by phosphatidylinositol 4,5-bisphosphate and phosphatidylinositol 3,4,5-trisphosphate. *J. Biol. Chem.* **1995**, *270*, 22412–22416.
(12) Toker, A.; Meyer, M.; Reddy, K. K.; Flack, J. R.; Aneja, R.; Aneja, S.; Parra, A.; Burns, D. J.; Ballas, L. M.; Cantley, L. C. Activation of protein kinase C family members by the novel polyphosphoinositides PI-3,4-P_2 and PI-3,4,5-P_3. *J. Biol. Chem.* **1994**, *269*, 32358–32367.
(13) Nakanishi, H.; Brewer, K. A.; Exton, J. H. Activation of the ζ Isozyme of Protein Kinase C by Phosphatidylinositol 3,4,5-trisphosphate. *J. Biol. Chem.* **1993**, *268*, 13–16.
(14) Schu, P. V.; Takegawa, K.; Fry, M. J.; Stack, J. H.; Waterfield, M. D.; Emr, S. D. Phosphatidylinositol 3-Kinase Encoded by Yeast *VPS*34 Gene Essential for Protein Sorting. *Science* **1993**, *260*, 88–91.
(15) Schultz, R. M.; Merriman, R. L.; Andis, S. L.; Bonjouklian, R.; Grindey, G. B.; Rutherford, P. G.; Gallegos, A.; Massey, K.; Powis, G. In vitro and in vivo antitumor activity of the phosphatidylinositol-3-kinase inhibitor, wortmannin. *Anticancer Res.* **1995**, *15*, 1135–1140.
(16) Kozikowski, A. P.; Kiddle, J. J.; Frew, T.; Berggren, M.; Powis, G. Synthesis and Biology of D-3-Deoxyphosphatidylinositol: A Putative Antimetabolite of Phosphatidylinositol-3-phosphate and an Inhibitor of Cancer Cell Colony Formation. *J. Med. Chem.* **1995**, *38*, 1053–1056.
(17) Kozikowski, A. P.; Powis, G.; Fauq, A. H.; Tückmantel, W.; Gallegos, A. Synthesis and Biological Activity of the D-3-Deoxy-3-fluoro and D-3-Chloro-3-deoxy Analogues of Phosphatidylinositol. *J. Org. Chem.* **1994**, *59*, 963–971.

(18) Khanavkar, B.; Ulbrich, F.; Gatzemeier, U.; Meyer-Schwicherath, E.; Lorenz, J.; Schreml, W.; Brugger, R.; Schichk, H.; von Pawel, J.; Nordstrom, R.; Drings, P. Treatment of Nonsmall Cell Lung Cancer with the Alkyllysophospholipid edelfosine-Intermediate Data Analysis. *Contrib. Oncol.* **1989**, *37*, 224–235.
(19) Powis, G.; Seewald, M. J.; Gratas, C.; Melder, D.; Riebow, J.; Modest, E. J. Selective Inhibition of Phosphatidylinositol Phospholipase C by cytotoxic Ether Lipid Analogues. *Cancer Res.* **1992**, *52*, 2835–2840.
(20) Augustine, J.; Berggren, M.; Powis, G.; Modest, E. Inhibition of Phosphatidyl Inositol-3'-Kinase by Ether Lipid Analogues of Phosphatidylinositol and Phosphatidylcholine. *Proc. Am. Assoc. Cancer Res.* **1992**, *33*, 415.
(21) Ishaq, K. S.; Capobianco, M.; Piantadosi, C.; Noseda, A.; Daniel, L. W.; Modest, E. J. Synthesis and Biological Evaluation of Ether-Linked Derivatives of Phosphatidylinositol. *Pharm. Res.* **1989**, *6*, 216–224 and references therein.
(22) Schwartz, P. W.; Tropp, B. E.; Engel, R. Phosphonolipids. The Synthesis of Chiral Vinylic Phosphonolipid Analogues of Phosphatidic Acid and Phosphatidyl Choline. *Chem. Phys. Lipids* **1988**, *48*, 1–7.
(23) Kozikowski, A. P.; Qiao, L.; Tückmantel, W.; Powis, G. Synthesis of 1D-3-Deoxy and -2,3-Dideoxyphosphatidylinositol. *Tetrahedron* **1997**, *53*, 14903–14914.
(24) Kozikowski, A. P.; Tückmantel, W.; Powis, G. Synthesis and Biological Activity of D-3-Deoxy-3-Fluorophosphatidylinositol – A New Direction in the Design of Non-DNA Targeted Anticancer Agents. *Angew. Chem., Int. Ed. Engl.* **1992**, *31*, 1379–1381.
(25) Sobkowska, A.; Sobkowski, M.; Cieslak, J.; Kraszewski, A. Aryl *H*-Phosphonates. 6. Synthetic Studies on the Preparation of Nucleoside *N*-Alkyl-*H*-phosphonamidates. *J. Org. Chem.* **1997**, *62*, 4791–4794.
(26) Hammond, P. R. A Simple Preparation of Alkyl Ammonium Phosphonates and Some Comments on the Reaction. *J. Chem. Soc.* **1962**, 2521–2522.
(27) Wu, R.; Saab, N. H.; Huang, H.; Wiest, L.; Pegg, A. E.; Casero, R. A., Jr.; Woster, P. M. Synthesis and Evaluation of a Polyamine Phosphinate and Phosphonamidate as Transition-State Analogue Inhibitors of Spermidine/Spermine-N^1-Acetyltransferase. *Bioorg. Med. Chem.* **1996**, *4*, 825–836.
(28) Vinod, T. K.; Griffith, O. H.; Keana, J. F. W. Synthesis of Isosteric and Isopolar Phosphonate Substrate Analogues Designed as Inhibitors for Phosphatidylinositol-Specific Phospholipase C from Bacillus Cereus. *Tetrahedron Lett.* **1994**, *35*, 7193–7196.
(29) Burford, D.; Flint, A. J.; Tonks, N. K. Crystal Structure of Human Protein Tyrosine Phosphatase 1B. *Science* **1994**, *263*, 1397–1404.
(30) Berggren, M.; Gallegos, A.; Dressler, L. A.; Modest, E. J.; Powis, G. Inhibition of the Signaling Enzyme Phosphatidylinositol-3-kinase by Antitumor Ether Lipid Analogues. *Cancer Res.* **1993**, *53*, 4297–4302.

JM980254J